Technische Universität München

Fakultät Wissenschaftszentrum Weihenstephan für Ernährung, Landnutzung und Umwelt

Lehrstuhl für Systembiologie der Pflanzen

Auxin transport regulation through dynamic efflux carrier phosphorylation

Benjamin A. L. Weller

Vollständiger Abdruck der von der Fakultät Wissenschaftszentrum Weihenstephan für Ernährung, Landnutzung und Umwelt der Technischen Universität München zur Erlangung des akademischen Grades eines

Doktors der Naturwissenschaften

genehmigten Dissertation.

Vorsitzender:	Prof. Dr. Kay H. Schneitz
Prüfer der Dissertation:	1. Prof. Dr. Claus Schwechheimer
	2. Dr. Ulrich Hammes

Die Dissertation wurde am 21.08.2017 bei der Technischen Universität München eingereicht und durch die Fakultät Wissenschaftszentrum Weihenstephan für Ernährung, Landnutzung und Umwelt am 17.10.2017 angenommen.

Für Albert, Gromi, O+O, Michael, Christine,
Lotte, Hissa, Pauline, Eli, Barbara, Dietrich,
Benno, Thore und Josephine.

Contents

Abstract

The continuous flux of the phytohormone auxin within plants is crucial for the control of a plethora of growth and developmental processes. The direction of auxin transport is largely provided by auxin efflux carriers of the PIN (PIN-FORMED) family, which are polarly distributed in the plasma membranes of many cells. In *Arabidopsis*, at least two AGCVIII protein kinases, D6PK (D6 PROTEIN KINASE) and PID (PINOID), phosphorylate PINs at conserved serines S1 - S4 and activate PIN-mediated auxin efflux. Additionally, PID was proposed to promote PIN1 polarity changes through phosphorylation at S1 - S3. D6PK, on the other hand, does not influence PIN1 polarity. Differential D6PK and PID phosphosite preferences were thought to be at the basis of these differential effects, although the two kinases differ also with regard to their intracellular localization and trafficking. Here, I examine the dynamics of PIN1 phosphorylation *in situ* in the context of PIN1 activation and polarity control. To this end, phosphosite-specific antibodies were generated for the PIN1 phosphosites S1 - S4. I show that PIN1 phosphorylation at all four serines occurs at the apical, as well as basal plasma membrane in different cell types of the root. Furthermore, my data suggests that basal phosphorylation is dependent on BFA (Brefeldin A)-sensitive protein kinases such as D6PK, whereas apical phosphorylation is BFA-insensitive and could thus involve the BFA-insensitive PID kinase. I find further that PIN1 polar distribution in a variety of tissues and cell types is independent of PIN1 phosphorylation. Instead, the phosphorylation patterns correlate well with hypothetical auxin transport streams during root gravitropic growth. I therefore argue that PIN1 phosphorylation at S1 - S4 indicates auxin efflux activity, while more complex models are needed to explain the PID-induced PIN1 polarity changes. Since PIN1 phosphorylation is maintained in higher order mutants of the D6PK and PID families, additional, BFA-sensitive PIN1 regulatory protein kinases must be expressed in *Arabidopsis* roots.

Zusammenfassung

Der kontinuierliche Flux des Phytohormons Auxin innerhalb von Pflanzen ist entscheidend für die Kontrolle einer Vielzahl von Wachstums- und Entwicklungsprozessen. Die Richtung des Auxintransports ist weitgehend durch die Auxineffluxtransporter der PIN (PIN-FORMED) Familie gegeben, welche polar an der Plasmamembran vieler Zellen verteilt sind. In *Arabidopsis* phosphorylieren mindestens zwei AGCVIII Proteinkinasen, D6PK (D6 PROTEIN KINASE) und PID (PINOID), die PINs an den konservierten Serinen S1 - S4 und aktivieren den PIN-vermittelten Auxinexport. Zusätzlich wurde vorgeschlagen, dass PID PIN1 Polaritätsveränderungen durch die Phosphorylierung von S1 - S3 hervorruft. D6PK dagegen, hat keinen Einfluss auf die PIN1 Polarität. Differentielle Phosphorylierungspräferenzen von D6PK und PID wurden als ein Grund für diese unterschiedlichen Effekte vermutet, obwohl sich beide Kinasen auch im Hinblick auf ihre intrazelluläre Lokalisation und den Transportwegen unterscheiden. Hier untersuche ich die Dynamik von PIN1 Phosphorylierungen *in situ* im Kontext der PIN1 Aktivierung und Polaritätskontrolle. Hierfür wurden Phosphorylierungsrest-spezifische Antikörper für die PIN1 Phosphorylierungsstellen S1 - S4 hergestellt. Ich zeige, dass eine PIN1 Phosphorylierung an der apikalen, sowie basalen Plasmamembran in verschiedenen Zelltypen der Wurzel stattfindet. Des weiteren weisen meine Daten darauf hin, dass die basale Phosphorylierung von BFA-sensitiven Kinasen wie D6PK abhängig ist, während apikale Phosphorylierungen BFA-insensitiv sind, und somit die BFA-insensitive PID Kinase involvieren könnten. Außerdem beobachte ich, dass die polare Verteilung von PIN1 in verschiedenen Geweben und Zelltypen unabhängig von der PIN1 Phosphorylierung ist. Vielmehr korrelieren die Phosphorylierungsmuster gut mit theoretischen Auxintransport-Strömen während des gravitropischen Wachstums der Wurzel. Ich argumentiere daher, dass die PIN1 Phosphorylierung an S1 - S4 auf die Auxinefflux-

aktivität hinweist, während komplexere Modelle notwendig sind, um PID-vermittelte Veränderungen der PIN1 Polarität zu erklären. Da die PIN1 Phosphorylierung in höheren Mutanten der D6PK und PID Familien jeweils erhalten bleibt, muss es weitere, BFA-sensitive PIN1 regulatorische Proteinkinasen geben, welche in *Arabidopsis* Wurzeln exprimiert sind.

List of figures

List of tables

Abbreviations

2,4-D	2,4-dichlorophenoxyacetic acid
AFB	AUXIN SIGNALING F-BOX
AGC	cAMP-DEPENDENT PROTEIN KINASE A, cGMP-DEPENDENT PROTEIN KINASE G AND PHOSPHOLIPID DEPENDENT PROTEIN KINASE C
AHA2	ATPase/hydrogen-exporting ATPase2
amiRNA	Artificial microRNA
ARF	ADENOSYL-RIBOSYLATION FACTOR
ARF-GAP	ARF-GUANINE NUCLEOTIDE ACTIVATING PROTEIN
ARF-GEF	ARF-GUANINE NUCLEOTIDE EXCHANGE FACTOR
ATP	Adenosine triphosphate
AUX	AUXIN RESISTANT
AUX/IAA	AUXIN/INDOLE-3-ACETIC ACID
BFA	Brefeldin A
BSA	Bovine serum albumin
Cdc42	CELL DIVISION CONTROL PROTEIN42
Col-0	Columbia-0
COP	COAT PROTEIN
Cy3	Cyanin 3
D6PK	D6 PROTEIN KINASE
D6PKL	D6 PROTEIN KINASE LIKE
DMSO	Dimethylsulfoxide
dNTP	Deoxyribonucleoside triphosphate
DR5	DIRECT REPEAT 5
EDTA	Ethylenediaminetetraacetic acid
FITC	Fluorescein isothiocyanate
FM4-64	N-(3-triethylammoniumpropyl)-4-(6-(4(diethylamino)phenyl)hexatrienyl) pyridinium dibromide
GDP	Guanosine diphosphate
GFP	GREEN FLOURESCENT PROTEIN
GLUT4	GLUCOSE TRANSPORTER4
GN	GNOM
GTP	Guanosine triphosphate
GTPase	GUANINE TRIPHOSPHATASE
GUS	ß-GLUCURONIDASE
DII	Domain II
H+ ATPase	Proton ADENOSINE TRIPHOSPHATASE
HRP	Horseradish peroxidase
IAA	Indole-3-acetic acid
KIPK	KCBP-INTERACTING PROTEIN KINASE
LAX	LIKE AUX
MAPK	MITOGEN-ACTIVATED PROTEIN KINASE
MDR/PGP	MULTIDRUG RESISTANCE/P-GLYCOPROTEIN
MES	2-(N-Morpholino)ethanesulfonic acid
NPH	NON-PHOTOTROPIC HYPOCOTYL
NPY	NAKED PINS IN YUCCA

PAR	PARTITIONING DEFECTIVE
PBS	Phosphate buffered saline
PCR	Polymerase chain reaction
phot	phototropin
PID	PINOID
PIDL	PINOID LIKE
PIN	PIN-FORMED
PKA	PROTEIN KINASE A
PKB	PROTEIN KINASE B
PKC	PROTEIN KINASE C
plgA	Polymeric immunoglobulin A
plgR	Polymeric immunoglobulin receptor
PMSF	Phenylmethylsulfonylfluoride
PP2A	PROTEIN PHOSPHATASE 2A
PPT	Phosphinothricin
PR	Ponceau rouge
PVDF	Polyvinylidene fluoride
RT-PCR	Reverse transcription PCR
SDS	Sodium dodecyl sulfate
Taq	*Thermus aquaticus*
T-DNA	Transfer DNA
TIR	TRANSPORT INHIBITOR RESPONSE
Tris	Tris(hydroxymethyl)aminomethane
UNC	UNICORN
WAG	WAVY GROWTH
XVE	LexA, VP16 and human estrogen receptor
YFP	YELLOW FLUORESCENT PROTEIN

1 Introduction

1.1 Auxin

Not least the experiments of Charles Darwin on "The power of movement in plants" and his resulting hypothesis about a transmittable "influence" residing in the tips of growing shoots and roots "endowed with diverse kinds of sensitiveness" for stimuli such as touch, light, gravity or moisture (Darwin, 1880), suggested that plants possess mobile factors that direct growth. Since then, a number of signaling molecules have been identified that classify as phytohormones. The chemical nature of Darwin's compound would remain elusive for another 50 years but was eventually confirmed to be what is now commonly referred to as auxin [reviewed in (Wildman, 1997)]. A striking feature of this important phytohormone, given its rather simple chemical nature, is its vast impact on plant development and growth. Moreover, the synthetic auxin 2,4-D (2,4-dichlorophenoxyacetic acid) finds its application as one of the most widely used herbicides in North America (Grossmann, 2010). These two aspects have made it vitally important to understand, at the molecular level, how auxin exerts its diverse functions. This work explores, through functional analysis of a particular auxin transporter, how auxin is distributed within plant tissues, thereby contributing a small piece to this no doubt complex puzzle.

IAA (indole-3-acetic acid), the most abundant naturally occurring auxin in plants, is produced primarily in young leaves and the apexes of the root and shoot via tryptophan biosynthesis depended and independent pathways (Ljung et al., 2001; Ljung et al., 2005; Petersson et al., 2009; Normanly, 2010). The perception of auxin inside cells occurs through the auxin receptor TIR1 (TRANSPORT INHIBITOR RESPONSE1) and its close homologues AFB1, 2, and 3 (AUXIN SIGNALING F-BOX1, 2 and 3) (Dharmasiri et al., 2005). In the presence of auxin, these receptors initiate a

transcriptional response by binding AUX/IAA (AUXIN/INDOLE-3-ACETIC ACID) proteins, targeting them for degradation. This releases AUXIN RESPONSE FACTOR transcription factors, which are otherwise sequestered by binding to AUX/IAAs, to initiate transcriptional changes (Ulmasov et al., 1997a; Ulmasov et al., 1997b; Vernoux et al., 2011). These changes in gene expression are extensive and constitute the best characterized cellular auxin response (Teale et al., 2006; Paponov et al., 2008).

However, some auxin responses are very rapid and occur within minutes, such as changes in membrane potential (Felle et al., 1991) and ion uptake (Marten et al., 1991) and thus cannot be explained by transcriptional regulation alone. Particularly, studies on the effects of auxin on proton secretion from plant cells through the activation of plasma membrane H+ ATPases (proton ADENOSINE TRIPHOSPHATASE) (Senn and Goldsmith, 1988; Hager et al., 1991; Frias et al., 1996) have revived the long standing acid growth hypothesis. The auxin-induced acidification of the apoplastic space surrounding plant cells activates enzymes such as expansins that loosen the cell wall, allowing cells to incresase in volume and thus plants to grow. [reviewed by (Rayle and Cleland, 1992)]. Interestingly, recent research has linked auxin-induced phosphorylation and concomitant activation of the H+ ATPase AHA2 to hypocotyl elongation, providing molecular evidence for such auxin responses. Moreover, the study showed that this occurs in a TIR1/AFB-independent manner (Takahashi et al., 2012), suggesting that alternative auxin perception mechanisms exist in *Arabidopsis*.

1.1.1 Auxin transport

An important observation already made by Darwin was the ability of auxin to move within the plant. The idea culminated in the Cholodny-Went hypothesis, which suggests that asymmetric stimuli such as light or gravity result in tissue-specific vari-

ations in auxin distribution, leading to a differential growth rate across the auxin gradient (Went, 1926). This aspect has since been confirmed to be important for the diverse effects of auxin on plant development, as these local concentration differences, maxima and minima, serve as readouts for proper cell elongation and division in the control of a wide range of developmental processes, such as embryogenesis, lateral organ formation, apical dominance, phylotaxis, apical hook formation and tropic growth (Friml et al., 2002a; Benkova et al., 2003; Friml et al., 2003; Ottenschlager et al., 2003; Teale et al., 2006; Sorefan et al., 2009; Zadnikova et al., 2010). The formation of these concentration gradients is in part facilitated by the

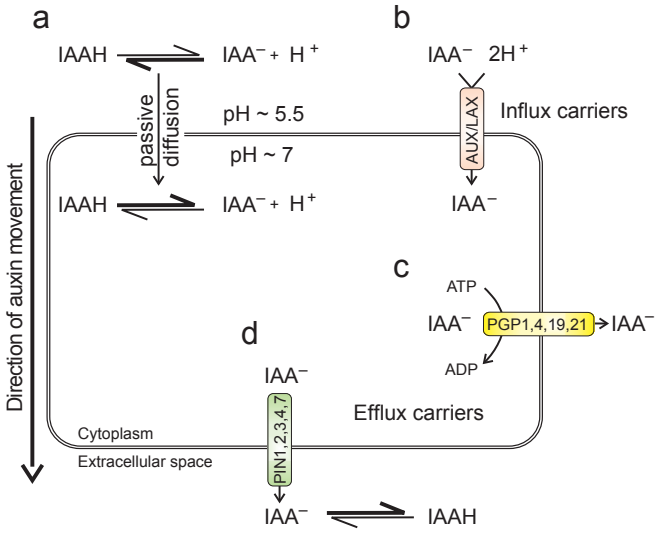

Figure 1: Cellular auxin transport.

(a) Chemiosmotic hypothesis, passive diffusion of auxin into the cell due to difrerences in pH between the cytoplasm and extracellular space. (b) Auxin influx carriers of the AUX/LAX family facilitate cellular auxin uptake. (c) MDR/PGP family transporters carry auxin across the plasma membrane in an ATP-dependent manner. PGP1 and PGP19 are auxin exporters, PGP4 and PGP21 are bi-directional transporters. (d) PIN1, 2, 3, 4 and 7 constitute auxin efflux carriers. Their often assymetrical distribution at the plasma membrane is thought to be crucial for the directionality of cellular auxin transport.
Figure modified from Petrasek and Friml, 2009.

ability of protonated auxin to diffuse into cells from the acidic apoplast, where the more alkaline pH of the cytosol causes de-protonation and entrapment inside the cell (Fig. 1a) (Rubery and Sheldrake, 1973).

Additionally, membrane-resident transporters assist in the directed movement of auxin between cells to form a complex transport system. Auxin influx carriers, namely AUX1 (AUXIN RESISTANT1) and its homologues LAX1, 2, 3 (LIKE AUX1, 2, 3) facilitate cellular auxin uptake (Fig. 1b). Their localization in the vascular tissue of

leaves and roots suggests that they might be involved in loading and unloading of auxin in source and sink tissues, respectively (Bennett et al., 1996; Marchant et al., 1999; Yang et al., 2006; Bainbridge et al., 2008; Swarup et al., 2008). A second class of proteins, MDRs/PGPs (MULTIDRUG RESISTANCE/P-GLYCOPROTEIN), also transport auxin and are thought to contribute to efficient long distance transport through the vasculature of the plant. PGP1 and PGP19 constitute efflux carriers, while PGP4 and PGP21 have been reported to have a bi-directional transport capacity (Fig. 1c) (Geisler et al., 2005; Terasaka et al., 2005; Geisler and Murphy, 2006; Cho et al., 2007; Yang and Murphy, 2009; Kamimoto et al., 2012).

The notion that auxin is able to enter, but not exit cells on its own led to the hypothesis that exporters could play an especially important role in controlling the path of auxin flow (Rubery and Sheldrake, 1974). Consequently, recent research has focused particularly on a family of auxin efflux carriers, the PIN (PIN-FORMED) proteins, which, due to their often polar distribution at the plasma membrane, have the potential to give directionality to the transport of auxin (Fig. 1d) [reviewed by (Habets and Offringa, 2014; Adamowski and Friml, 2015)]. This thesis particularly focuses on PIN1 from *Arabidopsis thaliana* and how its activity and polarity could influence auxin distribution. The PIN proteins will therefore be discussed in detail in section 1.2.

1.1.2 Auxin in plant development

The elucidation of the role of auxin transport in developmental and tropic growth processes has been greatly facilitated by the establishment of two different reporter constructs that permit the visualization of auxin activity at the cellular level. The first relies on a conserved motif found in the promoter regions of auxin responsive genes. These so-called auxin responsive elements were shown to be binding sites for the AUXIN RESPONSE FACTOR transcription factors and were used in tandem

repeats to form a synthetic, auxin-responsive promoter, DR5 (DIRECT REPEAT 5). DR5 allows the tracking of auxin-induced changes in gene expression when coupled to the expression of fluorescent or enzymatic markers, such as GFP (GREEN FLOURESCENT PROTEIN) or GUS (ß-GLUCURONIDASE) (Ulmasov et al., 1995; Ulmasov et al., 1997b).

More recently, a second reporter was established that makes use of auxin-induced, TIR1-mediated AUX/IAA degradation. The domain II (DII) of these AUX/IAA proteins that mediates the binding to TIR1 is coupled to a fluorescent marker, which leads, upon elevation of cellular auxin levels, to the degradation of the fusion protein and thus the disappearance of fluorescence. This reporter, referred to as DII-VENUS, does not rely on comparatively slow *de novo* transcription and therefore makes it possible to directly track relative changes in cellular auxin content at timescales of minutes (Brunoud et al., 2012). Although both reporters do not assess auxin concentrations *per se*, it was shown that the output obtained correlates well with direct measurements of auxin content within a given tissue (Casimiro et al., 2001; Friml et al., 2002b; Benková et al., 2003; Brunoud et al., 2012).

During embryogenesis, the earliest detectable signal from a DR5-GFP reporter appears specifically in the apical cell after the first cell division of the zygote, indicating an asymmetrical auxin distribution already at the two-cell stage. The DR5-GFP signal subsequently elevates in the proembryo, while it remains almost absent from the suspensor cells of the hypophysis. At the 32-cell stage, a reversal of the auxin distribution is observed towards the suspensor cells, suggesting that the direction of auxin transport, or the site of biosynthesis, changes at this point. At later stages of embryogenesis, DR5-GFP signals appear at incipient sites of cotyledon formation, in provasular strands, as well as in the cells that ultimately form the root apical meristem (Friml et al., 2003). This pattern of relative auxin distribution is largely main-

tained in the adult plant, where the reporters indicate local maxima in the quiescent center and columella cells of the root apical meristem, in vascular strands, as well as at the flanks of lateral organ initiation sites in the shoot (Sabatini et al., 1999; Friml et al., 2002b; Vernoux et al., 2010).

Studies on the process of lateral root formation have also benefited from the use of these reporter constructs. Initiation sites of lateral root primordia, pericycle cells adjacent to each xylem pole, can easily be identified based on the appearance of a cell-specific DR5-derived signal just before cell cycle activation. The formation of a local auxin maximum in these cells is indeed one of the earliest markers for the formation of a lateral root primordium and has been shown to be crucial in this process (Casimiro et al., 2001; Benková et al., 2003).

Dynamic changes in auxin distribution are also observed during tropic growth, a plant's response to external stimuli. Roots constantly orient themselves according

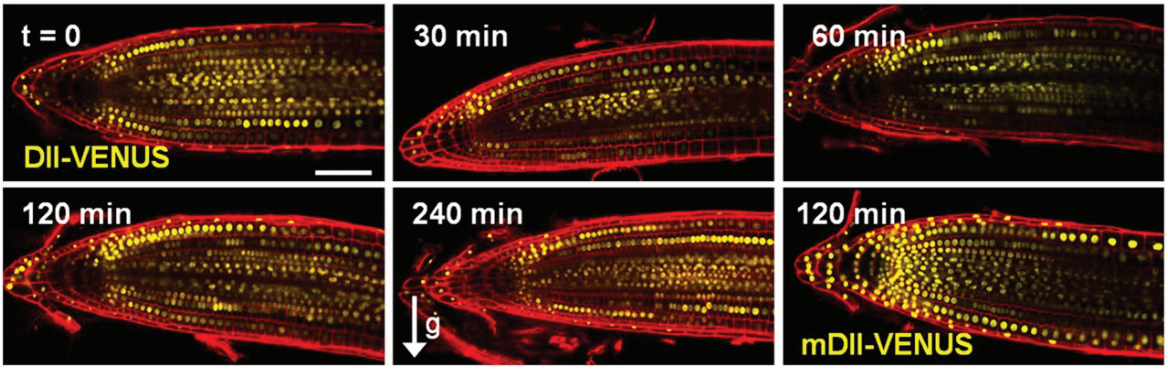

Figure 2: Asymmetric signal distribution of DII-VENUS auxin response marker after gravity stimulation.

Yellow circular structures represent nuclear localized DII-VENUS signals at the times indicated following a 90° gravity stimulus. Relative signal intensities between the upper and lower side of the root are comparable at t = 0 min. Over the first hour (t = 30 min and t = 60 min), the signal enriches at the upper side and is depleted from the lower side, in an inverse relationship to relative cellular auxin levels. This asymetric auxin distribution is transient, as symmetry is subsequently (at t = 120 min and t = 240 min) re-established. mDII-VENUS (last panel) serves as a negative control, as this mutagenized version of the reporter is not subject to auxin-induced proteasomal degradation. Consequently, no asymmetric signal distribution is observable following gravity stimulation. Red signal derives from propidium iodide staining of the cell wall to show cellular organization of the root tip.
Figure modified from Band et al., 2012.

to the vector of gravity. How plants exactly perceive this signal is not entirely understood; however, the use of auxin responsive reporters has revealed that a reorientation of the root tip with respect to gravity leads to an accumulation of auxin in epidermal cells facing downwards (Fig. 2). This asymmetric auxin distribution between the upper and lower sides of the meristem consequently inhibits cell expansion on the downward facing side, causing the root to bend in this direction (Boonsirichai et al., 2003; Ottenschlager et al., 2003; Band et al., 2012). Interestingly, recent data obtained with the highly dynamic DII reporter suggests that the lateralization of auxin is rapid, occuring within minutes of signal perception (Band et al., 2012).

The effects of uneven illumination on auxin distribution can be visualized in etiolated *Arabidopsis* hypocotyls, akin to the experiments of Darwin. Unilateral irradiation with blue light leads to an accumulation of auxin on the shaded side of the hypocotyl, which, in this tissue, has growth promoting effects, leading to organ bending towards the light source (Friml et al., 2002a; Ding et al., 2011).

1.2 The PIN auxin efflux carriers

Much of the available data suggests that these dynamic changes in auxin distribution are facilitated by the polar distribution of the PIN auxin efflux carriers [reviewed by (Michniewicz et al., 2007a)]. The earliest evolutionary appearance of PIN proteins can be found in unicellular green algae, such as *Klebsormidiales*, which contain a single PIN isoform. The biological function of this protein is not yet resolved and is not trivial to fathom, as auxin export from a unicellular organism is difficult to reconcile with most established functions for auxin in multicellular plants. However, it has been suggested that its role could be similar to quorum sensing in bacteria (Viaene et al., 2013). What is more evident is that the colonization of land by plants coincided with diversification of PIN protein structure and function and thus

with auxin biology (Bennett, 2015). The model plant *Arabidopsis thaliana* carries 8 PIN proteins in its genome. They are integral membrane proteins with 10 predicted transmembrane domains. Particular consideration will be given here to PIN1, 2, 3, 4 and 7, which have been shown to localize to the plasma membrane and feature a large cytosolic, hydrophillic loop that is not present in the other three PIN proteins, PIN5, 6 and 8 [reviewed by (Krecek et al., 2009)].

PIN1 was the first family member identified based on its striking loss-of-function phenotype in the form of pin-shaped inflorescences with undifferentiated floral organs, which results in complete sterility of the plant (Bowman et al., 1989; Okada et al., 1991). Other phenotypes of this mutant generally show a low penetrance and include a reduced number or discoid cotyledons and rosette leaves (Okada et al., 1991; Galweiler et al., 1998). A prominent feature of the PIN1 protein is its localization in distinct polar regions of the plasma membrane. In vascular tissue and stele cells of the root apical meristem it is enriched at the basal (rootward) side of the cell (Galweiler et al., 1998; Scarpella et al., 2006), whereas epidermal cells of the shoot apical meristem localize PIN1 apically (shootward) (Benková et al., 2003; Reinhardt et al., 2003; Heisler et al., 2005). During embryogenesis, PIN1 shows a dynamic distribution towards incipient sites of cotyledon initiation in the epidermal layer and towards the root pole in provascular cells (Steinmann et al., 1999; Benková et al., 2003).

PIN2 was also identified based on its mutant phenotype in several independent forward genetic screens (Chen et al., 1998; Luschnig et al., 1998; Muller et al., 1998; Utsuno et al., 1998). Mutation of this gene leads to agravitropic root growth, in line with its exclusive expression in cortex and epidermal cells of the root. The PIN2 protein is also restricted to distinct regions of the plasma membrane. In the root epidermis, as well as in differentiated root cortex cells, PIN2 is localized apically,

whereas it is found at the basal side of the cortex in the root apical meristem (Muller et al., 1998).

Based on the amino acid sequence of these two proteins, PIN3, 4 and 7 were identified as additional members of this family with high sequence similarity among each other (Friml et al., 2002b; Friml et al., 2002a; Friml et al., 2003). It might therefore not be surprising that single mutants of any one of these *PINs* display rather mild phenotypes, although the severity of these phenotypes increases with increasing mutant complexity (Benková et al., 2003; Friml et al., 2003; Blilou et al., 2005; Vieten et al., 2005; Willige et al., 2013). It has also been proposed that functional redundancy and ectopic expression of other *PINs* is able to compensate for defects arising in different *pin* mutant combinations (Vieten et al., 2005).

In plants with impaired PIN3 function, the gravitropic and phototropic responses, as well as apical hook maintenance are slightly impaired. PIN3 is located at the plasma membrane, specifically at the basal side of endodermis and stele of the root, as well as apolarly in columella cells and the endodermis of the shoot (Friml et al., 2002a; Ding et al., 2011). Mutants of *pin4* exhibit altered auxin distribution, as well as mild defects in cell fate and the division plane in the root apical meristem and during embryogenesis (Friml et al., 2002b). Likewise, *pin7* mutants have cell division defects during early embryogenesis; however, these embryos usually recover to form fertile adult plants. On the other hand, division plane and polarity defects during embryogenesis in double mutants of *pin4 pin7* are more persistent, leading to alterations in the organogenesis of cotyledons at the seedling stage (Friml et al., 2003). These phenotypes are enhanced further in *pin3 pin4 pin7* triple mutants, which also display a complete loss of photo- and gravitropism (Rakusova et al., 2011; Willige et al., 2013).

Importantly, the observed phenotypes of *pin* mutants can often be mimicked by

application of auxin transport inhibitors, suggesting that loss of PIN protein function results in improper auxin distribution within the plant (Okada et al., 1991; Muller et al., 1998; Benková et al., 2003; Blilou et al., 2005).

Moreover, in most tissues and cell types analyzed so far, where PIN function and auxin gradients have been shown to play a role, a strong correlation exists between the direction of PIN polarity and local auxin maxima (Wiśniewska et al., 2006; Zhang et al., 2010; Ding et al., 2011; Rakusova et al., 2011). This is particularly striking during embryogenesis, where the above mentioned polar PIN localization corresponds well with the observed patterns from auxin response markers (Fig. 3A and B) (Friml et al., 2003). Likewise, during lateral root initiation, an auxin response is observed in a pair of pericycle founder cells congruent with a change in PIN1 polarity in adjacent endodermal cells towards the initials (Benková et al., 2003). During subsequent formation of the lateral root, PIN1 polarity establishes towards a new auxin maximum at the primordium tip (Marhavy et al., 2014), similarly to what is observed in the primary root meristem (Fig. 3C and D).

Dynamic changes in PIN3 polarity have also been shown to coincide with local auxin maxima during photo- and gravitropic growth responses of the shoot and root (Friml et al., 2002a; Kleine-Vehn et al., 2010; Ding et al., 2011; Rakusova et al., 2011). In hypocotyl endodermal cells, PIN3 assumes a lateral polarity following a photo- or gravitropic stimulus towards the shaded, or downward facing side, respectively (Ding et al., 2011; Rakusova et al., 2011). Likewise, PIN3 in root columella cells is polarized towards the downward facing side upon gravity stimulation (Friml et al., 2002a; Kleine-Vehn et al., 2010). These polarization events are thought to initiate auxin concentration differences across the vertical plane of shoot and root tissue. Moreover, the accumulation of auxin could itself stabilize PIN membrane association and thus serve as its own positive feedback signal. This was shown for PIN1 in

root cells by auxin treatment (Paciorek et al., 2005) and for PIN2 in epidermal cells following a gravity stimulus (Abas et al., 2006).

Recent data suggests, however, that dynamic PIN polarity might not be sufficient to account for changes in auxin flux, particularly the rapid asymmetric auxin accumulation in roots following a gravity stimulus. There, experiments using the auxin response marker DII-VENUS, in combination with *in silico* modeling, predict a lateralization of auxin within a few minutes of stimulation (Band et al., 2012), while the polarization of PIN3 in columella cells is reported to take much longer (Kleine-Vehn et al., 2010). This has raised the question whether PIN activity, rather than polarity

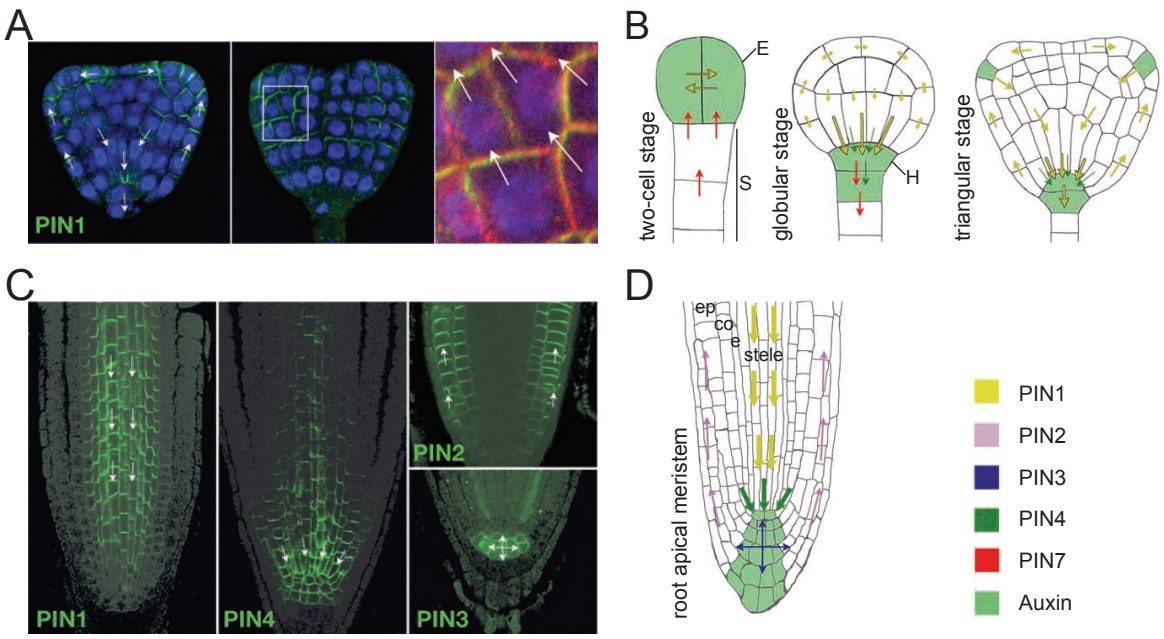

Figure 3: PIN polarity correlates with hypothetical auxin transport streams and observed auxin maxima.

(A) Polar plasma membrane localization of PIN1 (green) in immunostained *Arabidopsis thaliana* triangular stage embryos. White arrows depict the polarity of PIN1 in different cell types of the embryo. Close up from inset (right panel) shows apical PIN1 localization in epidermal cells towards incipient sites of cotyledon formation. (B and D) PIN polarity and hypothetical auxin transport streams at different stages of *Arabidopsis thaliana* embryogenesis (B) and the root apical meristem (D). Cells marked in green correspond to auxin maxima as observed with auxin responsive markers, such as DR5-GFP. Colored arrows depict hypothetical auxin transport streams as derived from the plasma membrane localization of the different PINs in their respective expression domains. (E = Embryo, S = Suspensor, H = Hypophysis, ep = Epidermis, co = Cortex, e = endodermis) (C) Localization of various PINs as indicated (green) at the plasma membrane of different cell types of immunostained *Arabidopsis thaliana* primary root meristems. White arrows depict PIN polarity as in A. Figure modified from Tanaka et al., 2006.

alone, might be another important regulatory component. In fact, the extent to which PINs actively transport auxin against a concentration gradient was long debated; however, it has since been validated in several independent studies using different heterologous systems, such as plant, yeast or human cell cultures (Petrasek et al., 2006), *Xenopus laevis* oocytes (Zourelidou et al., 2014), or *Arabidopsis* root hairs (Lee and Cho, 2006), that PINs are active auxin efflux carriers. Importantly, experiments in oocytes (Zourelidou et al., 2014), as well as root hairs (Lee and Cho, 2006), revealed that PINs require phosphorylation by specific kinases for transport activity. These particular phosphorylation events, specifically on the PIN1 cytoplasmic loop, as well as the kinases that mediate them, are the major topic of this thesis. Evidence will be provided that these sites, which are thought to be responsible for polarity regulation of PIN1, might rather be sites for transporter activation. A more detailed introduction on this will be provided in section 1.3.

1.2.1 PIN polarity through constitutive endocytosis

The polar distribution of PINs within cells and the resulting consequences on auxin transport and thus plant development have spawned intensive research on the mechanisms of polarity establishment in plants. While the animal field has amassed a wealth of knowledge on this subject, little is known about these mechanisms in plants to date [reviewed by (Petricka et al., 2009)]. All cells, however, regardless of the organism, are endowed with an inherent asymmetry in the form of vectorial polymers of actin and microtubule filaments that make up the cytoskeleton. Aside from shaping cellular morphology and providing stability, the cytoskeleton is utilized by the intracellular trafficking machinery of the endomembrane system to deliver membrane proteins and other cargo to the correct subcellular regions [reviewed by (Mullins, 2010)]. This can be accomplished by means of polarized secretion and/or selective recycling and endocytosis to and from the plasma membrane.

Membrane proteins translated into the lumen of the endoplasmatic reticulum are packaged into endosomes and delivered to the plasma membrane through the Golgi apparatus. Directionality in this process derives from movement of vesicles along the cytoskeleton, as well as the tightly controlled processes of vesicle fusion and budding. The former involves sequence-specific information from the cargo itself, as well as post translational modifications that specify the final intracellular address. The latter is coordinated by a large array of proteins. Clathrin and associated adaptor complexes regulate cargo endocytosis from the plasma membrane, while the cotamer complexes COPI and COPII regulate the trafficking between the endoplasmatic reticulum and Golgi apparatus. Vesicle formation is often coordinated by ARF (ADENOSYL-RIBOSYLATION FACTOR) proteins, which belong to the family of small GTPases (GUANOSINE TRIPHOSPHATASE) and are themselves regulated by ARF-GAPs (GUANINE NUCLEOTIDE ACTIVATING PROTEIN) and ARF-GEFs (GUANINE NUCLEOTIDE EXCHANGE FACTOR) that facilitate the exchange of GDP with GTP required for activation of the ARF [reviewed by (Mellman and Nelson, 2008; Orlando and Guo, 2009)].

All of these factors have been shown, through pharmacological inhibition of specific trafficking pathways, as well as analysis of mutants, to impact on polar PIN localization (Steinmann et al., 1999; Teh and Moore, 2007; Kleine-Vehn et al., 2008c; Heisler et al., 2010; Kitakura et al., 2011; Nagawa et al., 2012; Richter et al., 2012; Drdova et al., 2013; Tanaka et al., 2013; Tanaka et al., 2014; Doyle et al., 2015). Of particular relevance for this thesis is the application of the fungal toxin BFA (Brefeldin A). Its application to animal and yeast cells blocks retrograde trafficking from the Golgi to the endoplasmatic reticulum by inhibiting the ARF-GEF Arf1p, ultimately leading to collapse of the Golgi apparatus (Peyroche et al., 1999). Different effects of BFA, however, are observed in plant cells, possibly due to the strong diversifica-

tion of small GTPases between plants and animals (Richter et al., 2007). In plant cells, BFA inhibits the ARF-GEF GN (GNOM), which is normally responsible for the coordinated delivery of cargo vesicles from the trans Golgi network to the plasma membrane (Steinmann et al., 1999; Geldner et al., 2003). Fluorescent lipophillic dyes such as FM4-64 can undergo endocytosis and thereby make certain trafficking pathways visible. Under normal conditions, FM4-64 is taken up into small intracellular structures (Vida and Emr, 1995; Betz et al., 1996; Fischer-Parton et al., 2000); however, upon BFA application to plant cells, the dye accumulates in large, perinuclear structures called BFA compartments (Fig. 4).

The use of BFA, as well as analysis of *gn* mutants, suggests that selective endocytosis at the plasma membrane is crucial in the context of polar PIN targeting (Steinmann et al., 1999; Geldner et al., 2001; Geldner et al., 2003; Geldner et al., 2004). The root apical meristem has emerged as a model system to study this process, due to the differential polar localizations of PIN1 and PIN2 in this tissue as described in section 1.2.1 in conjunction with its accessibility to fluorescence microscopy techniques. These aspects, as will be evident, were also taken advantage of extensively in this thesis.

Treatment of *Arabidopsis* roots with BFA leads to PIN1 accumulation in BFA compartments (Geldner et al., 2001). It additionally results in loss of basal PIN1 polarity and prolonged treatments can even lead to its enrichment at the apical side, an observation also made when GN function is mutationally disrupted. While basal PIN2 in cortex cells behaves like PIN1 under these conditions, apical PIN2 localization in epidermal cells is maintained (Kleine-Vehn et al., 2008c). These observations led to the hypothesis that PINs undergo constitutive endocytosis at the plasma membrane to maintain their polarity and that GN regulates the delivery of PINs particularly, albeit not exclusively, to the basal plasma membrane (Richter et al., 2007; Kleine-

Vehn et al., 2008c; Kleine-Vehn et al., 2008a; Wolters et al., 2011).

Whether PINs, following translation into the endoplasmatic reticulum, are initially secreted polarly, or whether they gain polarity only upon selective endocytosis after apolar secretion was attempted to be resolved using an estradiol inducible expression system (*XVE>>PIN1*), or fluorescence recovery after photobleaching techniques. This report suggested that the latter scenario is valid, however, the corresponding manuscript has since been retracted (Dhonukshe et al., 2008). Whether PINs are initially distributed symmetrically is therefore unanswered.

Asymmetrically distributed cargo can also be redirected to other regions of the cell via a process termed transcytosis. Signals such as ubiquitination or phosphorylation on target proteins can be interpreted by the trafficking machinery to transfer cargo

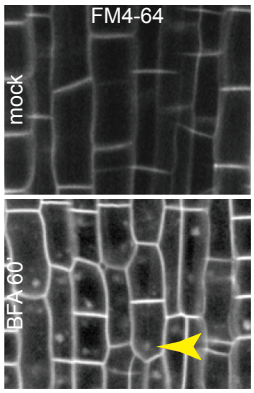

Figure 4: Intracellular endomembrane trafficking pathways visualized via imaging of the fluorescent lipophilic dye FM4-64.

Live imaging of intact *Arabidopsis* primary root meristem stele cells treated with mock or BFA and stained with FM4-64. The dye is able to incorporate itself into the plasma membrane and subsequently undergoes "passive" endocytosis along with other cellular cargo. BFA inhibits the recycling of endosomes back to the plasma membrane and thus causes apparent fusion or aggregation of endosomes over time. The resulting "BFA bodies" are marked with a yellow arrowhead.
Figure modified from Zourelidou et al., 2014.

to its new location via the trans Golgi network [reviewed by (Tuma and Hubbard, 2003)]. One prominent example from the animal field is the polymeric immunoglobulin receptor pIgR and its ligand pIgA. Binding of the ligand to the receptor at the baso-lateral membrane sets off a complex phosphorylation cascade, ultimately leading to endocytosis of the pIgA-PIgR complex and secretion at the apical membrane via apical recycling endosomes (Apodaca et al., 1994; Su et al., 2010). An analogous mechanism has been proposed to operate during polar PIN targeting. Specifically, experiments using photoconvertible fluorescent PIN constructs together with BFA

treatments suggested that distinct, GN-dependent and GN-independent trafficking pathways exist in plants and that PINs are able to interchange between these pathways depending on the intracellular destination (Kleine-Vehn et al., 2008c). Furthermore, the decision about which pathway is utilized by the cell was linked to a phosphorylation-based signal on the PIN cytoplasmic loop (Kleine-Vehn et al., 2009; Dhonukshe et al., 2010). The notion that such a signal does indeed exist is supported by the observations described in the next section.

1.2.2 PIN polarity signals involve phosphorylation

How exactly the selective endocytosis of PINs is regulated and whether it is essential for proper PIN polarity is as yet poorly understood. As mentioned above, information encoded on the cargo itself could also play an important role in the trafficking decisions made by the cell. Evidence for this comes from the observation that PIN1 expressed ectopically under the *PIN2* expression domain assumes a basal localization in epidermal cells, in contrast to the apical localization of endogenous PIN2 (Wiśniewska et al., 2006). Moreover, two different variants of transgenic lines that express GFP-tagged PIN1 from the promoter of *PIN2* show divergent polar targeting of PIN1 as a result of a variation in the positioning of the GFP-tag in the PIN1 cytoplasmic loop (Wiśniewska et al., 2006; Kleine-Vehn et al., 2008c; Kleine-Vehn et al., 2008a). Therefore, information must be encoded within the PIN protein sequence that determines its polar localization.

One such possible signal, a phosphorylated serine (S) or threonine (T) at positions 337 and 340, respectively, within the cytoplasmic loop of PIN1, was discovered by mass spectrometric analysis of immunoprecipitated PIN1-GFP. Introduction of a negatively charged glutamic acid (E) at either position, a phosphorylation-mimicking mutation, results in a polarity shift of the PIN1 protein from the basal to the apical membrane of root cells. Conversely, replacement with alanine (A), a neutral,

non-phosphorylatable residue at these positions causes a change from apical to basal in shoot epidermal cells (Zhang et al., 2010). Thus, a single amino acid exchange is sufficient in this case to change the polarity of the cargo in a tissue-specific manner.

The first candidate kinase that was considered to possibly target this site was the serine/threonine kinase PID (PINOID), since it was found that overexpression of PID in roots leads to a shift of PIN1 from a basal to a preferentially apical localization in the stele (Friml et al., 2004; Dhonukshe et al., 2010), as well as a basal to apical shift of PIN2 in cortex cells. While it was subsequently demonstrated that S337 is likely not targeted by PID directly, the observed basal-to-apical changes in PIN polarity upon overexpression of PID nevertheless led to an effort to identify potential target sites of PID on PIN1. *In silico* analysis, in combination with *in vitro* phosphorylation experiments indeed revealed additional phosphorylation sites directly targeted by PID within the PIN1 cytoplasmic loop (Fig. 5) (Huang et al., 2010). Paradoxically, however, these sites have since been attributed both to the regulation of PIN polarity (Kleine-Vehn et al., 2009; Dhonukshe et al., 2010; Huang et al., 2010), as well as PIN transport activity (Zourelidou et al., 2014). The possibly dual function of these specific phosphorylation events was investigated in detail in this thesis, by use of phosphorylation site-specific antibodies in combination with whole mount immunohistochemical experiments. A detailed introduction on this aspect of PIN regulation will therefore follow in the next section.

Aside from endosomal trafficking machinery components, other proteins have been identified that affect the polar localization of PIN proteins (Friml et al., 2004; Sauer et al., 2006; Michniewicz et al., 2007b; Furutani et al., 2011; Ballesteros et al., 2013; Gao et al., 2013). The discovery of important regulatory phosphorylation sites on the PIN cytoplasmic loop led to a series of important publications culminating in a phos-

phorylation-based model for PID-mediated regulation of PIN polarity. Moreover, it was found that PID activity can be counteracted by the PP2A (PROTEIN PHOSPHATASE 2A) complex, which may work by de-phosphorylating PINs and targeting them to the basal PM domain. Loss of function of multiple subunits of this complex, particularly of three a-type regulatory components (PP2Aa1-3) and two c-type catalytic subunits (PP2Ac3-4) sometimes leads to a basal-to-apical PIN polarity shift in roots (Michniewicz et al. 2007; Ballesteros et al. 2013). However, as the PP2A holoenzyme consists of at least three subunits of one A, B and C-type unit each, of which there are 3, 23 and 5 different genes present in the *Arabidopsis* genome, respectively, the complexity of possible PP2A compositions has made a more detailed analysis difficult.

1.3 AGCVIII kinases regulate PIN polarity and activity

1.3.1 PID regulates PIN1 polarity

PID belongs to the plant-specific AGCVIII (cAMP-DEPENDENT PROTEIN KINASE A, cGMP-DEPENDENT PROTEIN KINASE G AND PHOSPHOLIPID DEPENDENT PROTEIN KINASE C) family of kinases to which there are no direct orthologues in metazoans. The closest relatives to AGCVIII kinases by sequence homology are the mammalian kinase families PKA and PKC (Galvan-Ampudia and Offringa, 2007; Rademacher and Offringa, 2012). Additionally, an AGCVIII kinase from tomato was proposed to function orthologously to mammalian PKB, a master regulator of cell survival, growth, and proliferation (Devarenne et al., 2006). Interestingly, one function of PKB in animals is to promote the translocation of the glucose transporter GLUT4 from endosomes to the plasma membrane by phosphorylation of a Rab-GTPase activating protein (Sano et al., 2003; Zeigerer et al., 2004).

Whether this role of PKB is evolutionarily linked to the proposed effects of PID on

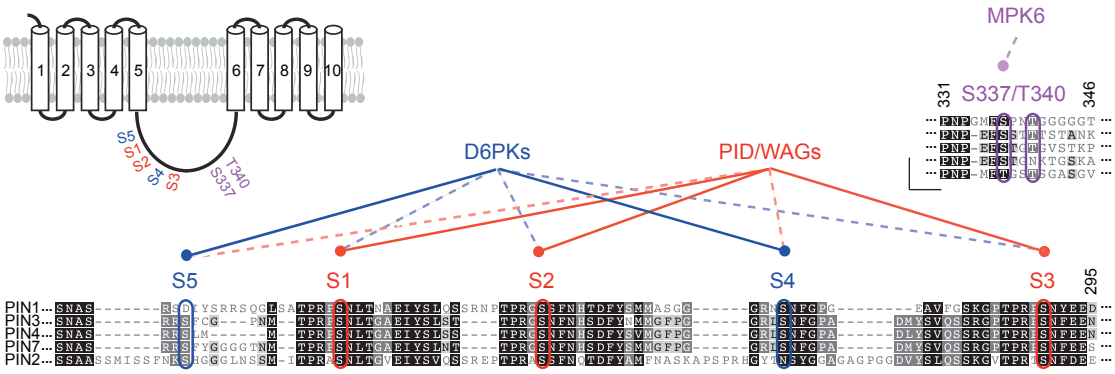

Figure 5: The cytoplasmic loop of plasma membrane-resident PINs harbors functionally important phosphorylation sites.

Predicted topology of PIN1 with 10 transmembrane domains separated by a large cytosolic loop and partial sequence alignment of this loop region from the plasma membrane-localized PINs, PIN1, 2, 3, 4 and 7. The relative positions of the phosphorylation sites discussed in this thesis are indicated and their conservation highlighted in the alignment. The phosphorylation site preference of kinases directly targeting the PIN cytoplasmic loop is depicted above the alignment. *In vitro*, PID/WAGs phosphorylate S1, S2 and S3 more efficiently comparred to S4, while the D6PKs show an inverse preference. Recently, MPK6 was shown to directly target S337.
Figure modified from Barbosa and Schwechheimer, 2014.

PIN polar targeting in *Arabidopsis* is speculative. Initial data suggested a role for PID either in regulating transcriptional auxin responses (Christensen et al., 2000) or as a positive regulator of auxin transport (Benjamins et al., 2001). The analysis of *pid* mutants nevertheless already hinted towards a functional interaction with PIN1, as they were isolated alongside *pin1* alleles in the same genetic screen for floral organ defective phenotypes (Bennett et al., 1995). Moreover, aside from the pin-shaped floral meristem similar to that of *pin1* mutants (Okada et al., 1991; Bennett et al., 1995), *pid* and *pin1* interact genetically during embryo axis and cotyledon formation (Furutani et al., 2004).

The current literature suggests that the *pid* mutant phenotypes are at least partly resulting from failure to correctly target PIN1 to the apical side of shoot epidermal cells. A mechanism was subsequently proposed by which PID mediates the apical targeting of PINs by phosphorylation of three serines (S1, S2 and S3) within a conserved TPRXS(N/S) motif in the PIN cytoplasmic loop (Fig. 5) (Dhonukshe et al., 2010; Huang et al., 2010). While the function of PID is not strictly required for apical

PIN targeting (Zhang et al., 2010), three main lines of evidence support a role for PID in this process:

Firstly, as mentioned, ectopic overexpression of PID in the root leads to mis-targeting of PINs towards the apical plasma membrane, while loss of *pid* function causes PIN1 to localize basally in shoot epidermal cells (Friml et al., 2004). Secondly, simultaneous mutations in PIN1 S1, S2 and S3 to non-phosphorylatable residues result in the same shift from apical to basal PIN1 polarity in shoot epidermal cells. Plants expressing this mutated transgene in a *pin1* mutant background partially phenocopy *pid* mutants. Mutating the same sites to residues mimicking constitutive phosphorylation has similar consequences as *PID* overexpression, in that this PIN1 variant localizes apically in roots (Huang et al., 2010). Thirdly, simultaneous mutation of *pid* and its closest homologues *wag1* and *wag2 (wavy growth1 and 2)* results in an agravitropic, short root phenotype, possibly due to a mislocalization of PIN2 in distal epidermal cells to the basal plasma membrane (Dhonukshe et al., 2010). The more complex *pid* quadruple mutant has, additionally, a fully penetrant no-cotyledon phenotype that correlates with a mislocalization of PIN1 in embryo epidermal cells (Cheng et al., 2008; Dhonukshe et al., 2010).

1.3.2 D6PK and PID activate PIN1 auxin efflux

While the effects on PIN polarity seem to be restricted to the function of PID, WAG1 and WAG2 (Dhonukshe et al., 2010), other kinases closely related to PID from the AGCVIII family have since been implicated in auxin transport-related processes. The blue light receptors phot1 and phot2 (phototropin 1 and 2), for example, activate the phototropic response [reviewed by (Liscum et al., 2014)], possibly in part through inhibition of PGP-mediated auxin transport by phot1 phosphorylation in the hypocotyl (Christie et al., 2011).

Another group of characterized AGCVIII kinases are the D6PKs (D6 PROTEIN KI-

NASEs), which have been strongly linked to activating the auxin efflux capacity of PINs (Zourelidou et al., 2009; Willige et al., 2013; Barbosa et al., 2014; Zourelidou et al., 2014). This is a second important regulatory element of PIN phosphorylation, which had already been attributed previously to PID activity (Lee and Cho, 2006). In stems and hypocotyls, chemically removing D6PK from the plasma membrane, as well as increasing *d6pk* mutant complexity, lead to decreased PIN phosphorylation and auxin transport (Zourelidou et al., 2009; Willige et al., 2013; Barbosa et al., 2014). Accordingly, complex *d6pk* mutants display auxin transport-related phenotypes, such as loss of photo- and gravitropism in hypocotyls, as well as defects in cotyledon and lateral root formation (Zourelidou et al., 2009; Willige et al., 2013). D6PK, as well as PID and at least WAG2, are able to activate PIN-mediated cellular auxin efflux in *Xenopus laevis* oocytes. In fact, the experiments in oocytes strongly suggested that PINs do not efficiently export auxin without a phosphorylating kinase added to the system. While PID/WAGs seemingly employ largely the same target serines (S1, S2 and S3) for activation and polarity regulation of PINs, D6PK preferentially targets an additional site, S4, which resides in the PIN cytoplasmic loop between S2 and S3 (Fig. 5). Phosphosite-mutant variants of PIN1 S4 are partially compromised in D6PK-mediated, but not PID-mediated activation of auxin efflux. Conversely, mutating PIN1 S1 - S3 affects activation by PID, but not D6PK. Importantly, however, mutations at all four serine residues are required to completely abolish PIN1 activation by both kinases, indicating that both are able to phosphorylate S1 - S4, albeit with different affinities (Fig. 5).

This target-site preference is also clearly present in *in vitro* phosphorylation experiments. Moreover, an *in vivo* analysis using selective reaction monitoring in inflorescence stems revealed that the relative amount of PIN1 S4 phosphorylation decreases with increasing *d6pk* mutant complexity, indicating that D6PK and its

closest homologues are the major contributors of PIN1 S4 phosphorylation at least in this tissue (Zourelidou et al., 2014).

An expanded search for phosphorylation target sites using the PIN3 sequence furthermore revealed an additional preferential target of D6PK on the PIN cytoplasmic loop, designated S5 (Fig. 5) (Zourelidou et al., 2014). D6PK-specificity for this site can, on the one hand, be detected in *in vitro* phosphorylation experiments. On the other, concomitant mutation of S4 and S5 to non-phosphorylatable alanine (A) residues in the PIN3 sequence strongly affects PIN3-mediated auxin efflux activation by D6PK, but not PID, in the oocyte system (Zourelidou et al., 2014). Therefore, differential regulation of PIN3 by D6PK and PID could be achieved by preferential phosphorylation of S4 and S5, or S1 - S3, respectively (Fig. 5).

While the closely related sequences of PIN3, 4 and 7 show strong conservation around S5, some algorythms align S5 to an aspartic acid (D) in the PIN1 sequence and thus a potentially phospho-mimicking residue (Fig. 5) (Barbosa and Schwechheimer, 2014). This has invited speculations that the phosphorylation target S5 arose evolutionarily, as an additional layer of D6PK-mediated activation of PIN3-driven auxin efflux, from an endogenous phosphomimic on PIN1. However, aside from *in vitro* phosphorylation by D6PK of a PIN1-derived peptide where the corresponding aspartic acid (D) residue is replaced by a serine at S5 (Zourelidou et al., 2014), no evidence exists to date that this residue is involved in the regulation of PIN1.

1.3.3 D6PK and PID are differentially regulated

Taken together, the phenotypic and biochemical data argue for a dual regulation of PIN polarity and activity by PID/WAG kinases through phosphorylation of the conserved target sites S1 - S3 and control of PIN activity through preferential phosphorylation at S4 and S5 by D6PK kinases in distinct but overlapping biological contexts. However, *in vitro* phosphorylation experiments, as well as the auxin transport exper-

iments in oocytes had suggested considerable promiscuity between D6PK and PID towards their respective preferential target sites on the PIN1 cytoplasmic loop (Fig. 5). At the onset of this thesis, it was therefore not resolved whether this differential phosphosite preference of the two kinases is sufficient to explain their divergent biological functions. Additionally, the biological connection between PID-mediated activation of PIN1 auxin efflux capacity and polarity control by use of the same target sites was not clear. At the cellular level, D6PK does not affect PIN polarity, neither in complex *d6pk* mutants, nor when strongly overexpressed (Zourelidou et al., 2009; Dhonukshe et al., 2010) (this thesis). D6PK and PID are also unable to complement their respective mutant phenotypes in promoter-swap experiments (Zourelidou et al., 2014), indicating that their biochemical similarities do not result in the same biological output. Other distinguishing factors, such as regulation of activity, interactors and cell biological properties exist between D6PK and PID that could result in their divergent functions.

PID, for example, has already been shown to interact with proteins other than PINs that could influence its activity or specificity (Benjamins, 2003). Furthermore, sequence divergence between D6PK and PID within an insertion domain that separates the highly conserved kinase domains suggests that the two kinase families might be differentially regulated. Recently, it was found that electrostatic interactions of a poly basic motif within this insertion domain are important for the affinity of both D6PK and PID to the highly negatively charged plasma membrane of plant cells (Barbosa et al., 2016; Simon et al., 2016). Particularly for D6PK, a biological relevance for this motif was shown (Barbosa et al., 2016). However, the consequences of these interactions on the intracellular distribution of the two kinases are clearly different.

In fact, intracellular trafficking and polar localization are perhaps the most notable

features that distinguish not only D6PK from PID, but also the two kinases from their PIN substrates (Fig. 6). Constitutive endocytic recycling, which is crucial for proper PIN polarity and function, also tightly regulates the activity of D6PK (Zourelidou et al., 2009; Barbosa et al., 2014). For PID, on the other hand, a regulatory function of this process is less clear. D6PK is itself polarly maintained at the basal plasma membrane and co-localizes there with basally targeted PINs (Zourelidou et al., 2009). D6PK, as well as PINs, constitutively recycle between the plasma membrane and internal compartments, but, as the highly differential kinetics suggest, do not share the same trafficking pathway (Barbosa et al., 2014). Inhibition of GN function by BFA leads to rapid and complete internalization of D6PK, while PINs respond relatively slowly and are never completely removed from the plasma membrane (Kleine-Vehn et al., 2009; Barbosa et al., 2014). The intracellular trafficking of PID on the other hand seems to be distinct from that of D6PK and possibly PINs. Importantly, PID is apolarly distributed at the plasma membrane (Kleine-Vehn et al., 2009; Dhonukshe et al., 2010) (this thesis) and this plasma membrane association does not seem to depend on GN function, as it is not affected by BFA treatment (Fig. 6) (Kleine-Vehn et al., 2009) (this thesis).

The differential intracellular trafficking of these three auxin transport components strongly suggests that interactions between D6PK or PID and PINs primarily occur at the plasma membrane, which had been hypothesized previously (Kleine-Vehn et al., 2009; Dhonukshe et al., 2010; Barbosa et al., 2014) (this thesis). This raises the question whether PIN1 polar localization and activity could be regulated by phosphorylation of essentially the same target sites on its cytoplasmic loop and to what extent phosphorylation at S1 - S4 differentially control these two processes. Additionally, the contribution to these phosphorylation events by differentially regulated kinases in different biological processes is still not clear.

1.4 Objectives of this thesis

The present study aimed to address the impact of specific phosphorylation events on the PIN1 cytoplasmic loop in terms of PIN1 polarity and auxin transport activity. Efficient PIN-mediated polar auxin transport in hypocotyls requires PIN phosphorylation at the plasma membrane (Willige et al., 2013; Barbosa et al., 2014). PIN1 phosphorylation at the conserved target sites S1 - S3 had previously been associ-

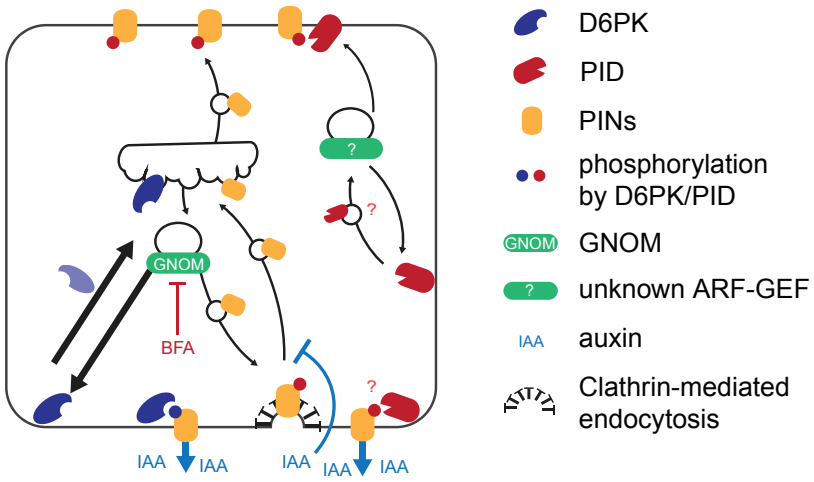

Figure 6: Intracellular trafficking of D6PK, PINs and PID via distinct pathways.

D6PK and PID phosphorylate and activate PINs at the plasma membrane. PID additionally influences PIN polar localization. PINs undergo clathrin-mediated endocytosis and are recycled back to the plasma membrane in a GNOM-dependent manner. Auxin may act as an inhibitor of endocytosis and thus PIN internalization. D6PK internalization is rapid and its recycling back to the plasma membrane also depends on functional GNOM. The molecular components mediating the intracellular trafficking of PID are unknown, however, GNOM is not among them.
Figure modified from Barbosa and Schwechheimer, 2014.

ated with the apical targeting of PIN1 and linked to the activity of PID and its close homologues (Kleine-Vehn et al., 2009; Dhonukshe et al., 2010; Huang et al., 2010). Auxin transport experiments in *Xenopus* oocytes from previous work of the group suggested that phosphorylation at S1 - S4 by D6PK or PID (and WAG2) jointly activate PIN1-mediated auxin efflux. In the same study, PIN1 S4 phosphorylation in inflorescence stems of *Arabidopsis* could be closely linked to D6PK activity at the plasma membrane and efficient auxin transport. PIN1 S4 phosphorylation was further examined in the root meristem by use of a PIN1 S4 phosphosite-specif-

ic antibody and shown to be dependent on BFA-sensitive kinases such as D6PK (Zourelidou et al., 2014). However, the differential contribution of phosphorylation at S1 - S4 to PIN1 activity and polarity *in planta* was unresolved.

In order to directly test the existing models on PIN1 polarity control by phosphorylation, and to assess whether cellular PIN1 phosphorylation patterns could predict its activity and thus hypothetical auxin streams at the tissue level, I examined PIN1 phosphorylation patterns *in situ* by whole mount immunohistochemistry. For this purpose, phosphosite-specific antibodies were generated that individually recognize the phosphorylated forms of PIN1 S1 to S4, respectively. The root apical meristem was chosen as the primary model system, due to its dynamic PIN polarities and accessibility to immunohistochemical techniques, to address whether specific phosphorylation events could be linked to polar PIN localization. I further made use of the DII-VENUS reporter, as well as root gravitropism as a proxy to correlate auxin accumulation and hypothetical auxin transport streams with PIN1 phosphorylation patterns at the tissue and organ levels. Finally, I explored whether dynamic PIN1 phosphorylation events at the plasma membrane could be correlated to the different trafficking behaviors of D6PK and PID family kinases, respectively, as well as the contribution of each of these kinase groups to phosphorylation of PIN1 in the root apical meristem.

2 Materials and methods

2.1 Materials

2.1.1 Biological material

All *Arabidopsis thaliana* lines used in this study are in the Columbia ecotype.

Table 1: Transgenic lines used in this study

Name	Construct / genetic background	Described in
PIN1-GFP	*PIN1p::PIN1-GFP*	Benkova et al., 2003
PIN1-YFP	*PIN1p::PIN1-YFP / pin1*(SALK_047613)	Zourelidou et al., 2014
PIN1-GFP2	*PIN2p::PIN1-GFP / pin2*	Wisniewska et al., 2006
PIN1-GFP3	*PIN2p::PIN1-GFP3 / pin2*	Wisniewska et al., 2006
PIN1-GFP S1A	*PIN1p::PIN1-GFP S1A / pin1*(SALK_047613)	Huang et al., 2010
PIN1-YFP S2A	*PIN1p::PIN1-YFP S2A / pin1*(SALK_047613)	This thesis
PIN1-YFP S3A	*PIN1p::PIN1-YFP S3A / pin1*(SALK_047613)	This thesis
PIN1-YFP S4A	*PIN1p::PIN1-YFP S4A / pin1*(SALK_047613)	Zourelidou et al., 2014
DII-VENUS	Col-0	Brunoud et al., 2012a
mDII-VENUS	Col-0	Brunoud et al., 2012a
XVE>>PID	*G10-90::XVE>>PID*	Dhonukshe et al., 2010
XVE>>PIN1	*G10-90::XVE>>PIN1*	Dhonukshe et al., 2010
$GNOM^{wt}$	*gnom (emb30-1)*	Geldner et al., 2003
$GNOM^{M696L}$	*gnom (emb30-1)*	Geldner et al., 2003
YFP-PID	*35S::YFP-PID*	This thesis
YFP-D6PK	*35S::YFP-D6PK*	Zourelidou et al., 2009
d6pk012	*d6pk d6pkl1 d6pkl2*	Zourelidou et al., 2009
pid/wag	*pid/PID pid2 wag1 wag2*	Haga et al., 2014
pid-1	*PIN1p::PIN1-GFP / pid-1*	Bennett et al., 1995

pid pid2 wag1 wag2 quadruple mutants were isolated from the progreny of *pid/PID pid2 wag1 wag2* based on the cotyledon formation-deficient phenotype specific for the quadruple mutant (Haga et al., 2014).

2.1.2 Primers

Table 2: Primers used for this study

Name	Purpose	Primer sequence (5' - 3'; phos, phosphorylation)
PIN1 S2A	Mutagenesis of S252 (S2) to A252 (S2A) in PIN1-YFP	phos-CCACGTGGCGCTAGTTTTAATCATAC

PIN1 S3A	Mutagenesis of S290 (S3) to A290 (S3A) in PIN1-YFP	phos-ACTCCGAGACCTGCCAACTACG
PIN1 S1E	Mutagenesis of S231 (S1) to E231 (S1E) in p002:PIN1	phos-ACACCTAGACCTGAAAATCTAAC
PIN1 S2E	Mutagenesis of S252 (S2) to E252 (S2E) in p002:PIN1	phos-GCCACGTGGCGAAAGTTTTAATCAT-AC
PIN1 S3E	Mutagenesis of S290 (S3) to E290 (S3E) in p002:PIN1	phos-ACTCCGAGACCTGAAAACTACG
PIN1 S4E	Mutagenesis of S271 (S4) to E271 (S4E) in p002:PIN1	phos-TGGTCGGAACGAAAACTTTGGTC
GW-PID-FW	Amplification and cloning of PID CDS in pGW-35S-MYC and pExtag-YFP-GW	GGGGACAAGTTTGTACAAAAAAGCAG-GCTTCATGTTACGAGAATCAGACGGT
GW-PID-RV1	Amplification and cloning of PID CDS in pGW-35S-MYC and pExtag-YFP-GW	GGGGACCACTTTGTACAAGAAAGCTGG-GTCTCAAAAGTAATCGAACGCCGCTG
pin1 LP	pin1 (SALK_047613) mutant genotyping: pin1 LP	CAAAAACACCCCCAAAATTTCTC
pin1 RP	pin1 (SALK_047613) mutant genotyping: pin1 RP	AATCATCACAGCCACTGATCC
LBb1.3	pin1 (SALK_047613) mutant genotyping: LBb1.3	ATTTTGCCGATTTCGGAAC
AGC1-5 FW	Amplification and cloning of AGC1-5	GGGGACAAGTTTGTACAAAAAAAGCAG-GTTAATGGACTTAGCTTCTAAGAAGAACAC
AGC1-5 RV	Amplification and cloning of AGC1-5	GGGGACCACTTTGTACAAGAAAGCTGGG-TACTAAAAGTACTCGAAATCTATATACGCC
KIPK FW	Amplification and cloning of KIPK	GGGGACAAGTTTGTACAAAAAAGCAG-GCTTAATGGGGTCGTTTGCAGG
KIPK RV	Amplification and cloning of KIPK	GGGGACCACTTTGTACAAGAAAGCTGGG-TATTAAAACAACTCGAACTCAAGATGATC
D6PKL3	Amplification and cloning of D6PKL3	GGGGACCACTTTGTACAAGAAAGCTGG-GTCCTGATAGTGAAAGAAATCACAAATCAG
D6PKL3	Amplification and cloning of D6PKL3	GGGGACAAGTTTGTACAAAAAAGCAG-GCTTAATGGATTCTTCTTCATCAGT

2.1.3 Peptides

Table 3: Peptides for immunization and purification of phosphosite-specific antibodies

Name	Amino acid sequence	Source
PIN1 S1(P)	N'-LSATPRP-S(P)-NLTNA-C'	Eurogentec, Liège, Belgium
PIN1 S2(P)	N'-RNPTPRG-S(P)-SFNHT-C'	Eurogentec, Liège, Belgium
PIN1 S3(P)	N'-GPTPRP-S(P)-NYEEDG-C'	Eurogentec, Liège, Belgium
PIN1 S4(P)	N'-SGGGRN-S(P)-NFGPGE-C'	Eurogentec, Liège, Belgium

Table 4: Additional peptides used in dot blot analysis

Name	Amino acid sequence	Source
PIN3/4/7 S1(P)	N'-NMTPRP-S(P)-NLTGAE-C'	Eurogentec, Liège, Belgium
PIN3/7 S4(P)	N'-FPGGRL-S(P)-NFGPAD-C'	Eurogentec, Liège, Belgium
PIN2 S1(P)	N'-SMITPRA-S(P)-NLTGV-C'	Eurogentec, Liège, Belgium

2.1.4 Antibodies

Table 5: Antibodies used in this study

Name	Dilution	Carrier	Source/described in
anti-GFP	1:3000	Rabbit	Life Technologies, Carlsbad, CA
anti-rabbit HRP	1:100,000	Goat	Sigma, Taufkirchen
anti-GFP	1:400	Mouse	Roche, Penzberg
anti-PIN1	1:1000	Rabbit	Geldner et al., 2001
anti-PIN1	1:400	Goat	Nottingham Arabidopsis Stock Centre, UK
anti-PIN1 S1-P	1:100	Rabbit	Eurogentec, Liège, Belgium/this thesis
anti-PIN1 S2-P	1:100	Rabbit	Eurogentec, Liège, Belgium/this thesis
anti-PIN1 S3-P	1:100	Rabbit	Eurogentec, Liège, Belgium/this thesis
anti-PIN1 S4-P	1:300	Rabbit	Eurogentec, Liège, Belgium/Zourelidou et al., 2014/this thesis
anti-mouse ALEXA488	1:500	n.a.	ThermoFisher, Ulm
anti-rabbit Cy3	1:500	Goat	Dianova, Hamburg
anti-goat FITC	1:100	Rabbit	Dianova, Hamburg

2.1.5 Chemicals

Table 6: Used chemicals

Name	Source
1,4-diazabicyclo[2.2.2]octane	Gift
2-(N-morpholino)ethanesulfonic acid (MES)	Applichem, Darmstadt
Acrylamide 4K-solution (30%) mixure 29:1	Applichem, Darmstadt
Agarose	Peqlab Biotechnologie, Erlangen
Amersham Hybond-ECL	GE Healthcare, München
BFA (Brefeldin A)	ThermoFisher, Ulm
Bio-Rad Protein Assay	Bio-Rad Laboratories, München
BSA (bovine serum albumin)	Applichem, Darmstadt
Calcium hypochloride	Roth, Karlsruhe
Cantharidin	Sigma-Aldrich, Taufkirchen
Deoxyribonucleoside triphosphate (dNTPs)	Fermentas, St. Leon-Rot
Dimethylsulfoxide (DMSO)	Roth, Karlsruhe
Disodium phosphate	Applichem, Darmstadt
Driselase	Sigma-Aldrich, Taufkirchen
Acetic acid	Roth, Karlsruhe
Estradiol	Sigma-Aldrich, Taufkirchen

Ethanol	Roth, Karlsruhe
Ethidium bromide	Roth, Karlsruhe
Ethylenediaminetetraacetic acid (EDTA)	Applichem, Darmstadt
GeneRuler 1kb DNA Ladder	Fermentas, St. Leon-Rot
Glucose	Applichem, Darmstadt
Glycerine	Applichem, Darmstadt
Isopropanol	Roth, Karlsruhe
Potassium chloride	Applichem, Darmstadt
Potassium dihydrogenphosphate	Applichem, Darmstadt
Potassium hydroxide	Applichem, Darmstadt
Skim milk powder	Applichem, Darmstadt
Magnesium chloride	Applichem, Darmstadt
Methanol	Roth, Karlsruhe
MG132	Enzo Life Sciences, Lörrach
Murashige & Skoog Medium & B5 Vitamins	Duchefa, Haarlem, Niederlande
Sodium chloride	Applichem, Darmstadt
Sodium dihydrogenphosphate	Merck, Darmstadt
Sodium hydroxide	Applichem, Darmstadt
Sodium dodecyl sulfate (SDS)	Applichem, Darmstadt
Nonidet P40	AppliChem, Darmstadt
PageRuler Plus Prestained Protein Ladder	Fermentas, St. Leon-Rot
Paraformaldehyde	Roth, Karlsruhe
Plant agar	Duchefa, Haarlem, Niederlande
Phenylmethylsulfonylfluoride (PMSF)	Sigma-Aldrich, Taufkirchen
PhosSTOP phosphatase inhibitor cocktail	Roche, Penzberg
Ponceau rouge (PR)	Sigma-Aldrich, Taufkirchen
Propidium iodide	Applichem, Darmstadt
Protease Inhibitor Cocktail	Sigma-Aldrich, Taufkirchen
PVDF membrane	Roth, Karlsruhe
Rotiphorese Gel (37,5:1)	Roth, Karlsruhe
Hydrochloric acid	Applichem, Darmstadt
Sucrose	Applichem, Darmstadt
Super Signal West Femto Max. Sens. Substrate	Thermo Fisher Sientific, Bonn
Tris(hydroxymethyl)aminomethane (Tris)	Applichem, Darmstadt
Triton X-100	Applichem, Darmstadt
Tween 20	Applichem, Darmstadt
β-Mercaptoethanol	Roth, Karlsruhe

2.1.6 Software

Table 7: Software applied in this study

Name	**Vertreiber**
MS Office	Microsoft, Unterschleißheim
ImageJ	NIH, Bethesda, USA

Fluoview	Olympus, Hamburg
Photoshop	Adobe Systems, Dublin, Republic of Ireland
Illustrator	Adobe Systems, Dublin, Republic of Ireland
InDesign	Adobe Systems, Dublin, Republic of Ireland

2.2 Methods

2.2.1 Molecular cloning

The following constructs and corresponding transgenic lines were kindly generated by Melina Zourelidou:

PIN1p::PIN1-YFP (PIN1-YFP) is a previously described plant transformation construct for the expression of a functional YFP-tagged PIN1 under control of the *PIN1* promoter fragment (Zourelidou et al., 2014). Mutagenesis of the PIN1 S2 and S3 phosphosites to alanine (A) yielded PIN1-YFP S2A and S3A, which were introduced in PIN1-YFP as previously described for PIN1-YFP S4A (Zourelidou et al., 2014). The constructs were transformed into heterozygous *PIN1/pin1* (SALK_047613) plants by Agrobacterium-mediated transformation (Clough and Bent, 1998) and *pin1* homozygous lines carrying the PIN1-YFP transgenes were isolated from the progeny and used for immunostaining.

The *PID* overexpression construct (*35S::PID*) was obtained by PCR amplification of the *PID* coding sequence with primers PID-GW-FW and PID-GW-RV. The resulting fragment was inserted into pDONR201 (LifeTechnologies, Carlsbad, CA) and from there into pGW-35S-MYC (a gift from Jane Parker, Cologne, Germany). A stop codon in PID-GW-RV prevents the in-frame fusion with the C-terminal MYC-tag of this vector. *35S::PID* was introduced in the Col-0 wild type background using the floral dip method (Clough and Bent, 1998).

A construct for the expression of YFP-tagged PID (YFP-PID) in *Arabidopsis* was obtained by PCR amplification of the *PID* coding sequence, insertion of the PCR

fragment into pDONR201 followed by the transfer into pExtag-YFP-GW (a gift from Jane Parker, Cologne, Germany). The transgenic construct was introduced into the Col-0 wild type using the floral dip method (Clough and Bent, 1998).

For auxin transport assays in *Xenopuslaevis* oocytes performed by Astrid Fastner and Ulrich Hammes, PIN1 S (serine) phosphosites were mutagenized by Melina Zourelidou in p002:PIN1 to potentially phosphorylation-mimicking E (glutamic acid) through several rounds of PCR mutagenesis (Zourelidou et al., 2014) with primers PIN1 S1E, PIN1 S2E, PIN1 S3E and PIN1 S4E.

For *in vitro* phosphorylation experiments, Lena Frank amplified cDNAs of the AGV-VIII protein kinases D6PKL3, AGC1-5 and KIPK using forward and reverse primers for the respective gene and transferred the amplification products via pDONR201 into pDEST15 using the Gateway cloning system (Invitrogen, Carlsbad, CA).

Expression constructs for D6PK, PID and PIN1 (cytoplasmic loop) were previously described (Zourelidou et al., 2014).

2.2.2 Genotyping of plant genomic DNA

Genomic DNA from *Arabidopsis* was extracted from ca. 300 µg of plant material frozen in liquid nitrogen. The ground material was taken up in 300 µL extraction buffer (250 mM NaCl, 200 mM Tris/HCl [pH 7,5], 25 mM EDTA [pH 8] and 0,5% SDS), left to incubate at room temperature for 10 min and centrifuged. 300 µL of the supernatant were added to 300 µL isopropanol for precipitation of DNA. After another centrifugation, the pellet was washed in 70% ethanol, dried and subsequently taken up in 100 µL sterile water.

For genotyping of *Arabidopsis* mutants via PCR, 20 µL reactions containing 11 µl H_2O, 4 µl genomic DNA, 2 µl polymerase buffer (200 mM Tris/HCl [pH 8,4], 500 mM KCl and 25 mM MgCl2), 2 µl dNTPs (2,5 mM dATP, dCTP, dGTP and dTTP, each), 1 µl primer [10 µM], each and 0,2 µl Taq-Polymerase (produced in the laboratory)

were subjected to the following thermal cycles: 5 min at 98°C, followed by 32 cycles of step 1: 95°C for 30 sec, step 2: 60°C for 25 sec, step 3: 72°C for 1 - 2 min and finally 5 min at 72°C. 2 µL of 6x loading buffer were then added to 10 µL of the finished reactions and loaded onto agarose gels containing ethidium bromide for analysis.

2.2.3 Plant growth conditions

Arabidopsis seeds were incubated in saturated calcium hypocloride for 20 min and subsequently washed five times in sterile water. Stratification of seeds was done at 4°C for two to three days.

For whole mount immunostaining of primary root meristems, as well as immunoblotting of root extracts, seedlings were grown at 21°C in continuous light (120 µmol m^{-2} s^{-1}) on standard growth medium (4.2 g/l Murashige and Skoog salts, 1% sucrose, 0.5 g/l 2-[N-morpholino-]ethanesulfonic acid, 5.5 g/l agar, pH 5.8) for 4 - 5 days on vertically placed, agar-containing plates.

For *pid1* immunostainings, plants were cultivated under sterile conditions on standard growth medium without sucrose for three weeks in continuous light and undifferentiated shoot apical meristems were dissected.

For live imaging of DII-VENUS, seedlings were grown on standard growth medium without sucrose in continuous light at 18°C for 4 days.

2.2.4 Physiological experiments

For gravitropic root growth assays, four day-old seedlings, grown vertically on standard growth medium without sucrose, were transferred to plates containing 10 µM BFA or the equivalent amount of solvent (DMSO) and the position of the root tip was marked. Plates were then transferred to the dark, kept in a vertical orientation and scanned after 18 hrs to determine root angles, root elongation as well as the

distance between the point of transfer and the final position of the root tip using Fiji (ImageJ). Root angles were assessed by measuring the angle between the initial and final positions of the root tip. The root curling index was calculated as the ratio between the direct distance of the root tip before and after transfer and root elongation over the duration of the experiment (18 hrs). For the relative root growth on BFA, root elongation for each genotype and treatment was ranked according to size and the ratio between BFA and solvent grown seedlings was compared for each genotype.

2.2.5 Histological methods

Where applicable, seedlings were treated in liquid growth medium supplemented with 50 µM BFA, 25 µM Cantharidin, 10 µM ß-Estradiol or a DMSO mock solvent control. Seedlings were fixed for 1 hr at room temperature under vacuum in 4% paraformaldehyde in PBS at pH 7.4. Samples were subsequently transferred to a liquid handling robot. Cell walls were partially digested for 30 min at 37°C with 2% (w/v) Driselase. Plasma membranes were permeabilized for 1 hr at room temperature with 3% Nonidet P40 in 10% DMSO/PBS. The samples were blocked for 1 hr at room temperature with 4% BSA in PBS. Primary and secondary antibodies were diluted in blocking solution and incubated for 4 hrs at 37°C. All steps were separated by 3 - 6 washes with 0.1% Triton X-100 in PBS (Sauer and Friml, 2010).

Dissected *pid1* shoot apical meristems were immunostained as described above with minor modifications: fixation was performed for 3 hrs, cell wall digestion was extended to 60 min, antibody incubation times were extended to 6 hrs for the primary antibodies and 6 hrs for the secondary antibodies. Samples were mounted in mounting solution (90% glycerol, 10% PBS, 25 mg/ml 1,4-diazabicyclo[2.2.2]octane, pH 9.0) for imaging.

For comparison of root apical meristem size, 4 day-old seedling roots were incubat-

ed in a 1:1000 dilution of 10 mg/ml stock solution of propidium iodide and directly mounted for imaging.

2.2.6 Microscopy and signal quantification

Confocal microscopy images were acquired with an Olympus BX61 microscope equipped with a FV1000 confocal laser scanning unit (Olympus, Hamburg). Images were processed only for brightness and contrast adjustments using Adobe Photoshop software.

PIN1 distribution and PIN1 polarity were determined using lateral signal distribution as a secondary parameter or obvious cell morphologies.

All quantitative fluorescence intensity measurements were performed in Fiji (ImageJ). Plasma membrane signal intensities were measured by drawing a line across the plasma membrane of individual cells. An additional line for every root was drawn outside the PIN1 expression domain and used for background correction. Overall root stele signal intensities were measured by drawing a box as shown in the image of the respective figure. An additional box outside the PIN1 expression domain was also measured and used as background correction for each root. For statistical evaluation, one-way ANOVA or Student's t-test were performed in Microsoft Excel and post-hoc Tukey HSD analysis using an online calculator (http://statistica.mooo.com).

2.2.7 Biochemical methods

For dot blot analysis, 20 µg of each peptide used for immunization or its non-phosphorylated counterpart were spotted onto PVDF membranes. Membranes were then blocked with PBS/2% BSA and incubated with primary antibody in blocking solution. After washing the membranes three times in PBS, they were incubated with an HRP-conjugated secondary antibody and washed again. The membranes

were then incubated in Super Signal West Femto substrate and the signal detected using a Luminescent Image Analyzer LAS-4000 mini series (Fujifilm).

For anti-GFP immunoblots, five days-old seedlings were treated in liquid growth medium supplemented with 50 µM BFA or a DMSO mock solvent control. Total protein extracts were prepared from roots in extraction buffer (50 mM Tris-HCl, pH 7.5, 150 mM NaCl, 0.5% Triton X-100, 0.1 mM MG132, 1 mM PMSF, protease inhibitor cocktail and PhosSTOP phosphatase inhibitor cocktail). Total protein content was measured with Bradford reagent and 10 µg protein were resuspended in 5x Laemli buffer and heated to 45°C for 15 min prior to loading onto 10% acrylamide gels. Proteins were then transferred to nitrocellulose membranes via semi-dry blotting. Membranes were then blocked in PBS/5% skim milk and subsequently left to incubate over night at 4°C in primary antibody diluted in blocking solution. After washing the membranes in PBS/0.5% tween 20 three times for 10 min, they were incubated in secondary antibody diluted in blocking solution and washed again. The membranes were then incubated in Super Signal West Femto substrate and the signal detected using a Luminescent Image Analyzer LAS-4000 mini series. Membranes were stained with Ponceau rouge to control for equal loading and transfer. Signal quantification was performed using Fiji (ImageJ) by drawing a box around the main band as well as the phosphorylation smear.

3 Results

3.1 Phosphosite-specific antibodies detect PIN1 phosphorylation *in situ*

Directed auxin transport is relevant for many growth and developmental processes in *Arabidopsis* and highly correlated to the efflux activity and polarity of PINs (Wiśniewska et al., 2006; Zhang et al., 2010; Ding et al., 2011; Rakusova et al., 2011). We could previously show that phosphorylation of PINs is a prerequisite for their capacity to efficiently transport auxin (Willige et al., 2013; Barbosa et al., 2014; Zourelidou et al., 2014). Phosphosite mutant analysis, as well as *in vitro* phosphorylation experiments suggested that four target serines within the PIN1 cytoplasmic loop, designated PIN1 S1 - S4, are the principal contributors to this activation. Furthermore, two kinases, D6PK and PID (likely together with their respective close homologues), were shown to target these sites with differential preference (Fig. 5) (Zourelidou et al., 2014). PIN1 S1 - S3 phosphorylation had already been correlated to PID activity and was proposed to direct apical PIN targeting (Kleine-Vehn et al., 2009; Dhonukshe et al., 2010; Huang et al., 2010). Our previous work identified PIN1 S4 as a preferential target of D6PK and showed that it contributed to PIN1-mediated auxin transport activity. Importantly, however, we proposed that this activation involves all four phosphosites (PIN1 S1 - S4) and can occur through PID and WAG2, as well as D6PK (Zourelidou et al., 2014). This raised the question how largely the same target sites on PIN1 could be used both as polarity determinants and to signal activation.

I therefore sought to examine PIN1 at the level of individual residue phosphorylation with sub-cellular resolution. To this end, I tested purified antibodies provided by a commercial distributer (Eurogentec, Lüttich, Belgium) raised against four distinct

phosphorylated peptides around the target sites S1 - S4 from the PIN1 cytoplasmic loop (Table 3). The distributer's protocol, following immunization of rabbits with the respective antigens, included purification of sera for enrichment of phospho-epitope specific antibodies. This was accomplished by running the sera first through a column containing the phosphorylated peptide on the matrix, thus binding specific, as well as non-specific antibodies. The eluate was subjected to a second column containing the respective non-phosphorylated peptide, which captured antibodies not specific for the phosphorylation. The flow through of this column in turn contained antibodies highly enriched for recognition of the phosphorylated epitope and I utilized this flow through (designated a-PIN1 S1-P to a-PIN1 S4-P) directly in whole mount immunohistochemical assays.

In order to assess the specificity of the individual antibodies, I immunoblotted each antibody against the phosphorylated peptides, as well as their respective unphosphorylated counterparts. Corresponding peptides covering the respective residues from other closely related PINs were included to detect potential cross-reactions. This analysis showed that all four antibodies recognized their respective phospho-epitopes with high affinity, although minimal cross reactivity was detected between a-PIN1 S4-P and the phosphorylated peptide from PIN3 and PIN7 corresponding to this site (Fig. 7A).

I further wanted to confirm the *in planta* specificity in immunohistochemical assays. For this purpose, Melina Zourelidou generated plants expressing PIN1-YFP*,* as well as PIN1-YFP carrying the single, non-phosphorylatable amino acid substitutions S2A, S3A and S4A, respectively, in the *pin1* mutant background. Additionally, plants expressing PIN1-GFP or PIN1-GFP S1A (*pin1*-/-) that were included in this analysis have previously been described (Huang et al., 2010). I confirmed the presence of a homozygous T-DNA insertion disrupting the *pin1* gene by PCR (Fig. 7B) and select-

ed the appropriate lines for my analysis.

In roots stele cells, immunohistochemical analysis revealed a signal corresponding to PIN1 phosphorylation at the plasma membrane at all four serines, co-localizing with the signal from an a-GFP antibody that was able to detect all respective PIN1 transgenes. However, in the case of a-PIN1 S1-P, S2-P and S4-P, this signal was

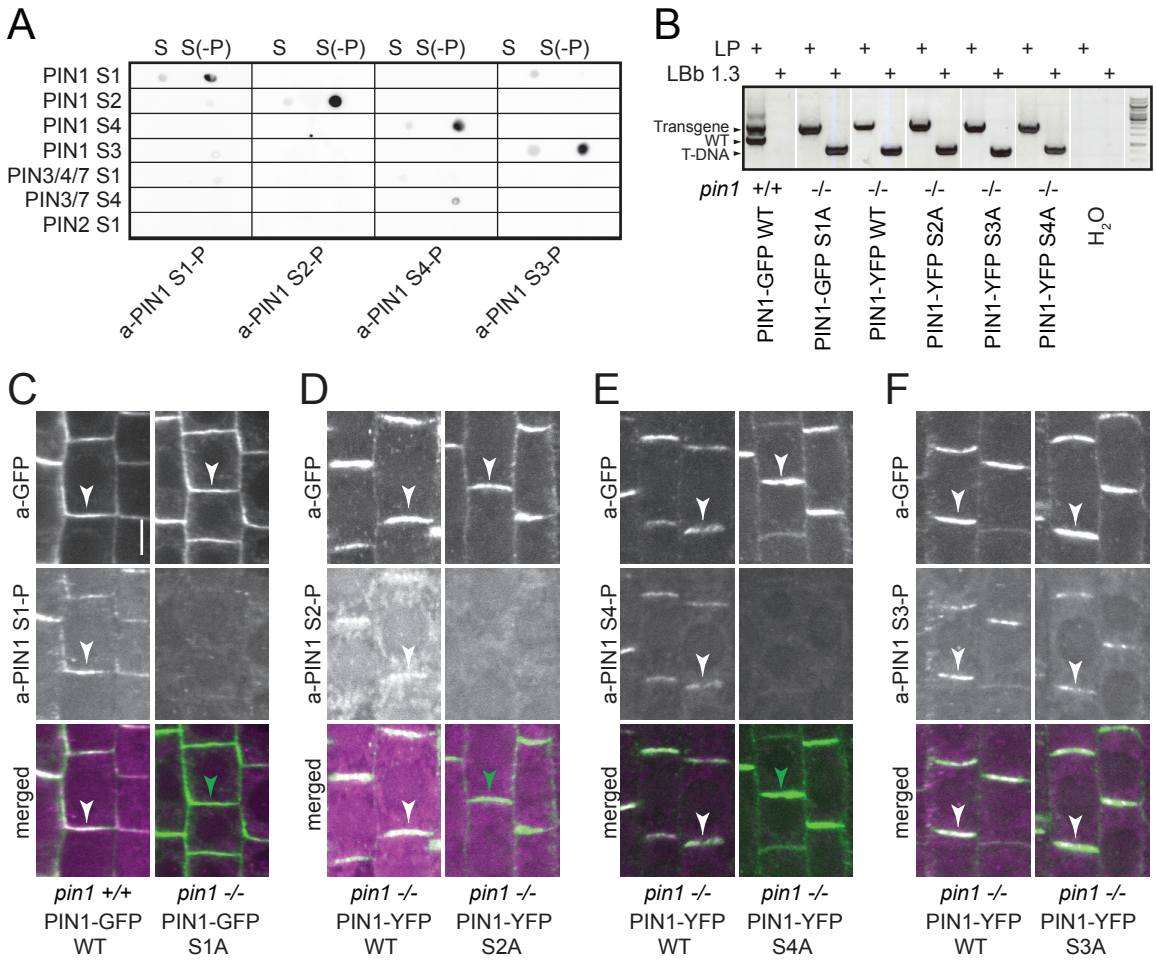

Figure 7: Three phosphorylation site-specific antibodies show high affinity for their respective phospho-epitopes *in vitro* and *in planta*.

(A) Dot blot immunoblot against unphosphorylated (S) and phosphorylated peptides S(-P) probed with anti-PIN1 S1-P through S4-P antibodies. (B) PCR analysis for the *pin1* (-/-) insertional mutation from genomic DNA of wild type *Arabidopsis* plants or *pin1* mutants transformed with PIN1-GFP or PIN1-YFP transgenes with alanine replacement mutations of S1 - S4. All reactions contain the reverse primer pin1 RP and the specified forward . (C - F) Representative confocal images of stele cells of the primary root after immunostaining of four days-old seedlings from plants as described in B stained with anti-GFP (a-GFP, PIN1-GFP) (green) and a-PIN1 S1-P (magenta) (C), a-PIN1 S2-P (magenta) (D), a-PIN1 S4-P (magenta) (E), or a-PIN1 S3-P (magenta) (F) antibodies. Overlap of green and magenta signals is indicated by white arrowheads in the merged images. Green arrowheads indicate the absence of a corresponding magenta signal from phosphosite-specific antibody staining. Scale bar = 5 µm.

lost when the respective target residue was rendered unphosphorylatable by mutation to A (Fig. 7C, D and E). Only a-PIN1 S3-P gave a signal in plants expressing a PIN1-YFP S3A construct (Fig. 7F). I judged that this signal could be produced by a cross reaction of a-PIN1 S3-P with the highly sequence-related epitopes at PIN1 S1 and/or S2, or with the corresponding epitope of related PIN proteins, which also share high sequence similarity (Fig. 5). Together, these results suggested that at least three antibodies, a-PIN1 S1-P, a-PIN1 S2-P and a-PIN1 S4-P, were site-specific towards the respective phosphorylated epitope in the PIN1 cytoplasmic loop.

3.2 PIN1 S1 - S4 phosphorylation in the root stele

3.2.1 PIN1 S1 - S4 phosphorylation at the basal plasma membrane is BFA-sensitive

PIN1, as well as D6PK, predominantly localize to the basal plasma membrane in stele cells of the root apical meristem (Galweiler et al., 1998; Zourelidou et al., 2009; Barbosa et al., 2014). While the polarity of PIN1 is not strictly maintained across all cell types of the stele, it is particularly discernible in the endodermal cell file by the baso-lateral pool of PIN1 at the inward facing plasma membrane. The signal obtained from the phosphosite-specific antibodies in PIN1-GFP transgenic lines prompted me to conduct a more directed approach to investigate the polarity and dynamics of PIN1 phosphorylation in these cells. Immunlocalization of PIN1-GFP expressing plants confirmed a signal at the basal plasma membrane for all four phosphosite antibodies, co-localizing there with the a-GFP PIN1 stained fusion protein in endodermal cells (Fig. 8).

We could previously show that PIN1 S4 phosphorylation at the plasma membrane of cells of the root apical meristem was highly sensitive to the endosomal trafficking inhibitor BFA (Zourelidou et al., 2014). We had judged that this site is preferential-

ly targeted by BFA-sensitive kinases such as D6PK. Both D6PK, as well as PIN1 constantly cycle between the plasma membrane and endosomal compartments (Geldner et al., 2001; Zourelidou et al., 2009; Barbosa et al., 2014); however, their trafficking kinetics are rather distinct. While the intracellular pool of D6PK is completely depleted from the plasma membrane within 10 minutes of BFA application (Barbosa et al., 2014), a fraction of the PIN pool remains persistently located to the cell periphery, even after prolonged treatments, but loses its basal polarity over time (Kleine-Vehn et al., 2008c).

The rapid disappearance of a phosphorylation signal at PIN1 S4 after BFA treatment could thus reflect the requirement for the presence of highly BFA-sensitive kinases at the plasma membrane. Since a signal was observed at the basal plasma membrane for all four phosphosites, I asked whether the remaining sites S1 - S3 were similarly BFA-sensitive. Indeed, PIN1 phosphorylation was strongly reduced, if not lost, following a 10 minute BFA treatment at all four phosphosites, while intracellular distribution of the a-GFP stained PIN1-GFP pool was unaffected (Fig. 8). Even though the signal obtained with a-PIN1 S3-P was not lost in transgenic *pin1* plants expressing PIN1-YFP S3A (Fig. 7F), this signal was still responsive to BFA treatments (Fig. 8D). I therefore concluded that this antibody is likely specific for phosphorylated epitopes, but might not exclusively recognize phosphorylated PIN1 S3.

PIN1 S1-S3 phosphorylation had previously been proposed to direct the apical targeting of PIN1 (Kleine-Vehn et al., 2009; Dhonukshe et al., 2010; Huang et al., 2010). My observation that these sites are phosphorylated at the basal plasma membrane in root stele cells is obviously in conflict with this hypothesis. Alternatively, my observed phosphorylation signals could constitute baseline levels of phosphorylation and hyperphosphorylation of these sites might be required to drive the apical targeting of PIN1. Another possibility is that they serve as an endosomal sorting signal

inside the cell. PIN1 polarity changes have been proposed to involve transcytosis from a BFA-sensitive basal trafficking pathway to a BFA-insensitive apical one. Fur-

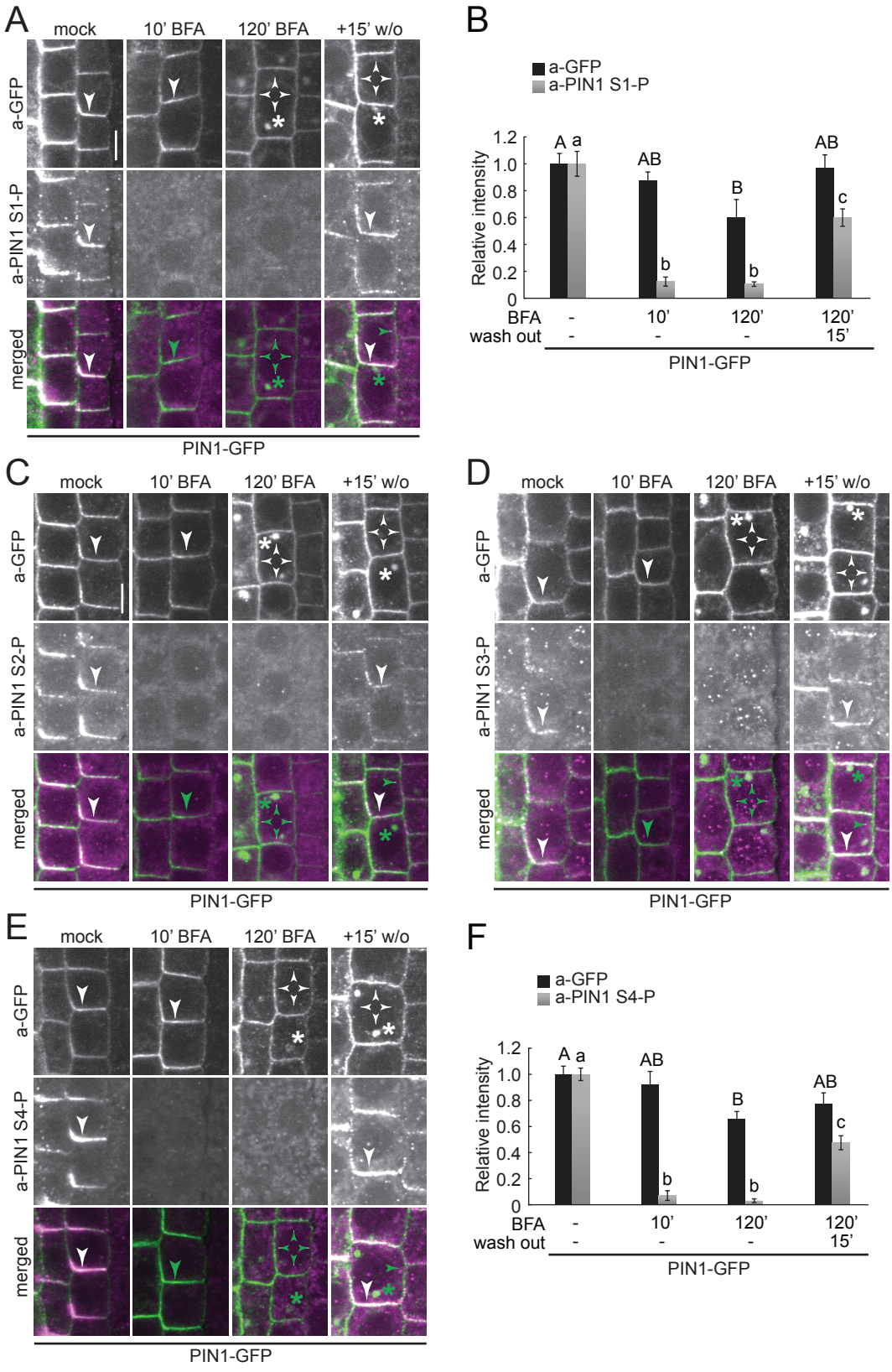

thermore, S1 - S3 phosphorylation was suggested to signal entry into the latter pathway for apical targeting of PIN1 (Kleine-Vehn et al., 2008c; Kleine-Vehn et al., 2009). The phosphosite-specific antibodies established here allowed me, in turn, to directly monitor the PIN1 phosphorylation status during changes in PIN1 polarity.

Prolonged BFA treatments lead to depolarization of basal PIN1 and its accumulation in BFA compartments (Geldner et al., 2001; Kleine-Vehn et al., 2008c). Under these conditions, I could not detect PIN1 S1 - S4 phosphorylation at the plasma membrane or in internal compartments. However, a 15 minute washout following 120 minutes of BFA treatment was sufficient to again detect PIN1 S1 - S4 phosphorylation at the basal plasma membrane (Fig. 8). The observed PIN1 phosphorylation patterns correlated well with the intracellular trafficking behavior of D6PK under the same experimental conditions, specifically with regard to its rapid and persistent internalization upon BFA application (Fig. 9), as well as its fast recycling dynamics at the basal plasma membrane (Barbosa et al., 2014).

In my hands, occasional accumulation of the bulk of the PIN1 pool at the lateral and apical sides of the cell only occurred after extended BFA treatments of 18 hours (Fig. 10). This is in disagreement with published data, where this apicalization is reported to occur faster (Kleine-Vehn et al., 2009). I nevertheless ascertained the

---

☜**Figure 8: PIN1 S1-S4 phosphorylation is BFA-sensitive.**

(A and C - E) Representative confocal images of primary root stele cells after immunostaining of four days-old PIN1-GFP seedlings with anti-GFP (a-GFP; PIN1-GFP) (green) and a-PIN1 S1-P (magenta) (A), a-PIN1 S2-P (magenta) (C), a-PIN1 S3-P (magenta) (D), or a-PIN1 S4-P (magenta) (E) antibodies. Seedlings were mock-treated or BFA [50 µM] -treated for 10 and 120 min, respectively. A 15 min w/o (wash out) followed the 120 min BFA treatment. Arrowheads mark strong and weak plasma membrane staining, asterisks mark intracellular BFA compartments. Overlap of green and magenta signals is indicated by white arrowheads in the merged images. Green arrowheads and asterisks indicate the absence of a corresponding magenta signal from phospho-specific antibodies. Scale bar = 5 µm. (B and F) Quantification of fluorescence intensity at the basal plasma membrane after immunostaining as shown in A and E. Data represents the average from two independent experiments (n = 50 cells). One way ANOVA and Tukey HSD datasets with no statistical difference fall in one group and were labeled accordingly. Upper and lower case letters serve to distinguish the results obtained with a-GFP and a-PIN1 S1-P or a-PIN1 S4-P, respectively. a-PIN1 S1-P and a-PIN1 S4-P signals were quantified, since these antibodies were chosen as representative for PID-specific and D6PK-specific target sites in subsequent experiments.

phosphorylation status of PIN1 at S1 and S4 in cases where, in my conditions, the a-GFP localized PIN1-GFP protein was enriched at the apical plasma membrane. A signal for both a-PIN1 S1-P and a-PIN1 S4-P, co-localizing with apical PIN1-GFP was observed occasionally. A mock treatment of the same duration in liquid medium had no impact on PIN1 phosphorylation or polarity (Fig. 10).

The phosphorylation patterns described above for the target sites S1 - S4 were observed throughout the entire root apical meristem (Fig. 11A - D). We and others have previously established that the overall phosphorylation state of PIN1 can be monitored on immunoblots using cell extracts of PIN1-GFP expressing plants or protoplasts (Michniewicz et al., 2007b; Barbosa et al., 2014; Zourelidou et al., 2014). There, the level of PIN1 phosphorylation correlates with distinguishable low

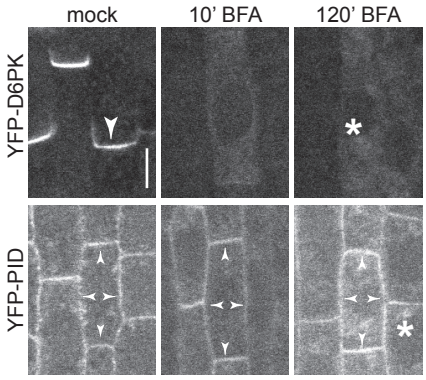

Figure 9: D6PK and PID differ in intracellular localization and trafficking in root stele cells.

Representative confocal images of stele cells of the primary root from four days-old YFP-D6PK and YFP-PID *Arabidopsis* seedlings after mock or BFA treatments as employed for the experiments shown in Fig. 8, followed by immunostaining with anti-GFP (a-GFP; YFP-D6PK or YFP-PID, respectively). Arrowheads mark strong and weak plasma membrane staining at the basal plasma membrane, asterisks mark intracellular compartments. Scale bar = 5 µm.

mobility, phosphatase-sensitive bands. I therefore asked whether the dynamics observed using the immunohisochemical approach for the sites S1 - S4 was applicable to the overall PIN1 phosphorylation state. Indeed, a-GFP immunoblots of whole root cell extracts of PIN1-GFP expressing plants under the same experimental conditions detected a phosphorylation pattern that reflected well those obtained with the phosphosite-specific antibodies, particularly prolonged dephosphorylation and rapid re-phosphorylation of PIN1 upon BFA treatment and subsequent washout, respectively (Fig. 11E and F). The BFA-sensitivity of PIN1 phosphorylation in the

root is thus likely not limited to the target sites S1 - S4 but a general feature of PIN1 phosphorylation in this tissue.

Taken together, these results suggested that the presence of BFA-sensitive kinases at the basal plasma membrane favors the phosphorylated state of PIN1 in cells of the root apical meristem. Long term interference with the BFA-sensitive basal targeting pathway could yet allow for BFA-insensitive kinases to counterbalance the loss of PIN1 phosphorylation at various sides of the plasma membrane. Importantly however, a phosphorylation signal was observed at the basal plasma membrane with high reproducibility, indicating that this is the predominant site of PIN1 S1 - S4 phosphorylation in the root.

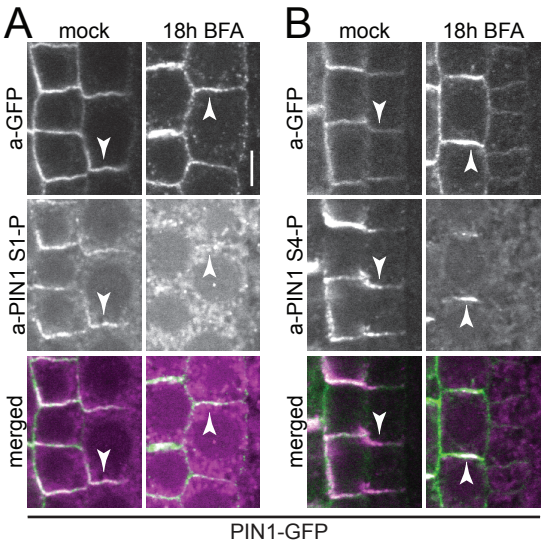

Figure 10: Effects of long-term BFA treatment on PIN1 polarity and phosphorylation.

(A and B) Representative confocal images of stele cells of the primary root from four days-old PIN1-GFP *Arabidopsis* seedlings after 18 hours mock or BFA [50] treatments followed by immunostaining with anti-GFP (a-GFP; PIN1-GFP) (green) and a-PIN1 S1-P (magenta) (A), or a-PIN1 S4-P (magenta) (B) antibodies. Arrowheads mark plasma membrane staining. Overlap of green and magenta signals is indicated by white arrowheads in the merged images. Scale bar = 5 µm.

Since the phosphosite-specific antibodies showed comparable behavior to this point in all experimental conditions, I chose a-PIN1 S1-P and a-PIN1 S4-P as representative phosphosites for further investigation.

3.2.2 PIN1 phosphorylation is GNOM-dependent

Basal plasma membrane localization of PIN1, as well as D6PK, requires functional activity of the ARF-GEF GN (Geldner et al., 2003; Barbosa et al., 2014), which controls the recycling of endosomal cargo to the plasma membrane. The fungal toxin

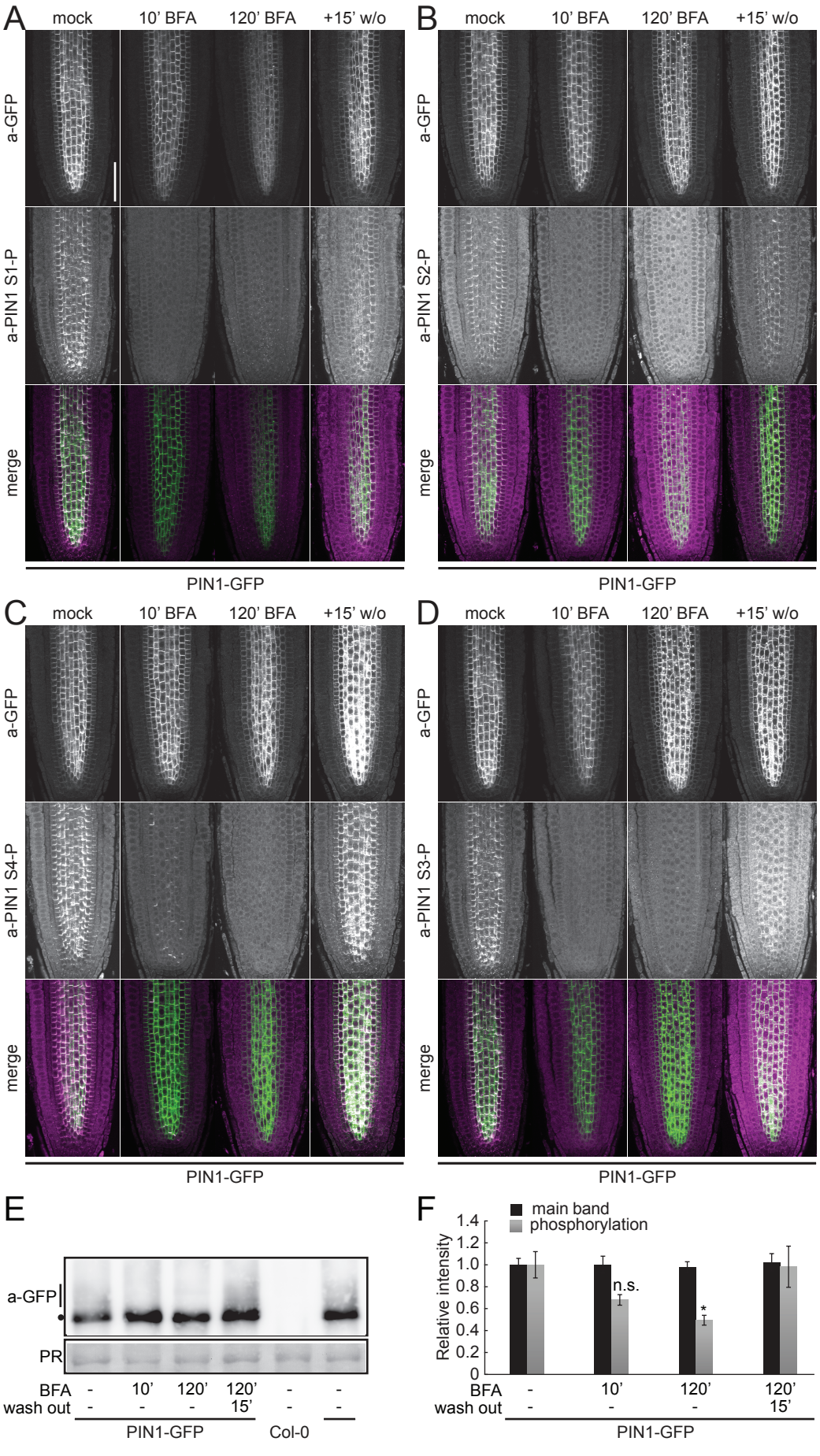
A
mock
10' BFA
120' BFA
+15' w/o
a-GFP
a-PIN1 S1-P
merge
PIN1-GFP
B
mock
10' BFA
120' BFA
+15' w/o
a-GFP
a-PIN1 S2-P
merge
PIN1-GFP
C
mock
10' BFA
120' BFA
+15' w/o
a-GFP
a-PIN1 S4-P
merge
PIN1-GFP
D
mock
10' BFA
120' BFA
+15' w/o
a-GFP
a-PIN1 S3-P
merge
PIN1-GFP
E
a-GFP
PR
BFA - 10' 120' 120' - -
wash out - - - 15' - -
PIN1-GFP
Col-0
F
main band
phosphorylation
Relative intensity
1.4
1.2
1.0
0.8
0.6
0.4
0.2
0
n.s.
*
BFA - 10' 120' 120'
wash out - - - 15'
PIN1-GFP

BFA inhibits GN function and its application to *Arabidopsis* roots leads to rapid and complete internalization of D6PK, as well as dephosphorylation of PINs at the plasma membrane (Fig. 8 - 11).

To test whether this rapid PIN1 dephosphorylation upon BFA treatment is dependent on proper GN activity, I made use of transgenic lines harboring a BFA-insensitive but functional GN variant. This construct contains a single amino acid substitution at position 696 from M (methionine) to L (leucine) (GN^{M696L}) that leads to steric hindrance in the docking site of the BFA molecule (Geldner et al., 2003). Plants carrying this construct are thus resistant to BFA treatments in terms of PIN1 (Geldner et al., 2003), as well as D6PK plasma membrane recycling (Barbosa et al., 2014).

When I immunlocalized endogenous PIN1 S1 and S4 phosphorylation using a-PIN1 S1-P and a-PIN1 S4-P in GN^{M696L} plants, the signal persisted at the plasma membrane even after 30 min BFA treatments. On the other hand, the same conditions applied to plants carrying a BFA-sensitive wild type version of GN (GN^{wt}) led to the expected loss of phosphorylation of PIN1 at S1 and S4 (Fig. 12). These results indicated that the phosphorylation of PIN1 at the plasma membrane is mediated by BFA-sensitive kinases and that the dynamics of these phosphorylations require GN-mediated intracellular trafficking.

☞ **Figure 11: PIN1 phosphorylation is BFA-sensitive throughout the *Arabidopsis* root.**
(A - D) Representative confocal images of primary roots from four days-old PIN1-GFP *Arabidopsis* seedlings after treatmets as described for Fig. 8, followed by immunostaining with anti-GFP (a-GFP; PIN1-GFP) (green) and a-PIN1 S1-P (magenta) (A), a-PIN1 S2-P (magenta) (B), a-PIN1 S4-P (magenta) (C), or a-PIN1 S3-P (magenta) (D) antibodies. White signal in merged images indicates overlap of green and magenta signals. Scale bar = 50 µm. (E) Anti-GFP (a-GFP; PIN1-GFP) immunoblot against 10µg total protein extract from five days-old PIN-GFP and wild type (Col-0) seedling roots. PR (Ponceau Rouge) staining was used as a protein loading control. The dot marks the main band that correlates with the migration of the non-phosphorylated protein, the line marks the higher molecular weight smear that corresponds to phosphorylated forms of the protein. (F) Quantification of the density profiles of the main band and the phosphorylation-dependent smear from four immunoblots (two biological and two technical replicates) as shown in E. Student's t-test: * $p \leq 0.05$; n.s., not significant.

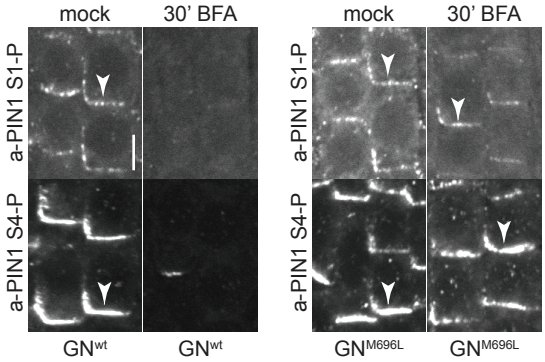

Figure 12: BFA-sensitivity of PIN1 phosphorylation is GNOM-dependent.

Representative confocal images of root stele cells after immunostaining of four days-old BFA-sensitive GN^{wt} and BFA-insensitive GN^{M696L} transgenic mock- and BFA [50] -treated *Arabidopsis* seedlings stained with a-PIN1 S1-P and a-PIN1 S4-P antibodies. Arrowheads mark the staining at the basal plasmamembrane. Scale bar = 5 µm.

3.2.3 The phosphatase inhibitor Cantharidin delays PIN1 dephosphorylation with consequences on auxin distribution in the root

My observations that phosphorylation of PIN1 at the basal plasma membrane was highly sensitive to the presence of BFA-sensitive kinases could imply that, in the absence of such kinases, PIN1 phosphorylation is counteracted by phosphatase activity. Previous reports have implicated particularly PP2A-type phosphatases in the control of PIN1 phosphorylation and also polarity. Mutant combinations of the regulatory subunits *pp2aa1-3* were shown to affect polar auxin transport, as well as the apical targeting of PINs, with consequences on embryo and root development, as well as gravitropism (Michniewicz et al., 2007b). An *in vivo* analysis of PIN phosphorylation suggested that PP2Aa1-3 might directly be involved in dephosphorylating PINs. The documented effects of mutations in the catalytic subunits PP2Ac3 and c4 are similar, their contribution to polar PIN1 distribution is less clear, however (Ballesteros et al., 2013). Interference of phosphatase activity by use of the inhibitor Cantharidin was shown to impact polar auxin transport, auxin distribution and gravitropism in *Arabidopsis* roots (Rashotte et al., 2001; Shin et al., 2005; Sukumar et al., 2009).

Experiments aimed at resolving the PIN1 phosphorylation state in the above mentioned mutants provided variable and inconclusive results. For example, attempts at reproducing the apicalization of PIN1 after tamoxifen induction of amiRNA lines tar-

geting PP2Aa1-3 (Michniewicz et al., 2007b) were unsuccessful in my hands. This could be due to the fact that I could not detect significant transcriptional downregulation of PP2Aa1-3 by semi quantitative RT-PCR in these lines following induction with tamoxifen, even though resistance to PPT (phosphinothricin) indicated the presence of a transgenic construct. Neither these amiRNA lines, nor mutants of *pp2aa1, pp2ac3, pp2ac4* or *pp2ac3/+ pp2ac4* showed significant alterations in PIN1 S1 and S4 phosphorylation or altered BFA-sensitivity of these phosphorylations (data not shown). These results could be indicative of a complex regulation by various phosphatase subunits. I therefore opted to use Cantharidin to block phosphatase activity more broadly in the presence of BFA.

Immunlocalization of a-PIN1 S1-P and a-PIN1 S4-P in root meristems of PIN1-GFP expressing plants treated with BFA in the presence of Cantharidin revealed a phosphatase inhibitor-specific delay in PIN1 dephosphorylation. Treatment with Cantharidin alone affected PIN1-GFP abundance and phosphorylation at S1 and S4 slightly (Fig. 13), pointing to possibly other pleiotropic effects of inhibition of phosphatase activity by Cantharidin. My observed incomplete attenuation of PIN1 dephosphorylation in roots treated with Cantharidin and BFA could be another indication for the complex regulation of PIN1 phosphorylation by a multitude of phosphatases.

We have previously shown by use of the auxin-labile DII-VENUS reporter that BFA affects auxin distribution patterns in the root apical meristem, correlating to the presence of D6PK at the plasma membrane (Barbosa et al., 2014). In order to corroborate my results on the effects of phosphatase inhibition on PIN1 dephosphorylation, I sought to correlate the observed PIN1 phosphorylation patterns with cellular auxin distribution via the same DII-VENUS reporter. As I expected a delay between changes in PIN1 phosphorylation and effects on cellular auxin distribution, I increased the duration of treatment for these experiments to allow for the latter to take place (Fig.

13 and 14). Additionally, plant growth conditions had to be adjusted to increase the sensitivity of the auxin reporter.

Live imaging of roots expressing the DII-VENUS construct treated with BFA confirmed our previous findings that BFA leads to elevated cellular auxin levels (Barbo-

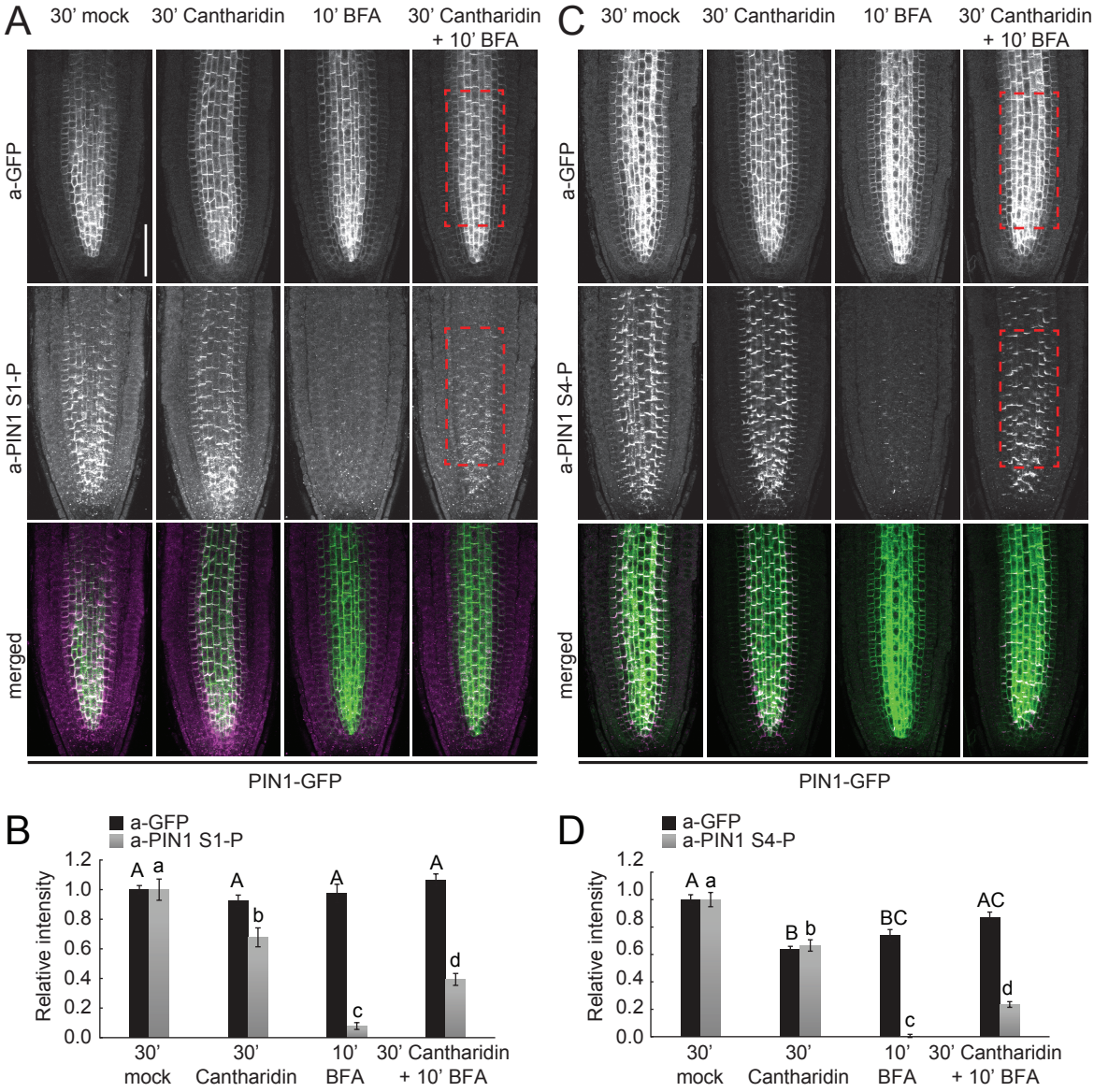

Figure 13: The phosphatase inhibitor Cantharidin delays PIN1 dephosphorylation.

(A and C) Representative images of primary roots after immunostaining of four days-old PIN1-GFP *Arabidopsis* seedlings following BFA [50] (10 min) and Cantharidin or mock (30 min) treatments with anti-GFP (a-GFP, PIN1-GFP) (green) and a-PIN1 S1-P (magenta) (A), or a-PIN1 S4-P (magenta) (C) antibodies. Scale bar = 50 µm. (B and D) Quantification of fluorescence intensity in the root stele after immunostaining as shown in A and C. The average from three independent experiments is shown (total n ≥ 44). One way ANOVA and Tukey HSD datasets with no statistical difference fall in one group and were labeled accordingly. Upper and lower case letters serve to distinguish the results obtained with a-GFP and a-PIN1 S1-P or a-PIN1 S4-P, respectively.

sa et al., 2014). When I exposed roots to BFA pretreated with Cantharidin, however, this decrease in DII-VENUS abundance, which indicates increased cellular auxin concentrations, was no longer observed. Roots treated with Cantharidin alone, on the other hand, did not produce significant changes in DII-VENUS fluorescence intensities (Fig. 14A and C). The auxin-insensitive mDII-VENUS construct served as a control and these plants did not respond to any of the treatments (Fig. 14B and C). These results substantiated my hypothesis that PIN1 phosphorylation levels in the root correlate with auxin efflux activity and thus with cellular auxin levels, as assessed via DII-VENUS reporter intensity.

Based on these experiments, as well as our previous work (Barbosa et al., 2014), I propose that a dynamic equilibrium of PIN1 phosphorylation exists at the plasma membrane that favors the phosphorylated state in the presence of kinases. In contrast, BFA-induced removal of kinases from the plasma membrane leads to efficient

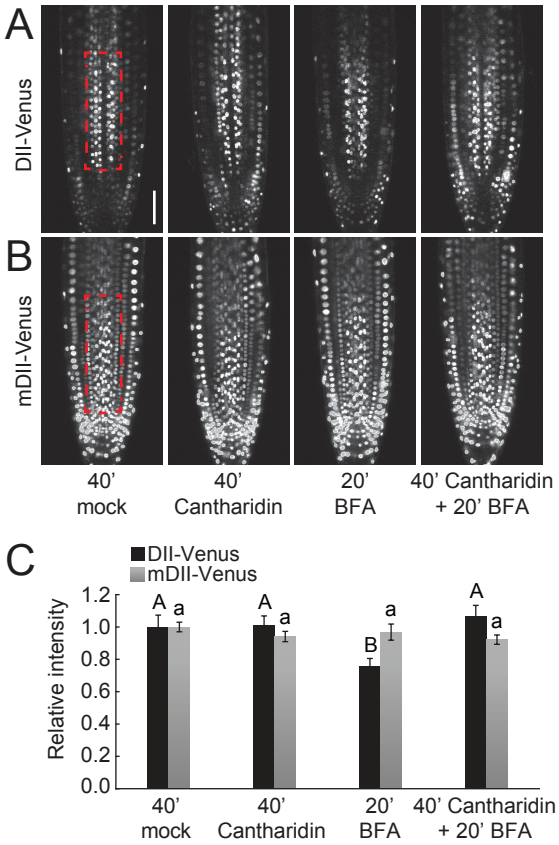

Figure 14: PIN1 phosphorylation dynamics correlate with auxin distribution in the root apical meristem.

(A and B) Representative live fluorescence microscopy images of root tips of four days-old *Arabidopsis* seedlings expressing the auxin-sensitive DII-VENUS (A) or the auxin-insensitive mDII-VENUS markers (B) subjected to BFA [50] (20 min) and Cantharidin or mock (40 min) treatments. Scale bar = 50µm. (C) Quantification of fluorescence intensities in the framed areas of the root stele as shown in A and B. The average from three independent experiments (n ≥ 7) is shown. One way ANOVA and Tukey HSD datasets with no statistical difference fall in one group and were labeled accordingly. Upper and lower case letters serve to distinguish the results obtained with the different series.

dephosphorylation of PIN1, which can, at least partially, be compromised by interfering with phosphatase activity. By establishing a close correlation between these PIN1 phosphorylation patterns and cellular auxin levels in the root apical meristem, I suggest that this equilibrium serves as a dynamic switch for PIN1-mediated auxin efflux activity.

3.2.4 PIN1 phosphorylation can be detected at the apical plasma membrane

Phosphorylation of the PIN1 cytoplasmic loop has been proposed to regulate its polar targeting, as well as efflux capacity. The AGCVIII kinases PID, WAG2 and D6PK were shown to activate PIN1-mediated auxin transport in *Xenopus* oocytes via phosphorylation at the sites S1 - S4 (Zourelidou et al., 2014). Additionally, PID, WAG1 and WAG2-dependent phosphorylation of PIN1 S1 - S3 at the plasma membrane was proposed to serve as a crucial sorting signal for apical targeting of PIN1 (Dhonukshe et al., 2010; Huang et al., 2010). The latter findings are partly based on observed PIN polarity phenotypes upon overexpression of these particular kinases (Friml et al., 2004; Michniewicz et al., 2007b; Dhonukshe et al., 2010). In plants containing a *35S::PID* transgene, PIN1 is often enriched at the apical side in root stele cells (Fig. 15A) (Friml et al., 2004). A PIN1 S123A phospho-mutant protein, however, is seemingly resistant to this change in polarity in the same genetic background, suggesting that PID-dependent targeting of these sites is driving PIN1 apicalization (Huang et al., 2010).

I report here, that phosphorylation of PIN1 at S1 - S4 could consistently be detected at the basal plasma membrane in cells of the root meristem. My data further suggest that BFA-sensitive kinases such as D6PK are the main contributors to these phosphorylation events. Only extended interference with the basal trafficking pathway could seemingly lead to phosphorylation of PIN1 also by BFA-insensitive kinases. These findings are difficult to reconcile with the current model of S1 - S3 phos-

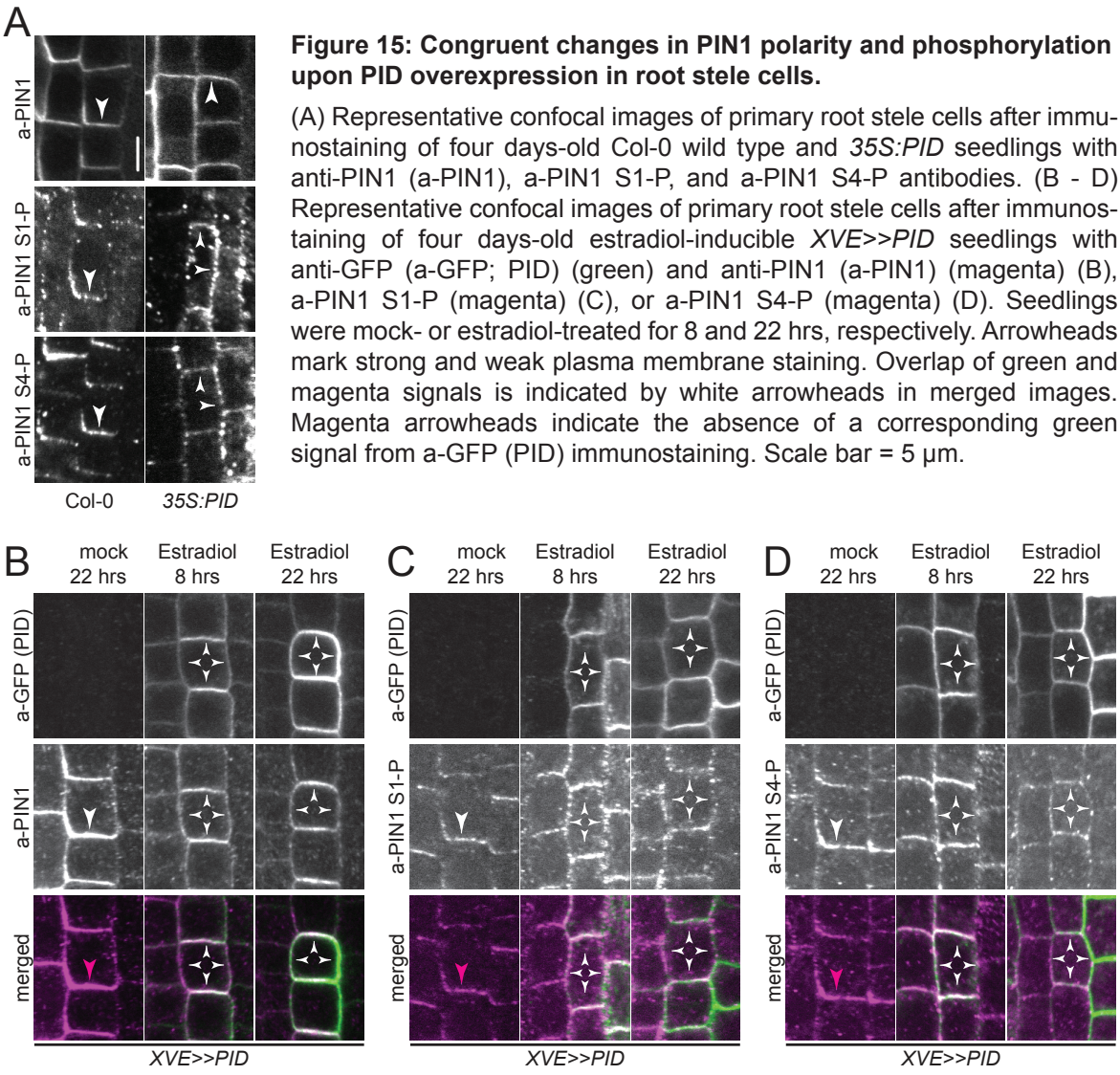

Figure 15: Congruent changes in PIN1 polarity and phosphorylation upon PID overexpression in root stele cells.

(A) Representative confocal images of primary root stele cells after immunostaining of four days-old Col-0 wild type and *35S:PID* seedlings with anti-PIN1 (a-PIN1), a-PIN1 S1-P, and a-PIN1 S4-P antibodies. (B - D) Representative confocal images of primary root stele cells after immunostaining of four days-old estradiol-inducible *XVE>>PID* seedlings with anti-GFP (a-GFP; PID) (green) and anti-PIN1 (a-PIN1) (magenta) (B), a-PIN1 S1-P (magenta) (C), or a-PIN1 S4-P (magenta) (D). Seedlings were mock- or estradiol-treated for 8 and 22 hrs, respectively. Arrowheads mark strong and weak plasma membrane staining. Overlap of green and magenta signals is indicated by white arrowheads in merged images. Magenta arrowheads indicate the absence of a corresponding green signal from a-GFP (PID) immunostaining. Scale bar = 5 µm.

phorylation by the BFA-insensitive PID serving as a sorting signal for apical PIN1 targeting.

I therefore used the antibodies established for this work to examine directly the effects of *PID* overexpression on PIN1 phosphorylation. First, I confirmed the reported PIN1 polarity phenotypes in transgenic *35S::PID* plants, which had been generated independently in our lab by Melina Zourelidou, by immunlocalization of endogenous PIN1 using an a-PIN1 antibody. I indeed detected an enrichment of PIN1 protein at the lateral and apical sides of many root endodermal cells in this line. Wild type roots, in contrast, displayed the expected basal PIN1 localization (Fig. 15A). Fur-

thermore, our *35S::PID* line displayed the previously characterized collapse of the root apical meristem (data not shown) (Friml et al., 2004). I then examined the phosphorylation status of PIN1 at S1 and S4 in *PID* overexpressing roots compared to wild type. A signal from a-PIN1 S1-P or a-PIN1 S4-P was detected at the lateral and apical regions in *35S::PID* lines, similarly to what I had observed for PIN1, whereas cells from wild type roots gave a signal at the basal plasma membrane (Fig. 15A).

In order to gain a better temporal resolution of the effects of *PID* overexpression on PIN1 localization and phosphorylation, I made use of previously characterized lines carrying an inducible *PID* overexpression construct (Dhonukshe et al., 2010). In these *XVE>>PID* lines, I observed a depolarization of basal PIN1 after 8 hours of *PID* induction, while 22 hours were required to consistently detect PIN1 enrichment at the apical side of many cells (Fig. 15B). In accordance with what I had observed

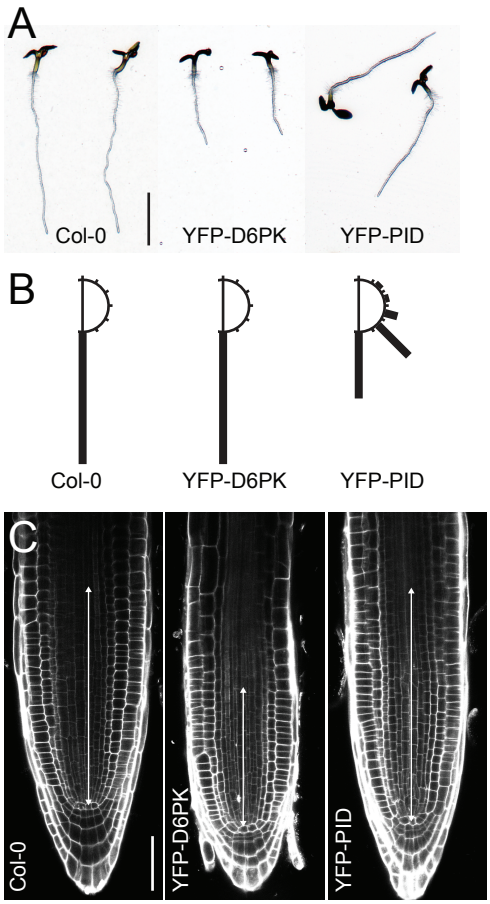

Figure 16: Roots of YFP-D6PK and YFP-PID display divergent phenotypes.

(A) Representative photographs of five day-old, light-grown *Arabidopsis* seedlings with the genotypes as indicated. Scale bar = 4 mm. (B) Quantification of root gravitropism in 30° windows from seedlings as shown in A. The sum of corresponding windows left and right from the vertical are shown. Data from one of three representative independent experiments are shown (n ≥ 30). (C) Representative confocal images of propidium iodide-stained root tips with the genotypes as indicated. The arrow marks the root meristematic zone as defined by the cell length to cell width ratio. Scale bar = 50 µm.

in *35S::PID* lines, the signals obtained from a-PIN1 S1-P and a-PIN1 S4-P mirrored the behavior of the overall pool of PIN1 in terms of plasma membrane distribution (Fig. 15C and D). I concluded that PIN1 phosphorylation followed PIN1 polar localization but was not specific for a particular side of the cell.

In the cells analyzed here, YFP-D6PK localized to the basal plasma membrane in a BFA-sensitive manner (Fig. 9) (Barbosa et al., 2014), whereas YFP-PID was found apolarly at the cell periphery. This distribution of YFP-PID, as well as the intracellular signal occasionally observed in mock-treated roots, likely from endosomal compartments, was not noticeably affected by BFA treatment (Fig. 9), in accordance with published data (Kleine-Vehn et al., 2009). The differential intracellular trafficking behavior of D6PK and PID could be one explanation for the phenotypic divergence observed upon overexpression of these kinases in the root.

In order to assess these phenotypes in comparable genetic material, I used roots from plants expressing YFP-D6PK or YFP-PID, which had previously been generated by Melina Zourelidou using an identical vector backbone. A striking effect of *D6PK* overexpression in YFP-D6PK was a shorter primary root compared to wild type, likely resulting from a shorter root apical meristem (Fig. 16A). While the gravitropic response was not affected by YFP-D6PK overexpression, roots from plants overexpressing YFP-PID grew highly agravitropically (Fig. 16B), as previously reported (Benjamins et al., 2001). However, this YFP-PID construct did not cause collapse of the primary root meristem (Fig. 16C), as was observed in other lines overexpressing *PID* (Friml et al., 2004), as well as the *35S::PID* plants analyzed here previously (data not shown).

As the meristem collapse had been attributed to *PID* overexpression-induced apicalization of PIN1 in stele cells, I analyzed the localization of PIN1 in the YFP-PID plants that did not show this phenotype. Surprisingly, also in this line, I observed

PIN1 enrichment at lateral and apical cell sides, although the localization of PIN1 overall was quite heterogeneous. In contrast, cells from YFP-D6PK roots localized PIN1 exclusively to the basal plasma membrane (Fig. 17A and D). This suggested that PIN1 apicalization might not be the primary cause for the PID-induced meristem collapse. Alternatively, the N-terminal YFP tag could interfere with some function of PID in YFP-PID lines, or these lines express PID at relatively lower levels.

Regardless, the differential phenotypes, along with altered PIN1 localization patterns in YFP-PID compared to YFP-D6PK, prompted me to investigate the BFA-sensitivity of apical PIN1 phosphorylation signals, since previous data had suggested that apically localized PIN1 is resistant towards BFA-induced internalization, specifically when phosphorylated at S1 - S3 (Kleine-Vehn et al., 2009; Huang et al., 2010). Using PIN1 S1 as a representative PID target, as well as PIN1 S4 as a D6PK targeted site, I compared, simultaneously and in the same cells, the BFA response of YFP-D6PK or YFP-PID, using a-GFP together with a-PIN1, a-PIN1 S1-P or a-PIN1 S4-P. YFP-D6PK plants localized PIN1 basally, as mentioned, and all components, D6PK, PIN1, PIN S1-P and PIN1 S4-P displayed the expected BFA sensitivity (Fig. 17A - C). As in *35S::PID* plants, however, PIN1, as well as PIN1 S1-P and PIN1 S4-P, were found at lateral and apical sides of cells expressing YFP-PID (Fig. 17D - F). Interestingly, while YFP-PID was targeted apolarly independently from BFA treatments, phosphorylation signals at PIN1 S1 and S4 were indeed, at least in some instances, resistant to BFA specifically at apico-lateral sides of the cell (Fig. 17E and F).

Taken together, these results suggested that, in the presence of PID, apico-lateral pools of phosphorylated PIN1 could be rendered insensitive to BFA-induced internalization, as reported previously (Kleine-Vehn et al., 2009). The BFA sensitivity of basal, compared to BFA insensitive apico-lateral phosphorylation correlated with

localization and trafficking behavior of YFP-D6PK and YFP-PID, respectively. However, PIN1 S1 and S4 phosphorylation were consistently associated with the predominant enrichment of PIN1 at a particular side of the cell. Consequently, while the different phenotypic effects of kinase overexpression could be attributed to the differential effects on PIN1 localization, phosphorylation of PIN1 at least at S1 or S4

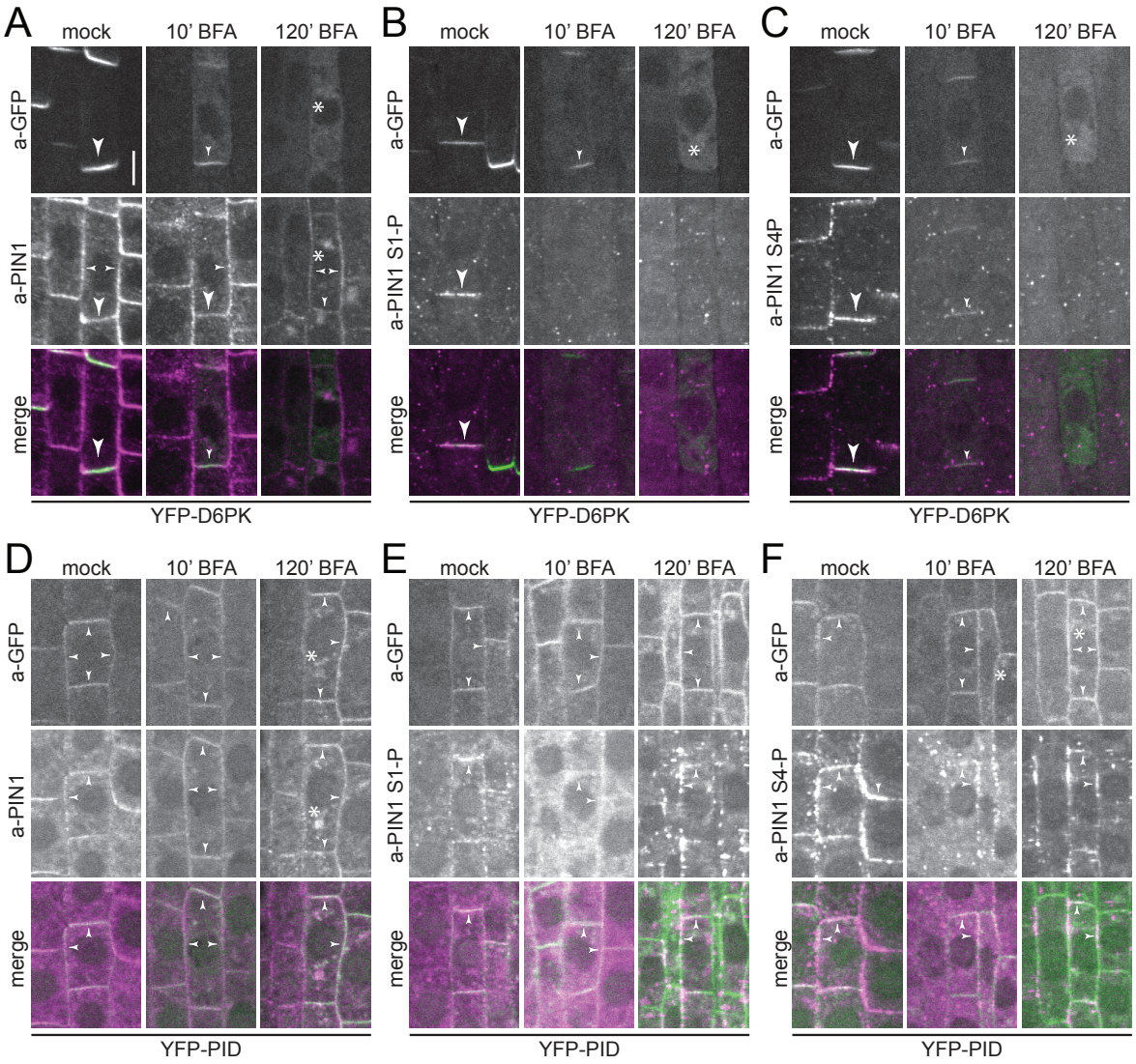

Figure 17: Apical PIN1 phosphorylation upon PID overexpression in stele cells is BFA-insensitive.

(A - F) Representative confocal images of root stele cells from four day-old seedlings overexpressing YFP-D6PK (A - C), or YFP-PID (D - F) after immunostaining with anti-GFP (a-GFP; YFP-D6PK or YFP-PID, respectively) (green) and anti-PIN1 (a-PIN1) (magenta) (A and D), a-PIN1 S1-P (magenta) (B and E), or a-PIN1 S4-P (magenta) (C and F) antibodies following a mock and a 10 or 120 min BFA [50] treatment. Arrowheads mark strong and weak plasma membrane staining, asterisks mark intracellular BFA compartments. Overlap of green and magenta signals is indicated by white arrowheads in the merged images. Scale bar = 5 µm.

at the plasma membrane is not sufficient to predict its polar targeting. Importantly, this would imply that the signaling by which PID induces changes in PIN1 polar localization likely involves other factors than phosphorylation at S1 (and likely S2 and S3) alone.

3.3 PIN1 S1 and S4 phosphorylation in cortex and epidermal cells

3.3.1 PIN1 phosphorylation is independent of PIN1 polar localization

The tissue-specific expression patterns of various AGCVIII kinases have been analyzed previously. GUS activity driven from the promoter of D6PK or its closest homologues D6PKL1 and D6PKL2 can be detected throughout the root apical meristem (Zourelidou et al., 2009). A more detailed microscopic analysis of a *D6PK* promoter-driven YFP-D6PK fusion protein revealed that D6PK localized to the basal plasma membrane in all cell types of the root (Zourelidou et al., 2009; Barbosa et al., 2014). I had focused my analysis to this point on PIN1 expressed in the root stele, particularly on endodermal cells. However, unlike D6PK, neither PID, nor WAG1 or WAG2 are endogenously found at detectable levels in the *PIN1* expression domain (Benjamins et al., 2001; Sukumar et al., 2009). The expression of *PID* in these cells therefore constitutes a non-physiological situation. Instead, *PID* or *WAG* promoter-driven YFP fusion proteins have been shown to localize apolarly at the plasma membrane specifically in root cortex and epidermal cells (Dhonukshe et al., 2010).
I therefore took advantage of two established transgenic variants that express PIN1 from the *PIN2* promoter, since both *D6PK* and *PID* are endogeneously expressed there. These PIN1 variants further show divergent polar targeting in epidermal cells, although they solely differ in the position of the GFP-tag within the PIN1 cytoplasmic loop. PIN1-GFP2 *(PIN2p::PIN1-GFP2)* expressing plants localize the PIN1 transgene to the basal plasma membrane in both cortex and epidermal cells, although in

the latter it is also detected around the entire cell periphery. The PIN1-GFP3 *(PIN-2p::PIN1-GFP3)* transgene localizes like endogenous PIN2, basally in the cortex and apically in epidermal cells (Fig. 18) (Wiśniewska et al., 2006). Using these lines I was able to monitor phosphorylation of PIN1 targeted to different regions within the same cell type, in the same genetic background. Immunlocalization revealed that the ectopically expressed PIN1 was phosphorylated at S1 and S4 independently of its polar localization (Fig. 18). This result suggested, congruent with our results from

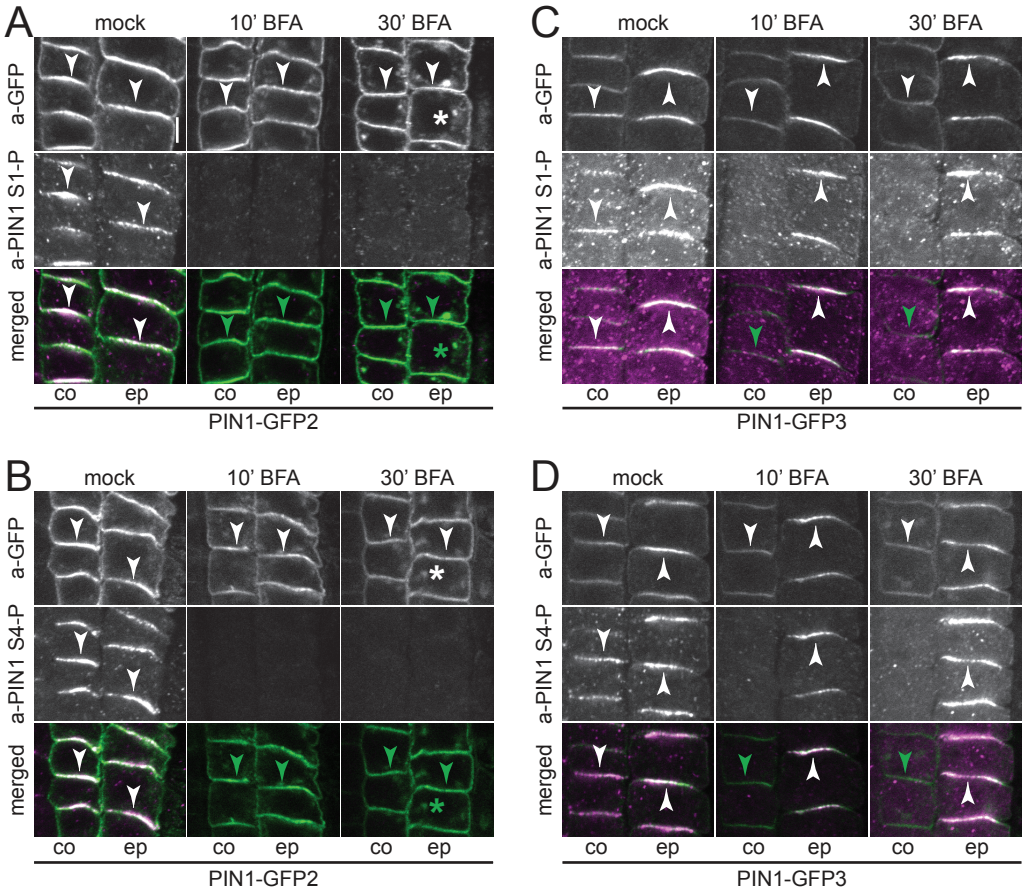

Figure 18: PIN1 phosphorylation in epidermal cells occurs at the basal and apical plasma membranes and is differentially BFA-sensitive.

(A - D) Representative confocal images of root cortex (co) and epidermal (ep) cells after immunostaining of four days-old PIN1-GFP2 and PIN1-GFP3 seedlings following mock or BFA [50] treatments (10 and 30 min) with anti-GFP (PIN1-GFP2 or PIN1-GFP3, respectively) (green) and a-PIN1 S1-P (magenta) (A and C), or a-PIN1 S4-P (magenta) (B and D). Arrowheads mark strong and weak plasma membrane staining, asterisks mark intracellular compartments. Overlap of green and magenta signals is indicated by white arrowheads in merged images. Green arrowheads and asterisks indicate the absence of a corresponding magenta signal from a-PIN1 S1-P or a-PIN1 S4-P immunostaining. Scale bar = 5 µm.

endodermal cells, that phosphorylation of PIN1 at S1 and S4 occurs independently from polarity control.

As I had observed a differential BFA sensitivity of PIN1 phosphorylation in root stele cells, I asked whether basal and apical PIN1 phosphorylation could respond differently towards BFA treatment in epidermal cells as well. Indeed, phosphorylation of basal PIN1 in cortex and epidermis cells was equally BFA sensitive, whereas when localized apically (PIN1-GFP3), it was largely insensitive to the treatments (Fig. 18C and D). These results correlate well with the distinct intracellular trafficking of D6PK and PID in terms of BFA sensitivity and cellular localization in epidermal cells (Fig. 19) (Barbosa et al., 2014). They furthermore corroborate my hypothesis that basal PIN1 phosphorylation is mediated by BFA sensitive kinases such as D6PK, while PID kinases are seemingly able to phosphorylate apical PIN1.

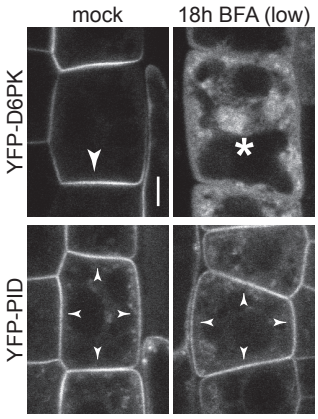

Figure 19: D6PK and PID differ in intracellular localization and trafficking in root epidermal cells.

Representative live fluorescence microscopy images of primary root epidermal cells of four days-old YFP-D6PK and YFP-PID *Arabidopsis* seedlings after 18 hours mock or BFA [10] treatments as employed for the experiments shown in Fig. 20. Arrowheads mark plasma membrane staining, asterisks mark intracellular compartments. Scale bar = 5 µm.

Interestingly, I could not detect PIN1-GFP2 phosphorylation at lateral and apical membranes of epidermal cells, even though an a-GFP antibody could detect this fusion protein there. While this could be due to the enrichment of the protein at the basal side and thus a technical issue of the detection limit of the phosphosite-specific antibodies, the observed phosphorylation pattern was highly congruent with the localization of D6PK in this cell type (Fig. 18A and B, Fig. 19). It is therefore inviting to speculate that this PIN1 variant preferentially interacts with D6PK family mem-

bers. Additionally, my observation that the apolar, BFA-insensitive PID is unable to maintain basal PIN1 phosphorylation in the presence of BFA could indicate that a BFA-sensitive factor is required for an interaction to take place at this plasma membrane region.

3.3.2 Differential effects of BFA on root gravitropism correlate with PIN1 phosphorylation patterns and hypothetical auxin transport in the *PIN2* expression domain

Opposite auxin streams in cortex and epidermis of the root apical meristem are crucial for proper gravitropic root growth. The differential localization of PIN2 in these cells directs auxin transport towards the root tip in young cortical cells and towards the elongation zone in the epidermis (Shin et al., 2005; Abas et al., 2006; Sukumar et al., 2009; Rahman et al., 2010). In line with this function, mutation of the *PIN2* gene results in agravitropic root growth (Muller et al., 1998). The constructs PIN1-GFP2 and PIN1-GFP3 under the control of the *PIN2* promoter had both been transformed into *pin2* plants and, as expected from their differential localization in epidermal cells, only PIN1-GFP3 was able to rescue the agravitropic root growth of the mutant (Wiśniewska et al., 2006).

This rescue is consistent with my observation that PIN1-GFP3 was phosphorylated at basal and apical plasma membranes (Fig. 18C and D), suggesting that this transgene is actively transporting auxin in the appropriate directions. Conversely, basal phosphorylation of PIN1-GFP2 in the epidermis indicated that the highly agravitropic root growth of these plants is a consequence of an improper orientation of auxin flow in these cells. Taken together with the observed differential BFA sensitivity of apical and basal PIN1 phosphorylation in epidermal cells (Fig. 18), I hypothesized that the agravitropism of PIN1-GFP2 plants should at least in part be rescued by BFA application, as this should inhibit the wrongly directed auxin transport stream

in the epidermal cell file. The BFA-insensitivity of apical phosphorylation of PIN1-GFP3 should, on the other hand, render this line at least partially resistant to BFA treatment.

In order to test these postulations, I grew plants vertically on agar-containing plates for four days and subsequently transferred the seedlings to plates containing 10 µM BFA, or the corresponding amount of solvent as control. After allowing the seedlings to grow vertically for an additional 18 hours in darkness, I assessed various root growth parameters. Wild type roots, in line with previous reports (Rahman et al., 2010), responded to BFA treatment with decreased gravitropic growth compared to control roots, as measured from the angle between the point of transfer and the final position of the root tip. The agravitropism of *pin2* mutants was not affected by BFA, indicating that proper PIN2 function is important in this context (Muller et al., 1998; Abas et al., 2006; Sukumar et al., 2009; Rahman et al., 2010).

When I subsequently analyzed seedlings expressing PIN1-GFP3 in the same assay, I saw that their gravitropic root growth was slightly decreased in control seedlings, compared to wild type roots (Fig. 20A and B), even though this line was previously reported to fully rescue the *pin2* agravitropism phenotype (Wiśniewska et al., 2006). The minor agravitropism I measured in control seedlings of this line, however, was not altered by growth on BFA, confirming my hypothesis that this line should be resistant to the treatment. This was in stark contrast my observations using PIN1-GFP2 seedlings. These seedlings grew highly agravitropically on control plates, as was shown previously (Wiśniewska et al., 2006). However, the gravitropic growth angles I measured on roots from BFA-containing plates were similar to those from PIN1-GFP3 seedlings or wild type roots of the same treatment (Fig. 20A and B). Importantly, the phenotypic rescue was beyond restoring gravitropic growth to the level of *pin2* mutant roots, the common genetic background.

It is noteworthy here that in the case of PIN1, prolonged BFA treatments over several hours lead to its depolarization from the basal membrane and eventual accumulation at the apical side of the cell (Fig. 10) (Kleine-Vehn et al., 2008c). These changes in PIN1 polarity are thought to involve transcytosis and are BFA concentration-dependent, occurring only at 25 - 50 µM (Rahman et al., 2010). As these concentrations of BFA completely inhibit root elongation, I employed a lower BFA concentration of 10 µM in physiological experiments, compared with the previously used 50 µM. Since it had been reported that basal PIN1 polarity in the stele is not affected at this lower BFA concentration (Rahman et al., 2010), I wanted to assess its effects on PIN1 phosphorylation. Immunlocalization of a-PIN1, a-PIN1 S1-P and a-PIN1 S4-P in wild type roots confirmed that this lower BFA concentration did not depolarize PIN1 from the basal plasma membrane, even after 18 hours. Additionally, neither S1 nor S4 phosphorylation was abolished following the same treatment (Fig. 20C), as opposed to my observations for short term treatments using 50 µM BFA (Fig. 8). This indicated that the agravitropism observed in wild type roots following BFA treatment was likely not due to a defect in PIN1-mediated auxin transport in the stele, but could rather stem from a defect in PIN2 function, as was postulated previously (Rahman et al., 2010). In order to exclude any differential effects of BFA treatment on root elongation and thus possibly the gravitropic response, I additionally measured the quantitative inhibition of 10 µM BFA on root elongation and recorded comparable inhibition rates across all genotypes tested (Fig. 20D).

As the results regarding the gravitropic growth of PIN1-GFP2 seedlings on BFA-containing plates were unexpected, I took roots from these assays for use in immunlocalization experiments, in order to get an insight into the molecular basis for this strong rescue. I first compared the behavior of the PIN1-GFP2 transgene in root cortex and epidermal cells between BFA-treated and control seedlings using an

a-GFP antibody. The preferentially basal enrichment of this protein observed in control roots was abolished following growth on BFA in both cell files. Instead, these cells displayed an apolar distribution with an occasional enrichment at the apical

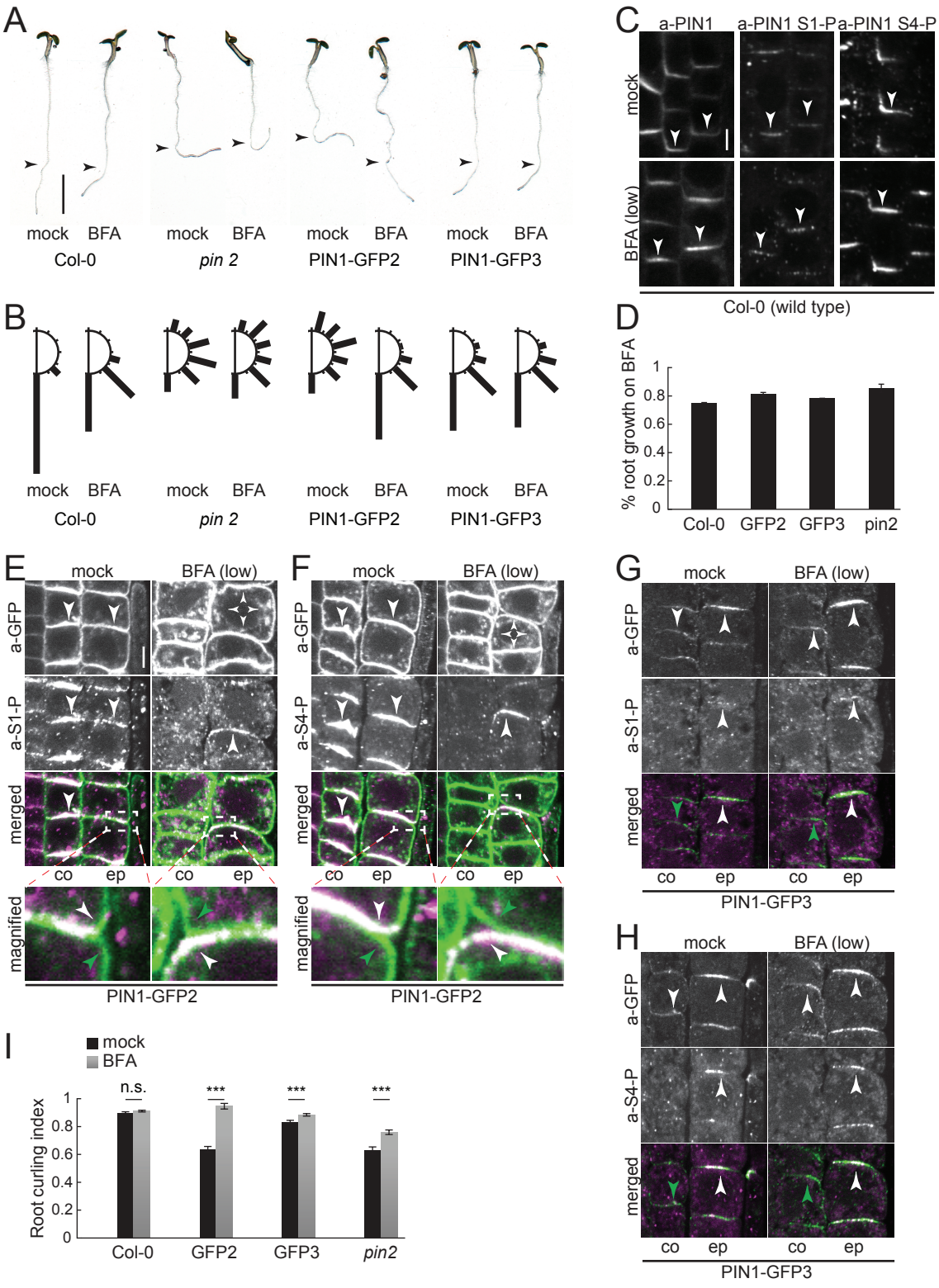

side, specifically in older epidermal cells (Fig. 20E and F, data not shown). Co-immunlocalization with either a-PIN1 S1-P or a-PIN1 S4-P in the same roots revealed that, as I had observed for short term 50 µM BFA treatments (Fig. 18), the basal phosphorylation signal in cortical cells was abolished also at this lower BFA concentration. As opposed to my previous results, however, growth on 10 µM BFA for 18 hours resulted in the occasional appearance of a phosphorylation signal at the apical plasma membrane of epidermal cells from PIN1-GFP2 roots. This was the case in 38% and 46% of cells for a-PIN1 S1-P and S4-P, respectively, to which a specific polarity could be assigned (Fig. 20E and F). In contrast, 65% and 91% of epidermal cells in mock-treated roots displayed the expected basal phosphorylation of S1 and S4, respectively.

I concluded that the strong rescue of agravitropic root growth on 10 µM BFA in PIN1-GFP2 seedlings could be due to a reversal in the direction of auxin transport in the

---

☜–**Figure 20: BFA-induced PIN1 phosphorylation changes in epidermal cells of PIN1-GFP2 roots correlate with a rescue of root gravitropic growth.**

(A) Representative photographs of five days-old light-grown *Arabidopsis* seedlings transferred for 18 hrs to medium with or without BFA [10 µM]. The arrowheads point to the position of the root tip at the point of transfer. Scale bar = 4mm (B) Quantification of root gravitropism in 30° windows from seedlings as shown in A. Seedlings with root angles corresponding to 30° windows left and right from the vertical axis were combined. Cumulative data from three independent experiments is shown (n ≥ 128 seedlings). (C) Representative confocal images of stele cells of the primary root after immunostaining of five days-old Col-0 wild type roots following the same treatment as in A with anti-PIN1 (a-PIN1), a-PIN1 S1-P, or a-PIN1 S4-P. Arrowheads indicate basal plasma membrane staining. Scale bar = 5 µm. (D) Relative growth of roots grown on BFA compared to mock from the same dataset as in B. (E - H) Representative confocal images of root cortex (co) and epidermis (ep) cells after immunostaining of five days-old PIN1-GFP2 (E and F) and PIN1-GFP3 (G and H) seedlings following the same treatment as in A, with anti-GFP (a-GFP; PIN1-GFP) (green) and a-PIN1 S1-P (magenta) (E and G), or a-PIN1 S4-P (magenta) (F and H). Arrowheads mark plasma membrane staining. Overlap of green and magenta signals is indicated by white arrowheads in merged images. Green arrowheads indicate the absence of a corresponding magenta signal from a-PIN1 S1-P or a-PIN1 S4-P immunostaining. In E, immunostained epidermal cells (51 of 79) showed a basal plasma membrane signal following the mock treatment and an apical signal after BFA treatment (92 of 240). In F, immunostained cells showed a basal plasma membrane signal (128 of 140) following the mock treatment and an apical signal after BFA treatment (81 of 177). In all cases, the remaining cells showed either no signal for a-PIN1 S1-P or a-PIN1 S4-P, or the polarity of that signal could not be unequivocally determined, based on the criteria as shown in the magnifications. Scale bar = 5 µm. (I) Quantification of root curling, measured by the shortest distance from the point of transfer to the root tip divided by root growth in 18 hrs from the same dataset as in B. Student's t-test: *** $p \leq 0.001$; n.s., not significant.

epidermis, as indicated by the change in PIN1 phosphorylation from strictly basal to preferentially apical. An active, apically localized PIN1 in epidermal cells could thereby serve to compensate for the mutational loss of PIN2 from these seedlings.

I also immunostained roots from PIN1-GFP3 seedlings, which had grown with comparable gravitropic angles independently from BFA treatments. In control roots, apical PIN1 in epidermal cells was phosphorylated at S1 and S4. This signal was maintained in roots grown on 10 µM BFA (Fig. 20G and H), as I had observed for short term treatments at 50 µM (Fig. 18).

Interestingly, a-GFP staining further revealed a reversal of PIN1-GFP3 polarity in cortical cells of roots grown on BFA from basal to apical (Fig. 20G and H). This had previously been reported to occur with PIN2 as well in these cells, under comparable experimental conditions (Rahman et al., 2010), indicating that PIN1-GFP3 and PIN2 are subject to similar intracellular trafficking regulation. The BFA-induced defect in gravitropic growth of wild type roots had been attributed to this apicalization of PIN2 in young cortical cells (Rahman et al., 2010).

Due to the relatively low expression of the PIN1-GFP3 transgene in cortical cells, I was unable to unequivocally determine the PIN1 phosphorylation status in these cells from my root growth assay. As I performed this assay in darkness, in order to exclude pleiotropic effects of light and phototropic responses, vacuolar degradation of the transgene could have occurred. This has been reported to occur with PIN2 in the dark and has subsequently been used widely as a marker for vacuolar protein degradation (Kleine-Vehn et al., 2008b; Laxmi et al., 2008; Isono et al., 2010) (see also section 3.3.3). Since I observed similar intracellular trafficking behavior for PIN1-GFP3, compared to what is reported for PIN2, a common degradation pathway is also conceivable. Whether the apical PIN1-GFP3 in the cortex is actively transporting auxin and thus contributing to a decrease in gravitropism could, how-

ever, not be resolved.

Nevertheless, the similar phosphorylation patterns of PIN1-GFP2 and PIN1-GFP3 grown on BFA were highly congruent with their gravitropic growth response, which could be an indication that polar phosphorylation of PIN1 is able to predict the direction of auxin transport at the tissue level. These results, taken together, are consistent with my proposal that PIN1 phosphorylation, at least at the target sites analyzed here, is not a determinant of PIN1 polarity, but rather of transporter activity. Furthermore, BFA-sensitive basal PIN1 phosphorylation correlated well with the intracellular trafficking behavior of D6PK family kinases, while BFA-insensitive apical PIN1 phosphorylation could involve the also insensitive PID kinases. This would not explain, however, why PID, in the absence of BFA-sensitive kinases, is seemingly unable to maintain PIN1 phosphorylation at the lateral and basal sides of the cell. These phosphorylation events could possibly require the presence of an as yet unidentified, BFA-sensitive factor. Alternatively, this basally localized factor could be unable to interact with PID family kinases.

While performing the gravitropic root growth assays, I noticed that *pin2* mutant seedlings, as well as *pin2* mutants expressing PIN1-GFP2 from control plates, displayed not only an agravitropic, but also a curled growth phenotype. I quantified this phenotype by measuring the distance of the root tip between the point of transfer and the final position after 18 hours of growth, in relation to total root elongation over the same time frame. This yielded a root curling index from control plates of ca. 0.6 for both *pin2* and PIN1-GFP2, compared to an index of around 0.9 for wild type and PIN1-GFP3 roots from control, as well as BFA-containing plates, indicating a relatively straight growth behavior. Interestingly, this phenotype was fully rescued in PIN1-GFP2 roots when grown on BFA, as indicated by a curling index of 0.9, while roots of *pin2* mutants were rescued only minimally to an index of 0.75 (Fig. 20I). This

was further indication that the effects of BFA on root gravitropic growth, specifically the phenotypic rescue of PIN1-GFP2 seedlings, were the result of alterations in auxin transport routes in the *PIN2* expression domain. Particularly the apical epidermal PIN1 phosphorylation of PIN1-GFP2 roots grown on BFA, compared to the absence of presumably any PIN in these cells in roots of *pin2* seedlings thus substantiates my hypothesis that polar PIN phosphorylation in these cells could predict physiological behavior based on hypothetical auxin transport streams.

3.3.3 The agravitropic root growth caused by inducible overexpression of PIN1 can be explained by polar PIN1 phosphorylation

It was previously suggested that newly synthesized PIN1 in epidermal cells is initially delivered to the PM in an apolar manner and subsequently attains its basal polarity upon selective endocytosis (Dhonukshe et al., 2008). Although this publication has since been retracted, I sought to analyze the same estradiol inducible *XVE>>PIN1* expression line, whose use led to this hypothesis in part, in order to trace the phosphorylation state of *de novo* synthesized PIN1 trafficking to the plasma membrane. I therefore grew *XVE>>PIN1* seedlings for four days on vertical agar-containing plates and subsequently transferred them to liquid medium containing 10 µM estradiol or the corresponding amount of solvent. I then immunostained these roots after different induction times with either a-PIN1, a-PIN1 S1-P, or a-PIN1 S4-P antibodies to take confocal images of root epidermal cells, the cell type in which the PIN1 polarization study had been performed. As PIN1 is not endogenously present in these cells, a signal observed there using the antibodies above should derive specifically from the induced PIN1 transgene.

At two hours of estradiol treatment, I observed a signal for a-PIN1 stained roots primarily in intracellular structures of epidermal cells and, albeit at low levels, apolarly distributed at the plasma membrane. These roots, however, did not produce a signal

for induction-specific conditions using a-PIN1 S1-P, while a-PIN1 S4-P-stained roots sometimes showed a very weak signal at the basal plasma membrane not present under non-inducing conditions. Cells of the stele, on the other hand, reliably produced a condition-independent signal (data not shown). Only after 4 hours of estradiol treatment, a clear induction-specific signal was observable for a-PIN1 S4-P at the basal plasma membrane of epidermal cells. At the same time, I detected PIN1 in intracellular structures and apolarly distributed at the plasma membrane in epidermal cells stained with a-PIN1. While I was unable to observe a clear signal using a-PIN1 S1-P under the same conditions, this could be attributed to the relatively low abundance of PIN1 after 4 hours of estradiol induction and possibly an inferior titer of this antibody.

It has to be noted here that a polarization of PIN1 towards the basal plasma membrane had been reported to occur well within four hours of estradiol induction (Dhonukshe et al., 2008). Nonetheless, I noticed with interest that apolar PIN1 distribution after 4 hours of induction was accompanied by an exclusively basal phosphorylation signal at S4 (Fig. 21A). Furthermore, prolonged induction times of 18 hours clearly resulted in a basal phosphorylation signal at both S1 and S4, with PIN1 preferentially enriched at the basal plasma membrane (Fig. 21B).

Phenotypically, It was demonstrated previously that induction of ectopic PIN1 overexpression in *XVE>>PIN1* lines leads to agravitropic root growth (Petrasek et al., 2006). In order to confirm this observation, I employed the root growth assay I had established previously, using *XVE>>PIN1* seedlings under inducing and non-inducing conditions. When I subsequently analyzed the gravitropic growth angle of these roots, I recorded a strong deviation from the vertical for roots grown on estradiol compared to control roots, as reported (Fig. 21C and D) (Petrasek et al., 2006). I reasoned that, akin to the scenario in PIN1-GFP2 seedlings, the wrongly direct-

ed auxin transport in epidermal cells, presumably the result of specifically basal PIN1 phosphorylation, could be causative for the agravitropic growth phenotype. It was therefore tempting to speculate that also estradiol-treated *XVE>>PIN1* roots should be rescued in their agravitropism by addition of BFA to the growth medium, as the basal PIN1 phosphorylation should again exhibit BFA sensitivity. I therefore expanded my root growth assay to include the presence or absence of BFA. Under control conditions, without estradiol induction, *XVE>>PIN1* roots behaved like wild

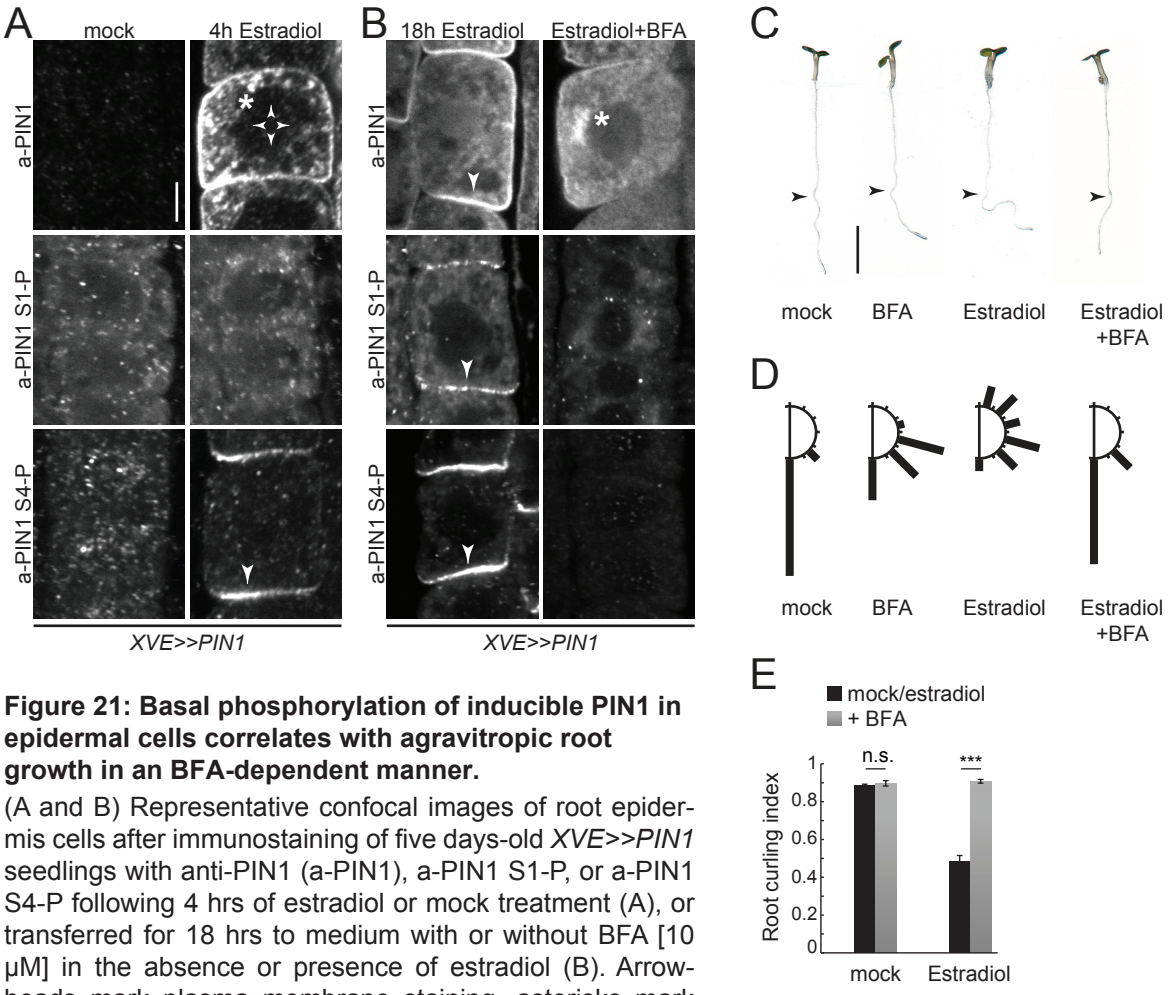

Figure 21: Basal phosphorylation of inducible PIN1 in epidermal cells correlates with agravitropic root growth in an BFA-dependent manner.

(A and B) Representative confocal images of root epidermis cells after immunostaining of five days-old *XVE>>PIN1* seedlings with anti-PIN1 (a-PIN1), a-PIN1 S1-P, or a-PIN1 S4-P following 4 hrs of estradiol or mock treatment (A), or transferred for 18 hrs to medium with or without BFA [10 µM] in the absence or presence of estradiol (B). Arrowheads mark plasma membrane staining, asterisks mark internal compartments. Scale bar = 5 µm. (C) Representative photographs of five days-old light-grown *XVE>>PIN1* seedlings following the same treatment as in B. The arrowheads point to the position of the root tip at the point of transfer. Scale bar = 4mm. (D) Quantification of root gravitropism in 30° windows from seedlings as shown in C. Seedlings with root angles corresponding to 30° windows left and right from the vertical axis were combined. Data from one of three representative independent experiments is shown (n ≥ 44 seedlings). (E) Quantification of root curling, measured by the shortest distance from the point of transfer to the root tip divided by root growth in 18 hrs from the same dataset as in D. Student's t-test: *** $p \leq 0.001$; n.s., not significant.

type (Fig. 20A and B), displaying mild agravitropic growth on BFA-containing plates. As mentioned, however, when the growth medium was supplemented with estradiol, these roots grew highly agravitropically. Conversely, when the medium was additionally supplemented with 10 µM BFA, gravitropic root growth could be restored almost to the level of control roots (Fig. 21C and D), in line with my hypothesis.

I noticed as well, that *XVE>>PIN1* seedlings grown on estradiol showed a similar root curling phenotype as PIN1-GFP2 or *pin2* seedlings (Fig. 20I). As the root curling index I had applied previously indicated, this phenotype was rescued as well in *XVE>>PIN1* roots on plates supplemented additionally with BFA. Importantly, as I had seen in wild type roots, BFA treatment alone did not affect root curling (Fig. 21E).

While attempting to validate my speculations at the molecular level, I was not able to identify a signal in epidermal cells for either, a-PIN1-S1-P, or a-PIN1-S4-P after immunostaining of *XVE>>PIN1* roots grown on estradiol + BFA, although a signal at the plasma membrane in stele cells could be detected (data not shown). This could be due to the fact that I did not reliably detect apicalization of PIN1 in estradiol + BFA-treated *XVE>>PIN1* root epidermal cells, as one could have expected from my observations using PIN1-GFP2 seedlings. Instead, PIN1 from a-PIN1-stained *XVE>>PIN1* epidermal cells from this treatment was either undetectable, or accumulated in BFA compartments (Fig. 21B). These observations point to the complex intracellular trafficking routes for PIN proteins operating in this context (see section 3.3.2) and could be explained by the fact that the *XVE>>PIN1* construct does not carry a GFP-tag within its cytoplasmic loop, the presence of which clearly affects the trafficking of this protein (see sections 1.2.2 and 3.3.2).

The low levels or intracellular accumulation of PIN1 in *XVE>>PIN1* epidermal cells grown on estradiol + BFA, in conjunction with undetectable levels of PIN1 phosphor-

ylation would be in line with PIN1 phosphorylation occuring primarily at the plasma membrane. Moreover, these results substantiate my hypothesis, since the strong phenotypic rescue of *XVE>>PIN1* roots grown on estradiol + BFA is yet attributable to the presence of endogenous PIN2, which is genetically mutated in PIN1-GFP2 seedlings. Importantly, highly agravitropic and curled root growth in the presence of basal PIN1 phosphorylation in estradiol-treated epidermal cells, compared to levels of PIN1 phosphorylation below detection limits in roots grown on estradiol + BFA and concomitant phenotypic rescue, support my model that PIN1 phosphorylation at the plasma membrane is able to predict the directional flow of auxin and, hence, the phenotypic responses to these auxin transport streams at the tissue level.

Furthermore, my observations with regard to the PIN1 phosphorylation dynamics at the basal plasma membrane in epidermal cells of *XVE>>PIN1* roots were reflected by the localization of D6PK under the same conditions (Fig. 19), indicating a possible preferential interaction with this PIN1 transgene. Whether these phosphorylation dynamics are linked to the polar targeting of PIN1 to the basal plasma membrane can only be speculated at this point. The absence of intracellular PIN1 phosphorylation signals for *de novo* synthesized protein (data not shown), as well as after prolongued BFA treatment, further suggest, however, that PIN1 phosphorylation occurs primarily at the plasma membrane.

3.4 Basal PIN1 is phosphorylated at S1 and S4 in *pid* mutants

The most prominent phenotype of *pin1* mutants is their name-giving pin-shaped inflorescence meristem (Okada et al., 1991). This is thought to arise in part from defective auxin transport up towards the meristem in epidermal cells, normally carried out by apically localized PIN1 (Benková et al., 2003; Reinhardt et al., 2003; Heisler et al., 2005). The presence of PID in these cells was proposed to maintain this apical

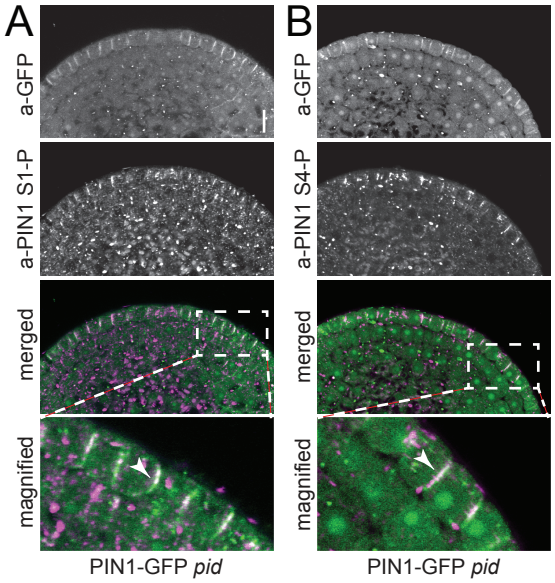

Figure 22: Basal PIN1 in epidermal cells of *pid* mutants is phosphorylated at S1 and S4.

(A and B) Representative confocal images of non-differentiated PIN1-GFP *pid* mutant shoot apical meristems stained with a-GFP (a-GFP; PIN1-GFP; green) and a-PIN1 S1-P (magenta) (A), or a-PIN1 S4-P (magenta) (B) antibodies. White arrowheads mark the staining at the plasma membrane in the merged images. Scale bar = 10 µm.

PIN1 polarization through phosphorylation of S1 - S3 (Huang et al., 2010). Evidence for this comes from the observation that *pid* mutants mislocalize PIN1 to the basal side in epidermal cells (Friml et al., 2004), which is thought to be causative for the similar pin-shaped phenotype. Additionally, a PIN1-GFP S123A transgene, where S1 - S3 are rendered unphosphorylatable, is equally mislocalized in inflorescence meristems and cannot rescue *pin1* mutants (Huang et al., 2010). Therefore, according to the current model of PIN1 polarity control, basal PIN1 in epidermal cells of *pid* mutants should be deficient at least in S1 phosphorylation.

When I probed undifferentiated floral meristems of *pid* plants expressing PIN1-GFP, for PIN1 polarity and phosphorylation in epidermal cells, I detected PIN1, using an a-GFP antibody, at the basal plasma membrane, as reported (Friml et al., 2004). This signal additionally co-localized with a-PIN1 S1-P or a-PIN1 S4-P derived signals, respectively (Fig. 22). Due to the more complex anatomy of differentiated floral meristems, I was unable to obtain a reliable signal from my phosphosite-specific antibodies as control in wild type meristems (data not shown). Particularly S1 phosphorylation of basally localized PIN1-GFP in *pid* mutant meristems, however, does not support a role for this phosphorylation signal in driving PIN1 apicalization.

3.5 Unknown kinases act redundantly with D6PK and PID in phosphorylating PIN1 in the root

Our results suggest that PIN1 phosphorylation is required for PIN1 activity. D6PK, as well as PID and the related WAG2 kinases phosphorylate and activate PIN1 (Zourelidou et al., 2014) and D6PK and PID are being treated in this study as representative members of their respective protein kinase families. Higher order mutants of three *D6PK* genes, namely the *d6pk d6pkl1 d6pkl2* mutant, and four *PID/WAG* genes, *pid pidl2 wag1 wag2*, have been described and show impaired development that can be explained by defects in PIN-dependent auxin transport and PIN polarity

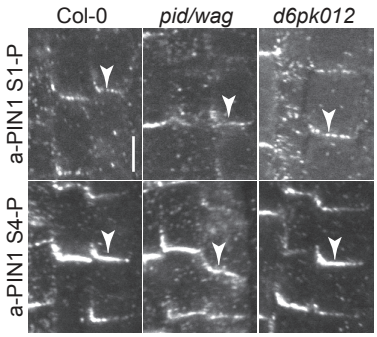

Figure 23: PIN1 phosphorylation is maintained in *pid/wag* quadruple and *d6pk* triple mutants.

Representative confocal images of primary root stele cells after immunostaining of four days-old Col-0 (wild type) seedlings, as well as *d6kp012* (*d6pk d6pkl1 d6pkl2*) and *pid/wag* (*pid pid-like2 wag1 wag2*) mutant seedlings with a-PIN1 S1-P, or a-PIN1 S4-P antibodies. Arrowheads mark the staining at the basal plasma membrane. Scale bar = 5 µm.

(Cheng et al., 2008; Zourelidou et al., 2009; Dhonukshe et al., 2010; Willige et al., 2013; Barbosa et al., 2014; Haga et al., 2014).

I used these available mutants to understand to what extent PIN1 phosphorylation was dependent on these kinases in the root apical meristem. In both cases, I observed that PIN1 phosphorlyation at S1 and S4 was maintained in root stele cells (Fig. 23), suggesting that other kinases may act redundantly with D6PKs and PID/WAGs in this tissue. Both of these groups of kinases belong to the larger AGCVIII family comprising 23 members in total [reviewed by (Galvan-Ampudia and Offringa, 2007)], many of which have yet to be functionally characterized. These kinases potentially qualify as additional PIN1 regulatory kinases.

4 Discussion

4.1 Phosphorylation dynamics of PIN1

4.1.1 PIN1 phosphorylation follows PIN1 distribution at the plasma membrane

Auxin regulates a plethora of developmental and growth processes in plants, including embryogenesis, stem cell maintenance, lateral organ formation and responses to tropic stimuli. How this relatively small molecule is able to influence such a remarkable diversity of processes has been intensively investigated. It is currently thought that the relative distribution of auxin within a tissue, or even between individual cells, is critical. The cellular transporters of auxin have therefore received particular attention, specifically auxin exporters of the PIN family, as they are often enriched in distinct polar regions of the plasma membrane to facilitate directional auxin transport. Moreover, relative auxin distribution patterns, visualized by cellular auxin response markers, generally correlate well with the polar orientation of PINs within a given tissue (Benková et al., 2003; Friml et al., 2003; Marhavy et al., 2014). However, the establishment of polarity in plant cells is poorly understood to date. Research on how PINs are polarly targeted within cells has thus emerged as not only important in the context of auxin transport, but also in terms of polar protein trafficking in plants in general.

For this thesis, I established phosphosite-specific antibodies against the previously characterized PIN1 phosphorylation sites S1 - S4 and at least three of these antibodies directed against S1, S2 and S4 showed high specificity towards their respective phosphorylated epitopes. The sites S1 - S3 had previously been linked to the control of PIN1 polarity (Kleine-Vehn et al., 2009; Dhonukshe et al., 2010; Huang et al., 2010), while all four sites were shown, in *Xenopus* oocytes, to regulate

PIN1 transport activity (Zourelidou et al., 2014). Employing the phosphosite-specific antibodies in whole mount immunlocalization experiments enabled me to directly assess the contribution of each individual site to PIN1 polarity and activity. I could show that PIN1 was phosphorylated at all four sites at the basal plasma membrane (Fig. 8 and 11), as well as at lateral and apical sides upon overexpression of *PID,* as well as extended BFA treatment in roots (Fig. 10, 15 and 17). Furthermore, differentially GFP-tagged PIN1 targeted to the basal or apical plasma membrane in epidermal cells showed localization-independent phosphorylation (Fig. 18).

My results suggest that PIN1 phosphorylation was not associated with a particular plasma membrane region. Instead, the phosphorylation signals followed the general distribution of PIN1. Interestingly, in *Arabidopsis* embryo tissue, PIN1 endogeneously assumes different polarities, depending on cell type. Apically localized PIN1 in the epidermis directs auxin streams towards incipient cotyledon initiation sites and basal PIN1 in the inner cells helps establish the early auxin maximum above the hypophysis (Friml et al., 2003). According to my findings here, both of these differentially localized PIN1 pools should show a phosphorylation signal, as PIN1

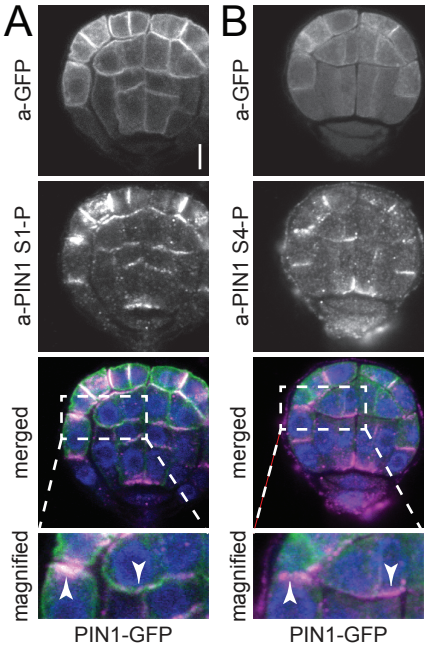

Figure 24: PIN1 is phosphorylated at apical and basal plasma membranes of *Arabidopsis* embryos.

Representative confocal images of Arabidopsis PIN1-GFP embryos stained with anti-GFP (a-GFP; PIN1-GFP (green) and a-PIN1 S1-P (magenta) (A) or a-PIN1 S4-P (magenta) (B) antibodies. Arrowheads mark the immunostaining at the plasma membrane. Merged images also include DAPI staining of nuclei (blue). Scale bar = 5 µm.
Experiments were performed by Sandra Richter and Gerd Jürgens (University of Tübingen).

phosphorylation was not associated with a particular polar region. In order to test this hypothesis, I collaborated with Sandra Richter and Gerd Jürgens (University of Tübingen) to probe *Arabidopsis* embryos for their PIN1 phosphorylation status, using PIN1-GFP transgenic lines. Indeed, they could observe apically, as well as basally localized PIN1-GFP phosphorylated at S1 and S4 in epidermal and provasular cells, respectively (Fig. 24). PIN1 phosphorylation at S1 and S4 therefore occurred independently from polarity control also in the complex tissue of *Arabidopsis* embryos, where PIN1 is endogenously differentially localized. These results are also consistent with our previous data that phosphorylation of PIN1 is required for transporter activity (Willige et al., 2013; Barbosa et al., 2014; Zourelidou et al., 2014), as both PIN1 pools in the embryo should be actively transporting auxin.

4.1.2 PIN1 phosphorylation dynamics correlate with differentially trafficking kinases

Basal PIN1 phosphorylation in root tissue was highly sensitive to the endosomal trafficking inhibitor BFA (Fig. 8, 11, 17 and 18). In cases where PIN1 was preferentially enriched at the apical plasma membrane, on the other hand, phosphorylation was largely insensitive to BFA treatments (Fig. 17 and 18). The AGCVIII kinase D6PK was previously shown to localize to the basal plasma membrane in a BFA-sensitive manner (Fig. 9 and 19) (Barbosa et al., 2014), whereas the apolar distribution and abundance of the structurally related PID kinase at the plasma membrane is largely BFA-insensitive (Fig. 9 and 19) (Kleine-Vehn et al., 2009).

The PIN1 phosphorylation dynamics I observed at the basal plasma membrane of root cells was highly congruent to the intracellular trafficking behavior of BFA-sensitive kinases such as D6PK. The rapid return of a specifically basal phosphorylation signal after washout of BFA at all four phosphosites is especially intriguing, as D6PK follows very similar kinetics under comparable conditions (Barbosa et al.,

2014). Moreover, basal phosphorylation was detectable well before PIN1 polarity is re-established (Fig. 8), a process that reportedly occurs only after several hours of BFA removal (Dhonukshe et al., 2008; Kleine-Vehn et al., 2008c) (Dhonukshe et al., 2008, retracted, see section 3.3.3).

Interestingly, I also observed selective basal phosphorylation of PIN1 in PIN1-GFP2, as well as estradiol-treated *XVE>>PIN1* root epidermal cells (Fig. 18 and 21), which reflected D6PK, rather than PID plasma membrane association patterns (Fig. 19) in cells where both kinases are endogenously expressed. In both cases, PIN1 was enriched at the basal plasma membrane, but could clearly be detected at lateral and apical membranes as well. While the failure to detect phosphorylation at lateral and apical membranes could be due to the relatively low abundance of PIN1 and thus an issue of detection limit by the phosphosite-specific antibodies, it suggests that these PIN1 variants preferentially interact with D6PK family kinases. The BFA-sensitivity of basal PIN1 phosphorylation supports this notion.

Prolonged BFA treatments on the other hand sometimes led to selectively apical PIN1 phosphorylation signals (Fig. 10 and 20) and apical PIN1-GFP3 phosphorylation was selectively BFA insensitive in epidermal cells (Fig. 20). BFA-insensitive apical phosphorylation could thus be mediated by correspondingly unresponsive PID family kinases. Earlier reports had already indicated that PIN1 plasma membrane association is selectively sensitive to BFA at the basal plasma membrane (Kleine-Vehn et al., 2008c; Kleine-Vehn et al., 2009). My results could thus reflect the general insensitivity of the apical trafficking pathway to BFA. Interestingly, BFA treatment induces the expression of *PID* and leads to immobilization of PP2A phosphatases that antagonize PIN1 phosphorylation (Rahman et al., 2010). The appearance of apical PIN1 phosphorylation in PIN1-GFP2 epidermal cells (Fig. 20) and of endogenous PIN1 in the stele (Fig. 10), both after prolonged BFA treatments, could thus

have resulted from elevated levels of PID. An important question that remains unresolved, however, is why apolar, BFA-insensitive kinases such as PID are seemingly unable to maintain basal PIN1 phosphorylation in the absence of BFA-sensitive kinases at the plasma membrane. Additional, basally localized, BFA-sensitive factors could be required for the maintenance of these phosphorylation events.

4.1.3 Differential phosphosite preference does not explain divergent biological functions of D6PK and PID

We had argued previously that differential phosphosite preference of D6PK and PID observable *in vitro* towards S4 and S1 - S3, respectively (Fig. 5) (Zourelidou et al., 2014), could explain the different biological functions of these two kinases *in vivo*. I had therefore chosen a-PIN1 S1-P and a-PIN1 S4-P as representative sites for detailed analysis. I could not find evidence, however, for a differential regulation of any of the four phosphorylation targets investigated here. While potential differences in antibody affinity or epitope accessibility precluded a more stringent direct comparison of the four target sites, the phosphorylation dynamics of all four sites were similarly sensitive to BFA and S1 and S4 phosphorylation patterns were highly congruent throughout my experiments. Moreover, the BFA-dependent phosphorylation dynamics as visualized with the individual site-specific antibodies could be reproduced biochemically in immunoblots (Fig. 11) and thus likely reflect the general phosphorylation state of PIN1 in root tissue. In light of these results, our interpretation that phosphosite preference underlies the differential effects of D6PK and PID on PIN1 polarity is no longer suitable. The similar phosphorylation dynamics rather suggest that S1 - S4 phosphorylations are mediated by the same kinases, depending on the polar localization of PIN1. The effects of PID on PIN1 polarity therefore likely involve additional components, as will be discussed in section 4.3.3.

4.2 Establishment of polarity in animals and plants

The mechanisms by which plants establish and maintain polarity within a given cell are poorly understood. The animal field, on the other hand, has amassed a large body of knowledge on the subject of polarity establishment. A master regulator of polarity in animals is the small GTPase Cdc42 (CELL DIVISION CONTROL PROTEIN42). It is able to locally modify the actin cytoskeleton by selective recruitment of actin polymerization factors [reviewed by (Slaughter et al., 2009)]. In multicellular organisms, the establishment of polarity, occurring before the first cell division of the zygote, is crucial for proper development. The discovery of *partitioning defective* mutants in the model system *Caenorhabditis elegans* was a crucial step in this analysis. There, two sets of functionally diverse proteins organize in a mutually exclusive manner at the anterior (Par3, Par6, aPKC) and posterior (Par1, Par2) poles of the zygote, respectively. This is thought to be initiated by the entry of the sperm nucleus, followed by cytoskeletal rearrangement and asymmetrical cortical contractions that lead to the accumulation of Par3, Par6 and aPKC at the anterior pole. A phosphorylation-dependent feedback loop then reinforces the separation of the partitioning factors at the plasma membrane. aPKC is able to phosphorylate Par1, leading to its dissociation from the plasma membrane. Conversely, Par1 can phosphorylate Par3, which causes dissociation of Par3 oligomers and loss of membrane affinity. In this manner, the two complexes mutually exclude each other from their respective plasma membrane domains. These polarly localized protein complexes then serve as an instructive signal scaffold for correct orientation of the cell division plane and proper delivery of asymmetrically distributed cargo, such as membrane proteins and phospholipids, within the cell [reviewed by (McCaffrey and Macara, 2009; Munro and Bowerman, 2009)].

The Par complexes, as well as the role of Cdc42, are highly conserved across

metazoans and are utilized as polarization determinants in many different cell types. However, these proteins are absent from plant genomes. Multicellularity evolved independently in animals and plants. Moreover, whereas animal cells are able to migrate relative to each other, plant cells, due to the existence of a rigid cell wall, are "locked in space", elevating the importance for accurate positional information between cells. Consequently, the components for the establishment and maintenance of polarity seem to be quite distinct. How exactly the axis of polarity during plant embryogenesis is initially established, or whether there exists an initial extrinsic cue for polarization, is still poorly understood. However, polarization defects observed in mutants of the MAPKKK (MITOGEN ACTIVATED PROTEIN KINASE KINASE KINASE) *YODA* could be an indication for the presence of such an external signal, as MAPK signaling generally involves the integration of external stimuli. An intriguing candidate is auxin derived from the maternal endosperm. This notion finds support in the embryonic polarity defects of *pin* mutants, as well as those of the transcriptional auxin signaling components *monopteros* and *bodenlos*. Furthermore, auxin distribution during embryogenesis is dynamically asymmetrical from the first cell division event onwards. Accurate intracellular PIN localization is therefore likely to be one of the earliest polarization events during plant development and elucidation of the underlying mechanisms crucial for advancing our understanding of the establishment of cellular polarity in plants [reviewed by (Geldner, 2009; Petricka et al., 2009; Shao and Dong, 2016)].

The well documented effects of PID on PIN polarity are not disputed in this thesis but could in fact be largely confirmed. However, specifically my experiments using plants with inducible overexpression of PID (Fig. 15), which are in line with published data (Friml et al., 2004), show that prolonged induction times of 22 hours were necessary to reliably observe PIN1 polarity changes, indicating that the effects

could be indirect.

While the above mentioned differences between plants and animals in terms of polarity establishment have made direct mechanistic comparisons difficult, transcytosis described in the animal literature are reported to occur much faster. The two examples given in the introduction, namely the phosphorylation-dependent translocation of GLUT4 and pIgR are reported to occur approximately within 30 - 60 minutes (Sano et al., 2003; Zeigerer et al., 2004; Su et al., 2010). The relatively slow effects of PID-dependent phosphorylation on PIN1 apicalization in root stele tissue could therefore indicate that other important regulatory components required for PID activity are absent from these cells. The phosphorylation of PIN1 S1 - S4 by two different kinase families, D6PK and PID, resulting in apparently diverging biological outcomes strengthen this argument. PID has been shown to interact with other proteins aside from PIN1 that could influence its activity (Benjamins, 2003, 2004). Differences in intracellular trafficking and localization, as well as sequence-specific variations between D6PK and PID family kinases suggest that the molecular interactions of these two families could also be divergent and thus allow for the differential biological outputs that result from phosphorylating the same target sites on PINs. Additionally, PID-independent PIN1 polarization mechanisms have been reported (Zhang et al., 2010; Jia et al., 2016), pointing to the complexity of this process.

4.3 PIN1 polarity regulation

4.3.1 PIN1 S1 phosphorylation is not a polarity determinant

Phosphorylation of S1 - S3 by the AGCVIII kinase PID was proposed to direct the apical targeting of PIN1 in root and shoot tissue (Dhonukshe et al., 2010; Huang et al., 2010). Based on sequence homology for the PIN1 phosphorylation sites around S1, S2 and S3 (Fig. 5), which all lie within a conserved TPRXS(N/S) motif,

phosphorylation and concomitant apical targeting were proposed to be a conserved mechanism among the plasma membrane-resident PINs. As described above, however, the data presented in this thesis, particularly phosphorylation of PIN1 S1 for apically, as well as basally targeted PIN1 in epidermal cells, argue against this model. Intriguingly, a previous report had investigated the cellular dynamics of PIN2 in the root epidermis, the endogenously expressed PIN in these cells. There, cell biological analysis of a PIN2 S123A phospho-mutant construct revealed that this transgene was only mistargeted in the cells adjacent to the root cap, while the remaining epidermal cells of the meristem targeted this construct apically, like wild type PIN2 (Dhonukshe et al., 2010). Taken together, these results dispute a conserved role for phosphorylation of S1 - S3 in mediating the apical targeting of PINs.

It is currently unknown how root epidermal cells differentially localize PIN1-GFP2 and PIN1-GFP3. However, removal of the GFP-tag results in basal PIN1 polarity in these cells (Wiśniewska et al., 2006). Therefore, the insertion of GFP close to PIN1 S1 in the PIN1-GFP2 construct is not expected to interfere with the targeting of this transgene. Instead, it seems that the differentially positioned GFP-tag results in alternative molecular interactions with the intracellular trafficking machinery or other polarity determinants. Importantly, however, my phosphorylation analysis suggests that the interaction of different kinases such as D6PK and PID with PIN1 is not a determinant of, but rather dependent on PIN1 polar localization.

Previous reports had suggested that S1 - S3 phosphorylation directs PIN1 towards the BFA-insensitive apical trafficking pathway (Kleine-Vehn et al., 2009). I could not find evidence, however, for PIN1 S1 - S4 phosphorylation during intracellular transport, as I was unable to detect phosphorylation signals when PIN1 was allowed to accumulate in the so-called BFA compartments. Although the phosphosite-specific antibodies recognized intracellular structures, these structures did not reliably

co-localize with a-GFP (PIN1-GFP) signals inside the cell. I therefore judged the signals from these structures to be unspecific background. While the expertise and kind technical support from Peter Marhavý and Eva Benkova at the Institute of Science and Technology in Vienna enabled me to reduce this unspecific binding over the years, I failed to completely abolish it. Nevertheless, the clearest evidence that these punctae represented unspecific signals came from the observation that they were also present outside of the *PIN1* expression domain (Fig. 25). My findings therefore do not support the proposed role for S1 - S3 phosphorylation in regulating intracellular PIN1 trafficking. My findings rather indicated that PIN1 phosphorylation occurred exclusively at the plasma membrane, a notion that was already proposed

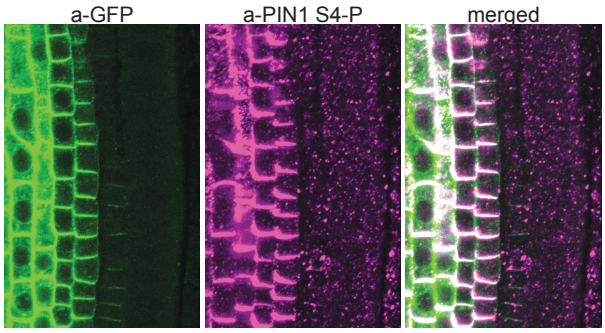

Figure 25: Punctae produced by phosphosite-specific antibodies constitute background signal.
Representative confocal image of an *Arabidopsis* PIN1-GFP root meristem stained with anti-GFP (a-GFP; PIN1-GFP (green) and a-PIN1 S4-P (magenta) antibodies. Punctate structures are clearly present outside the PIN1 expression domain and there is no clear overlap between these structures and the PIN1 signal obtained from PIN1:GFP in intracellular structures.

previously (Kleine-Vehn et al., 2009; Barbosa et al., 2014).

I further argue against an involvement of at least S1 in PIN1 polarity control, as phosphorylation of this site was not associated with a particular localization of PIN1. This was even the case in the shoot apical meristem of *pid* mutant plants. There, it was thought that the basal mistargeting of PIN1 in the epidermis was due to a lack of PID-mediated phosphorylation of S1 - S3 (Huang et al., 2010). My analysis of such meristems revealed PIN1 phosphorylation at the basal plasma membrane in the absence of PID (Fig. 22). While redundantly acting kinases such as WAG1 and WAG2 could be mediating these phosphorylation events (Dhonukshe et al., 2010),

my observations offer no indication that S1 phosphorylation mediates the apical targeting of PIN1 in this tissue.

4.3.2 PIN1 phospho-mimetics do not show auxin transport activity

Our earlier work showed that PIN1 S1 - S4 phosphorylation is essential for PIN1 auxin transport activity in *Xenopus* oocytes. Furthermore, phospho-mutant variants of PIN1, where S1 - S4 had been mutated to unphosphorylatable alanine (A) residues PIN1 S1234A, were no longer subject to kinase-mediated activation (Zourelidou et al., 2014). On the other hand, evidence for an involvement of S1 - S3 phosphorylation in PIN1 polarity control came in part from observations that a PIN1 S123A variant was mistargeted basally in shoot epidermal cells and was no longer apicalized upon PID overexpression in the root. Conversely, a phospho-mimetic PIN1 S123E version did not polarize properly to the basal plasma membrane in root cells. As expected, based on the functionally important PIN1 trafficking dynamics, neither PIN1 S123A, nor PIN1 S123E were able to rescue the *pin1* mutant phenotypes (Huang et al., 2010).

We had previously shown that a PIN1 S1234A construct was no longer subject to kinase-mediated activation in *Xenopus* oocytes (Zourelidou et al., 2014) and my findings in this thesis support a biological significance of phosphorylation-dependent efflux activation at S1 - S4. It could thus be argued that a PIN1 S123E, or the more complex PIN1 S1234E phospho-mimetic variant, should show constitutive kinase-independent transport activity. I therefore collaborated with Astrid Fastner and Ulrich Hammes (University of Regensburg) to analyze these phospho-mimetic constructs for auxin transport activity in *Xenopus* oocytes. Interestingly, they found that neither PIN1 S123E, nor PIN1 S1234E, showed kinase-independent activity, nor were they activatable by addition of D6PK or PID to the system (Fig. 26). The phospho-mimetic constructs thus rather behaved like the PIN1 S1234A phospho-mutant

version, indicating that, at least in terms of auxin transport capacity, PIN1 S1234E constituted a transporter with reduced functionality. While this does not rule out the possibility that the intracellular trafficking machinery might still recognize the S - E replacements as phospho-mimics, it could imply that mistargeting of this PIN1 variant *in planta* is the result of transporter inactivity.

Plants expressing PIN1 S123E in the *pin1* mutant background did not show a collapse of the root meristem associated with phosphorylation at these sites. This had been attributed to the need for apicalization of multiple PINs in root tissue (Huang et al., 2010). The insufficiency, however, of both PIN1 S1234A and PIN1 S123E to induce root meristem collapse can also be explained by the auxin transport deficiency of both constructs. The inactivity of PIN1 S1234E in the oocyte system could in fact be interpreted as conflicting with our hypothesis that S1 - S4 phosphorylation is essential for transporter activity. I propose, however, that this primarily reflects the need for dynamic phosphorylation of PIN1 and possibly dynamic kinase interaction at the plasma membrane for proper transporter functionality in terms of activity, as

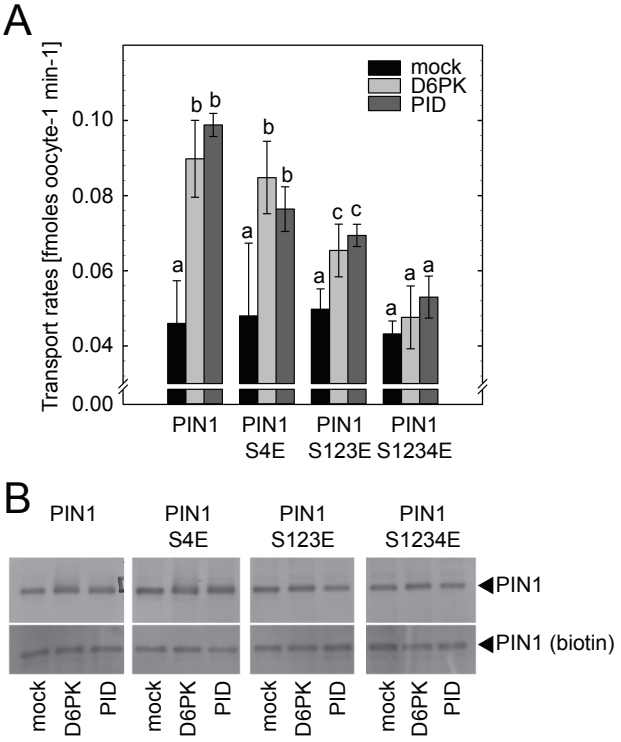

Figure 26: A PIN1 S1234E phospho-mimic variant behaves like a functionally compromised transporter in *Xenopus* oocytes.
A. Auxin (indole-3-acetic acid, IAA) transport rates of Xenopus oocytes injected with PIN1 or PIN1 variants where S (serine) phosphosites had been replaced by possibly phosphorylation-mimicking E (glutamic acid) residues, together with protein kinases or a mock control injection as specified in the legend. B. Immunoblot analysis of Xenopus oocytes injected with PIN1 variants and protein kinases (or mock) as specified. Upper panel, membrane fraction; lower panel, immunoblots of proteins following surface biotinylation demonstrating the presence of equal amounts of PIN1 in the plasma membrane of all oocytes.
Experiments were performed by Astrid Fastner and Ulrich Hammes (University of Regensburg).

well as polarization.

4.3.3 PIN1 polarity control involves many players

In my hands, PIN1 apicalization upon *PID* overexpression was observed to varying degrees across different cell files of the root stele in lines generated for this study by Melina Zourelidou (Fig. 15 and 17), as well as from previously published work (Fig. 15) (Dhonukshe et al., 2010). Additionally, my analysis of PIN1 S123E polarity in the root meristem presented a rather heterogeneous localization (data not shown), as was indicated in the original publication (Huang et al., 2010). While, as stated, the effects of *PID* overexpression on PIN polarity are not disputed here, I argue that more complex models are required, as my observations show that a PIN1 S1 - S3 phosphorylation-dependent mechanism is not sufficient to explain differential PIN1 targeting to the apical plasma membrane. This is also evident from the reported effects on PIN polarity that occur independently from PID activity. The phosphorylation of S/T 337/340 within the PIN1 cytoplasmic loop was shown to be sufficient for apicalization of PIN1 in roots (Zhang et al., 2010). Furthermore, this site was recently demonstrated to be phosphorylated by a MAPK cascade involving MPK6 and to be targeted by a peptidyl-prolyl *cis*/*trans* isomerase, Pin1At. This enzyme is able to induce a conformational change at phosphorylated serine/threonine-proline motifs and may thereby, apparently, influence the polar localization of PIN1 (Jia et al., 2016).

Another interesting class of proteins that have emerged as PIN polarity regulators belong to the NPH3 (NON PHOTOTROPIC HYPOCOTYL3) family of proteins. As the name suggests, the founding member of this large gene family in *Arabidopsis* was identified in a genetic screen for mutants defective in hypocotyl phototropism (Liscum and Briggs, 1995). Its interaction with the blue light receptor phot1 was shown to promote ubiquitination-mediated modulation of the phototropic response

(Roberts et al., 2011).

Several independent forward genetic screens subsequently identified the related NPH3-like protein ENP/MAB4/NPY1 (NAKED PINS IN YUCCA1) as a genetic enhancer of *pid*-mediated phenotypes, particularly during embryonic cotyledon formation (Treml et al., 2005; Cheng et al., 2007; Furutani et al., 2007). These findings hinted at a functional module by which AGCVIII kinases and NPH3-like proteins modulate PIN polarity and auxin-mediated organogenesis concertedly (Cheng et al., 2008). For D6PK, however, a possible interaction with NPH3-like proteins has as yet not been reported. Importantly, mutation of NPY1 and its close homologues NPY2-5 were shown to lead to drastic PIN polarity defects and auxin-related phenotypes, such as defects in embryonic development, floral organ formation and root gravitropism (Cheng et al., 2008; Furutani et al., 2011; Furutani et al., 2014), independently from PID activity. NPY proteins themselves are polarly localized at the plasma membrane and, intriguingly, mimic the polar localization of PIN proteins in all tissues and cells analyzed. Moreover, NPY4, which is normally expressed in root stele cells and co-localizes there with basal PIN1, assumes an apical polarization in epidermal cells when ectopically expressed there (Furutani et al., 2011). It is therefore tempting to speculate that NPY proteins are crucial structural anchors for PIN proteins at specific plasma membrane regions.

Recently, another enhancer of *pid*-mediated cotyledon development, AtMOB1a, was identified. Mutation of this gene leads to decreased cellular auxin responses and to decreased expression of *PIN1* in the *pid* mutant background, whereas PIN1 polar localization was not reported to be affected in the double mutant (Cui et al., 2016). Similarly, close examination of the different NPY proteins suggested that, while some seem to be directly involved in the polarization of PINs, others might control downstream cellular auxin responses not directly related to PIN plasma membrane

localization or activity (Ito et al., 2011). An anchoring function for PINs has even been attributed to the cell wall, which seems to limit the lateral diffusion of PINs at the plasma membrane (Feraru et al., 2011). Taken together, the available data suggest that PID, as well as its genetic interactors do not merely influence polar PIN distribution, but are also involved in other auxin responses that might not directly be related to the polarity of PINs. Conversely, the emerging picture suggests that dynamic polarization of PINs at the plasma membrane involves many players that regulate this process at many levels. While PID is no doubt one of these players, I argue that its phosphorylation of the PIN1 target sites S1 - S3 promotes auxin efflux, and that its involvement in the regulation of PIN polarity involves other components and additional signaling mechanisms yet to be identified.

4.4 PIN1 S1 - S4 phosphorylation regulates PIN1 transport activity *in planta*

We previously reported that PIN phosphorylation at the plasma membrane is a prerequisite for efficient PIN-mediated auxin transport (Willige et al., 2013; Barbosa et al., 2014; Zourelidou et al., 2014). Multiple lines of evidence suggest that the dynamics of these phosphorylation events are crucial in the regulation of auxin efflux-dependent processes. Importantly, we were able to closely correlate dynamic PIN phosphorylation to the intracellular trafficking dynamics of the AGCVIII kinase D6PK. Chemical or genetic interference with the proper function of *D6PK* family genes results in reduced PIN phosphorylation and causes defects in auxin transport related processes such as gravitropic growth or phototropic bending of *Arabidopsis* hypocotyls (Willige et al., 2013; Barbosa et al., 2014). We could, in fact, demonstrate that the basipetal auxin transport in these hypocotyls is severely reduced (Willige et al., 2013). The negative correlation between D6PK kinase family function and

efficient basipetal auxin transport is also evident in inflorescence stems. There, our analysis using selective reaction monitoring mass spectrometry indicated that PIN1 phosphorylation, specifically at the target site S4, was strongly reduced in complex *d6pk* mutants (Zourelidou et al., 2014).

While the highly dynamic auxin transport streams in *Arabidopsis* roots have complicated the establishment of similar correlations between D6PK function and auxin transport at the organ level, the use of cellular auxin response markers has facilitated tissue-specific analysis. Application of the exocytosis inhibitor BFA to cells of the root apical meristem results in rapid and reversible depletion of D6PK from the basal plasma membrane, congruent with a similarly reversible loss of PIN1 phosphorylation, monitored by a phosphatase-sensitive, low mobility smear on PIN1-GFP immunoblots. The effects of BFA can further be correlated to intracellular accumulation of auxin in the same cells, as measured by a quantitative decrease in DII-VENUS reporter signal intensity (Fig. 14) (Barbosa et al., 2014). I thus propose a mechanism by which dynamic PIN phosphorylation at the plasma membrane regulates auxin efflux-dependent growth.

One implication of such a mechanism would be the presence of phosphatases at the plasma membrane acting to dephosphorylate PINs in the absence of active kinases. PP2A-type phosphatases have previously been implicated in the regulation of PIN phosphorylation; however, effects of genetic interference, particularly of PP2A regulatory subunits such as *rcn1,* were generally linked to the polar localization of the transporters and the therein resulting alterations in auxin transport streams (Michniewicz et al., 2007b). Genetic analysis in this context has been complicated by high redundancy among closely related sub-complexes of the phosphatase holoenzymes. Pharmacological inhibition of phosphatase activity has therefore been used as a tool to study their involvement in plant development and growth.

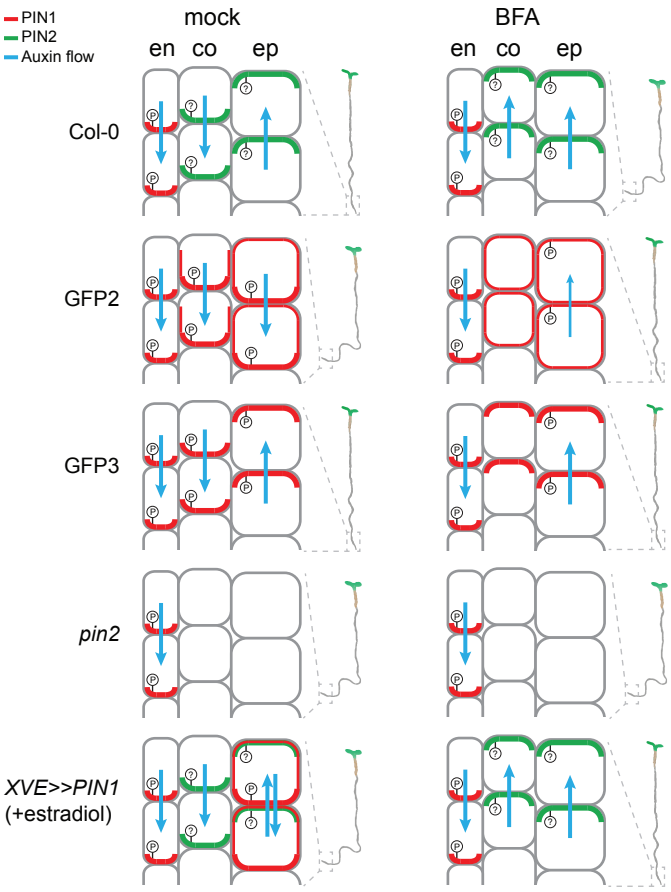

Figure 27: Model for the correlation of PIN1 phosphorylation patterns with hypothetical auxin transport streams and the consequences on root gravitropic growth.

Illustration depicting PIN1 and PIN2 polarization, as well as PIN1 phosphorylation in different cell files of the *Arabidopsis* primary root meristem, as specified in the legend. The direction of the blue arrows depicting the flow of auxin is derived from BFA-dependent polar PIN1 phosphorylation patterns at the plasma membrane, as well as from previously published data on BFA-dependent PIN2 polarity during root gravitropic growth (Rahman et al., 2010). en = endodermis; co = cortex; ep = epidermis.

Interpretation of such experiments has to be conducted carefully, due to the surely pleiotropic effects of such inhibitors. Nevertheless, analyses using the phosphatase inhibitor Cantharidin had suggested an involvement of protein dephosphorylation in negatively regulating root and hypocotyl elongation, emergence of lateral roots and root and shoot gravity responses, which could all be explained by alterations in auxin transport (Rashotte et al., 2001; Shin et al., 2005; Rahman et al., 2010).

In this thesis, I provide further evidence for the importance of dynamic PIN1 phosphorylation at the plasma membrane in controlling efficient cellular auxin efflux. My analysis of specific phosphorylation events further suggests that PIN1 phosphorylation at S1 - S4 follows these dynamics quite accurately. Not only could I correlate PIN1 S1 - S4 phosphorylation to the presence of BFA-sensitive kinases such as D6PK at the plasma membrane, I was also able to establish a close relationship between PIN1 phosphorylation dynamics and cellular auxin accumulation by com-

bining immunohistochemical PIN1 phosphorylation experiments with live imaging of DII-VENUS reporter lines. Particularly the Cantharidin-mediated inhibition of phosphatase activity in combination with BFA treatments delayed both dephosphorylation of PIN1 and BFA-induced cellular auxin accumulation (Fig. 13 and 14).

It was previously suggested that the polar localization of PIN proteins is sufficient to explain the directionality of auxin transport streams at the tissue level (Wiśniewska et al., 2006). However, the treatments in the experiments described above affected the polar localization of PIN1 only minimally, while the effects on PIN1 phosphorylation and DII-VENUS signal intensities were statistically significant. This suggests that PIN polarity might in fact not be adequate to explain all dynamic changes in auxin transport. In order to corroborate this claim, I made use of gravitropic root growth as a physiological readout for the effects of PIN1 phosphorylation on the well described dynamic auxin transport streams governing this growth response. There, I was able to correlate BFA-induced changes in the PIN1 phosphorylation status at S1 and S4 with a rescue in gravitropism (Fig. 20 and 21). Importantly, as the illustra-

Figure 28: Alignment of the PIN1 protein sequence from agriculturally relevant species.

Muscle alignment of the PIN1 protein sequence from *Arabidopsis thaliana* (*A.th.*) (highlighted as reference sequence, partial sequences shown), *Solanum lycopersicum* (*So.ly.*), *Oryza sativa* (*Or.sa.*), *Zea maize* (*Z.m.*) and the moss *Physcomitrella patens* (*P.p.*). The highly conserved target serines and surrounding motifs are marked in red (S1 - S3) or blue (S4). The less conserved motif around the target site S337 is also marked in black.

tion in figure 27 describes, the observed PIN1 phosphorylation patterns, not simply PIN1 polarity, accurately predicted putative dynamic auxin transport routes at the tissue level that occur during the complex process of gravitropic root growth.

Overall, the available evidence points to a functional regulation of auxin efflux activity at the plasma membrane at least of PIN1 by reversible phosphorylation in general, as well as specifically at the target sites S1 - S4 within the PIN1 cytoplasmic loop. The phosphosite-specific antibodies targeting S1 - S4 established in this thesis will therefore be an important tool for future investigations into developmental and environmental growth responses governed by PIN-mediated auxin transport. Moreover, the PIN cytoplasmic loop contains other functionally relevant phosphorylation sites, for which the type of analysis performed here could shed light on the *in planta* role at cellular resolution. Finally, phosphorylation-dependent auxin transport by PINs appears to be conserved among agriculturally relevant plant species, such as rice. High sequence homology around many of the known PIN1 phosphorylation sites in crop plants like rice, maize and tomato argues for functional conservation of the herein proposed regulation of PIN1 in those species (Fig. 28). As the immunohistochemical techniques applied in this work do not strictly require often arduous genetic manipulation of the organism studied, a transfer of this kind of methodology to many other species is feasible and will surely expand our understanding of cellular auxin transport beyond the model plant *Arabidopsis thaliana*.

4.5 Additional kinases phosphorylate PIN1

The plant-specific class of AGCVIII kinases comprises 23 members in the *Arabidopsis* genome (Galvan-Ampudia and Offringa, 2007). Genetic analysis has revealed at least partial functional redundancy among three or four D6PK family members D6PK0, D6PKL1, D6PKL2 and possibly D6PKL3 (Zourelidou et al., 2009), as well

as among at least three of the four members of the PID family, including WAG1 and WAG2 (Cheng et al., 2008; Dhonukshe et al., 2010). A functional role for PIDL2 has not been reported as yet specifically, however the complex quadruple mutant displays some enhancement of phenotypes, such as defects in cotyledon development (Cheng et al., 2008).

My analysis of complex mutants of these two kinase families in terms of their contribution to PIN1 phosphorylation in the root apical meristem indicated that as yet unknown kinases could be involved in regulating PIN1 through phosphorylation (Fig. 23). It is thus reasonable to speculate that members of the AGCVIII class still awaiting functional characterization are among those kinases.

The phot2 blue light receptor, as well as UNC (UNICORN) were previously found not to activate PIN1-mediated auxin transport in *Xenopus* oocytes (Zourelidou et al., 2014), suggesting that this function might be restricted to a subgroup of AGCVIII kinases in close evolutionary proximity to the D6PK and PID families. To investigate this idea, Lena Frank, as part of her master thesis, performed *in vitro* phosphorylation experiments using the PIN1 cytoplasmic loop as a substrate. Interestingly, she was able to observe auto-, as well as trans-phosphorylation not only when adding recombinantly expressed D6PK or PID, respectively, the related kinases D6PKL3, AGC1-5 and KIPK displayed similar activity towards the PIN1 substrate (Fig. 29). The latter kinases thus qualify as additional PIN1 phospho-regulators. Their careful genetic, biochemical and cell biological analysis will be vital, if we are to paint a more complete picture of PIN-mediated auxin transport processes. The phospho-site-specific antibodies established here, as well as others designed for novel target sites, will then be instrumental in ongoing investigations into not only auxin biology,

but such fundamental processes as the establishment of cellular polarity in plants.

4.6 Concluding remarks

In this thesis I analyzed the *in planta* functional impact of specific phosphorylation events at the previously identified target serines S1 - S4 on the cytoplasmic loop of the PIN1 auxin efflux carrier in *Arabidopsis thaliana*. Phosphorylation of these sites by the AGCVIII kinases D6PK, PID and WAG2 was previously shown to be essential for PIN1-mediated auxin transport in *Xenopus* oocytes (Zourelidou et al., 2014). Since prior studies had already linked phosphorylation of S1 - S3 specifically

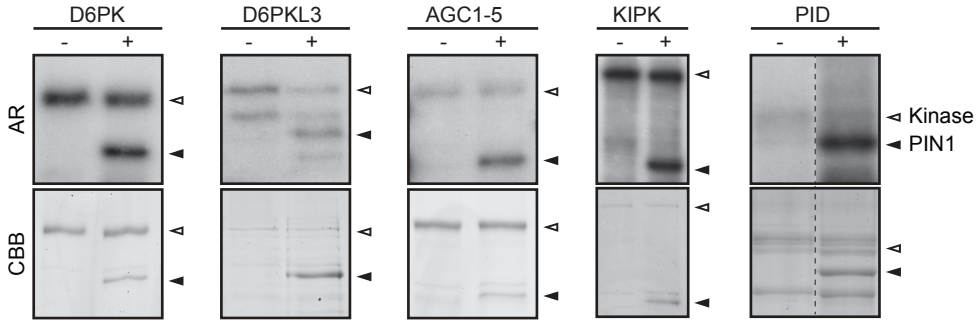

Figure 29: Related kinases from the AGCVIII family phosphorylate the PIN1 cytoplasmic loop *in vitro*.

Results from a phosphorylation experiment using recombinant AGCVIII kinases (Kinase) as specified and a PIN1 cytoplasmic loop substrate (PIN1). AR, autoradiograph; CBB, Coomassie Brilliant Blue-stained gel as a loading control.
Experiments were performed by Lena Frank and Melina Zourelidou.

by the PID sub-family (including WAG1 and WAG2) of AGCVIII kinases to the polar targeting of PIN1 towards the apical plasma membrane in various tissues and cell types (Kleine-Vehn et al., 2009; Dhonukshe et al., 2010; Huang et al., 2010), I aimed to determine the consequences of S1 - S4 phosphorylation in terms of PIN1 polarity and activity regulation, as well as the contribution of the different AGCVIII kinase sub-families to these phosphorylations. To this end, I established phosphosite-specific antibodies for use in immunohistochemical experiments and at least three, directed against PIN1 S1, S2 and S4, showed high specificity towards the respective

phosphorylated epitope.

I find that PIN1 is phosphorylated at all four phosphosites when present at the basal plasma membrane in the root. Furthermore, PIN1 S1 and S4 phosphorylation could be detected at the apical, as well as basal side of the plasma membrane in different cell types and tissues, often in accordance with the prevailing PIN1 distribution pattern. Except when PIN1 was allowed to accumulate in BFA compartments, no phosphorylation signal could be detected, providing corroborating evidence for preferential PIN phosphorylation at the plasma membrane. I further show that apical and basal PIN1 phosphorylation are differentially BFA-sensitive, suggesting the involvement of kinases with contrasting intracellular trafficking behavior.

I conclude that PIN1 S1 - S4 phosphorylation does not allow predicting PIN1 polarity in different cell types of various tissues. My data challenge the existing model of PIN1 polarity control by PID-dependent phosphorylation at specific phosphosites and rather argue for PIN auxin efflux transporter activation as the primary activity of PIN phosphorylation at the target sites investigated here. Therefore, differential phosphosite preference of D6PK and PID likely does not contribute to their divergent effects on PIN1 polarity. Instead, additional, as yet unidentified factors contribute to PID-dependent polarity control of PINs. Finally, this work implicates novel regulators of PIN phosphorylation among specific, closely related AGCVIII kinases, whose characterization should be exciting future research.

Interestingly, the absence of supposedly efflux-activating phosphorylations on intracellular PIN1 pools as described in this thesis are in disagreement with a longstanding proposal that constitutive intracellular PIN recycling could serve a "neurotransmitter-like" mechanism by which PIN-containing endosomes would be loaded with auxin and subsequently fuse with the plasma membrane to release the cargo extracellularly (Baluska et al., 2003; Schlicht et al., 2006; Baluska et al., 2008; Ra-

makrishna et al., 2011; Mettbach et al., 2017). This type of mechanism would, however, require PINs to be active while residing on internal compartments, for which I could not find evidence. An alternative speculation would be that continuous cycles of ATP-dependent phosphorylation-dephosphorylation of PINs at the plasma membrane provide the energy required to transport auxin against its concentration gradient. This idea would be supported by the rapid phosphorylation dynamics I observed, but also by the apparent importance of the recycling dynamics of D6PK kinases in efficient cellular auxin transport (Barbosa et al., 2014). Kinase-mediated phosphorylation of transporters as a direct source for energy-dependent transport processes has, to my knowledge, not been reported previously. Intriguingly nonetheless, this would add a hitherto unknown layer of regulation to such processes through dynamic and direct activity control by kinases. Future experiments, possibly involving the phosphosite-specific antibodies established here, should be able to tackle these interesting questions.

Bibliography

Abas, L., Benjamins, R., Malenica, N., Paciorek, T., Wisniewska, J., Moulinier-Anzola, J.C., Sieberer, T., Friml, J., and Luschnig, C. (2006). Intracellular trafficking and proteolysis of the *Arabidopsis* auxin-efflux facilitator PIN2 are involved in root gravitropism. Nat Cell Biol **8,** 249-256.

Adamowski, M., and Friml, J. (2015). PIN-dependent auxin transport: action, regulation, and evolution. Plant Cell **27,** 20-32.

Apodaca, G., Katz, L.A., and Mostov, K.E. (1994). Receptor-mediated transcytosis of IgA in MDCK cells is via apical recycling endosomes. J Cell Biol **125,** 67-86.

Bainbridge, K., Guyomarc'h, S., Bayer, E., Swarup, R., Bennett, M., Mandel, T., and Kuhlemeier, C. (2008). Auxin influx carriers stabilize phyllotactic patterning. Genes Dev **22,** 810-823.

Ballesteros, I., Dominguez, T., Sauer, M., Paredes, P., Duprat, A., Rojo, E., Sanmartin, M., and Sanchez-Serrano, J.J. (2013). Specialized functions of the PP2A subfamily II catalytic subunits PP2A-C3 and PP2A-C4 in the distribution of auxin fluxes and development in *Arabidopsis*. Plant J **73,** 862-872.

Baluska, F., Samaj, J., and Menzel, D. (2003). Polar transport of auxin: carrier-mediated flux across the plasma membrane or neurotransmitter-like secretion? Trends Cell Biol **13,** 282-285.

Baluska, F., Schlicht, M., Volkmann, D., and Mancuso, S. (2008). Vesicular secretion of auxin: Evidences and implications. Plant Signal Behav **3,** 254-256.

Band, L.R., Wells, D.M., Larrieu, A., Sun, J., Middleton, A.M., French, A.P., Brunoud, G., Sato, E.M., Wilson, M.H., Péret, B., Oliva, M., Swarup, R., Sairanen, I., Parry, G., Ljung, K., Beeckman, T., Garibaldi, J.M., Estelle, M., Owen, M.R., Vissenberg, K., Hodgman, T.C., Pridmore, T.P., King, J.R., Vernoux, T., and Bennett, M.J. (2012). Root gravitropism is regulated by a transient lateral auxin gradient controlled by a tipping-point mechanism. Proc Natl Acad Sci U S A **109,** 4668-4673.

Barbosa, I.C., and Schwechheimer, C. (2014). Dynamic control of auxin transport-dependent growth by AGCVIII protein kinases. Curr Opin Plant Biol **22,** 108-115.

Barbosa, I.C., Zourelidou, M., Willige, B.C., Weller, B., and Schwechheimer, C. (2014). D6 PROTEIN KINASE activates auxin transport-dependent growth and PIN-FORMED phosphorylation at the plasma membrane. Dev Cell **29,** 674-685.

Barbosa, I.C., Shikata, H., Zourelidou, M., Heilmann, M., Heilmann, I., and Schwechheimer, C. (2016). Phospholipid composition and a polybasic motif determine D6 PROTEIN KINASE polar association with the plasma membrane and tropic responses. Development **143,** 4687-4700.

Benjamins, R. (2003). PINOID-Mediated Signaling Involves Calcium-Binding Proteins. Plant Physiol **132,** 1623-1630.

Benjamins, R. (2004). Functional analysis of the PINOID protein kinase in *Arabidopsis* thaliana. Leiden University, PhD thesis.

Benjamins, R., Quint, A., Weijers, D., Hooykaas, P., and Offringa, R. (2001). The PINOID protein kinase regulates organ development in *Arabidopsis* by enhancing polar auxin transport. Development **128,** 4057-4067.

Benkova, E., Michniewicz, M., Sauer, M., Teichmann, T., Seifertova, D., Jurgens, G., and Friml, J. (2003). Local, efflux-dependent auxin gradients as a common module for plant organ formation. Cell **115,** 591-602.

Benková, E., Michniewicz, M., Sauer, M., Teichmann, T., Seifertová, D., Jürgens, G., and Friml, J. (2003). Local, Efflux-Dependent Auxin Gradients as a Common Module for Plant Organ Formation. Cell **115,** 591-602.

Bennett, M.J., Marchant, A., Green, H.G., May, S.T., Ward, S.P., Millner, P.A., Walker, A.R., Schulz, B., and Feldmann, K.A. (1996). *Arabidopsis* AUX1 gene: a permease-like regulator of root gravitropism. Science **273,** 948-950.

Bennett, S.R.M., Alvarez, J., Bossinger, G., and Smyth, D.R. (1995). Morphogenesis in pinoid mutants of *Arabidopsis* thaliana. Plant J **8,** 505-520.

Bennett, T. (2015). PIN proteins and the evolution of plant development. Trends Plant Sci **20,** 498-507.

Betz, W.J., Mao, F., and Smith, C.B. (1996). Imaging exocytosis and endocytosis. Curr Opin Neurobiol **6,** 365-371.

Blilou, I., Xu, J., Wildwater, M., Willemsen, V., Paponov, I., Friml, J., Heidstra, R., Aida, M., Palme, K., and Scheres, B. (2005). The PIN auxin efflux facilitator network controls growth and patterning in *Arabidopsis* roots. Nature **433,** 39-44.

Boonsirichai, K., Sedbrook, J.C., Chen, R., Gilroy, S., and Masson, P.H. (2003). ALTERED RESPONSE TO GRAVITY is a peripheral membrane protein that modulates gravity-induced cytoplasmic alkalinization and lateral auxin transport in plant statocytes. Plant Cell **15,** 2612-2625.

Bowman, J.L., Smyth, D.R., and Meyerowitz, E.M. (1989). Genes Directing Flower Development in *Arabidopsis*. Plant Cell **1,** 37-52.

Brunoud, G., Wells, D.M., Oliva, M., Larrieu, A., Mirabet, V., Burrow, A.H., Beeckman, T., Kepinski, S., Traas, J., Bennett, M.J., and Vernoux, T. (2012). A novel sensor to map auxin response and distribution at high spatio-temporal resolution. Nature **482,** 103-106.

Casimiro, I., Marchant, A., Bhalerao, R.P., Beeckman, T., Dhooge, S., Swarup, R., Graham, N., Inze, D., Sandberg, G., Casero, P.J., and Bennett, M. (2001). Auxin transport promotes *Arabidopsis* lateral root initiation. Plant Cell **13,** 843-852.

Chen, R., Hilson, P., Sedbrook, J., Rosen, E., Caspar, T., and Masson, P.H. (1998). The *arabidopsis* thaliana AGRAVITROPIC 1 gene encodes a component of the polar-auxin-transport efflux carrier. Proc Natl Acad Sci U S A **95,** 15112-15117.

Cheng, Y., Qin, G., Dai, X., and Zhao, Y. (2007). NPY1, a BTB-NPH3-like protein, plays a critical role in auxin-regulated organogenesis in *Arabidopsis*. Proc Natl Acad Sci U S A **104,** 18825-18829.

Cheng, Y., Qin, G., Dai, X., and Zhao, Y. (2008). NPY genes and AGC kinases define two key steps in auxin-mediated organogenesis in *Arabidopsis*. Proc Natl Acad Sci U S A **105,** 21017-21022.

Cho, M., Lee, S.H., and Cho, H.T. (2007). P-glycoprotein4 displays auxin efflux transporter-like action in *Arabidopsis* root hair cells and tobacco cells. Plant Cell **19,** 3930-3943.

Christensen, S.K., Dagenais, N., Chory, J., and Weigel, D. (2000). Regulation of Auxin Response by the Protein Kinase PINOID. Cell **100,** 469-478.

Christie, J.M., Yang, H., Richter, G.L., Sullivan, S., Thomson, C.E., Lin, J., Titapiwatanakun, B., Ennis, M., Kaiserli, E., Lee, O.R., Adamec, J., Peer, W.A., and Murphy, A.S. (2011). phot1 inhibition of ABCB19 primes lateral auxin fluxes in the shoot apex required for phototropism. PLoS Biol **9,** e1001076.

Clough, S.J., and Bent, A.F. (1998). Floral dip: a simplified method for Agrobacterium-mediated transformation of *Arabidopsis* thaliana. Plant J **16,** 735-743.

Cui, X., Guo, Z., Song, L., Wang, Y., and Cheng, Y. (2016). NCP1/AtMOB1A Plays Key Roles in Auxin-Mediated *Arabidopsis* Development. PLoS Genet **12,** e1005923.

Darwin, C.R. (1880). The Power of Movement in Plants. (London: Murray).

Devarenne, T.P., Ekengren, S.K., Pedley, K.F., and Martin, G.B. (2006). Adi3 is a Pdk1-interacting AGC kinase that negatively regulates plant cell death. Embo j **25,** 255-265.

Dharmasiri, N., Dharmasiri, S., and Estelle, M. (2005). The F-box protein TIR1 is an auxin receptor. Nature **435,** 441-445.

Dhonukshe, P., Huang, F., Galvan-Ampudia, C.S., Mahonen, A.P., Kleine-Vehn, J., Xu, J., Quint, A., Prasad, K., Friml, J., Scheres, B., and Offringa, R. (2010). Plasma membrane-bound AGC3 kinases phosphorylate PIN auxin carriers at TPRXS(N/S) motifs to direct apical PIN recycling. Development **137,** 3245-3255.

Dhonukshe, P., Tanaka, H., Goh, T., Ebine, K., Mahonen, A.P., Prasad, K., Blilou, I., Geldner, N., Xu, J., Uemura, T., Chory, J., Ueda, T., Nakano, A., Scheres, B., and Friml, J. (2008). Generation of cell polarity in plants links endocytosis, auxin distribution and cell fate decisions. Nature **456,** 962-966.

Ding, Z., Galvan-Ampudia, C.S., Demarsy, E., Langowski, L., Kleine-Vehn, J., Fan, Y., Morita, M.T., Tasaka, M., Fankhauser, C., Offringa, R., and Friml, J. (2011). Light-mediated polarization of the PIN3 auxin transporter for the phototropic response in *Arabidopsis*. Nat Cell Biol **13,** 447-452.

Doyle, S.M., Haeger, A., Vain, T., Rigal, A., Viotti, C., Langowska, M., Ma, Q., Friml, J., Raikhel, N.V., Hicks, G.R., and Robert, S. (2015). An early secretory pathway mediated by GNOM-LIKE 1 and GNOM is essential for basal polarity establishment in *Arabidopsis* thaliana. Proc Natl Acad Sci U S A **112,** E806-815.

Drdova, E.J., Synek, L., Pecenkova, T., Hala, M., Kulich, I., Fowler, J.E., Murphy, A.S., and Zarsky, V. (2013). The exocyst complex contributes to PIN auxin efflux carrier recycling and polar auxin transport in *Arabidopsis*. Plant J **73,** 709-719.

Felle, H., Peters, W., and Palme, K. (1991). The electrical response of maize to auxins. Biochim Biophys Acta **1064,** 199-204.

Feraru, E., Feraru, M.I., Kleine-Vehn, J., Martiniere, A., Mouille, G., Vanneste, S., Vernhettes, S., Runions, J., and Friml, J. (2011). PIN polarity maintenance by the cell wall in *Arabidopsis*. Curr Biol **21,** 338-343.

Fischer-Parton, S., Parton, R.M., Hickey, P.C., Dijksterhuis, J., Atkinson, H.A., and Read, N.D. (2000). Confocal microscopy of FM4-64 as a tool for analysing endocytosis and vesicle trafficking in living fungal hyphae. J Microsc **198,** 246-259.

Frias, I., Caldeira, M.T., Perez-Castineira, J.R., Navarro-Avino, J.P., Culianez-Macia, F.A., Kuppinger, O., Stransky, H., Pages, M., Hager, A., and Serrano, R. (1996). A major isoform of the maize plasma membrane H(+)-ATPase: characterization and induction by auxin in coleoptiles. Plant Cell **8,** 1533-1544.

Friml, J., Wisniewska, J., Benkova, E., Mendgen, K., and Palme, K. (2002a). Lateral relocation of auxin efflux regulator PIN3 mediates tropism in *Arabidopsis*. Nature **415,** 806-809.

Friml, J., Vieten, A., Sauer, M., Weijers, D., Schwarz, H., Hamann, T., Offringa, R., and Jurgens, G. (2003). Efflux-dependent auxin gradients establish the apical-basal axis of *Arabidopsis*. Nature **426,** 147-153.

Friml, J., Benkova, E., Blilou, I., Wisniewska, J., Hamann, T., Ljung, K., Woody, S., Sandberg, G., Scheres, B., Jurgens, G., and Palme, K. (2002b). AtPIN4 mediates sink-driven auxin gradients and root patterning in *Arabidopsis*. Cell **108,** 661-673.

Friml, J., Yang, X., Michniewicz, M., Weijers, D., Quint, A., Tietz, O., Benjamins, R., Ouwerkerk, P.B., Ljung, K., Sandberg, G., Hooykaas, P.J., Palme, K., and Offringa, R. (2004). A PINOID-dependent binary switch in apical-basal PIN polar targeting directs auxin efflux. Science **306,** 862-865.

Furutani, M., Nakano, Y., and Tasaka, M. (2014). MAB4-induced auxin sink generates local auxin gradients in *Arabidopsis* organ formation. Proc Natl Acad Sci U S A **111,** 1198-1203.

Furutani, M., Vernoux, T., Traas, J., Kato, T., Tasaka, M., and Aida, M. (2004). PIN-FORMED1 and PINOID regulate boundary formation and cotyledon development in *Arabidopsis* embryogenesis. Development **131,** 5021-5030.

Furutani, M., Kajiwara, T., Kato, T., Treml, B.S., Stockum, C., Torres-Ruiz, R.A., and Tasaka, M. (2007). The gene MACCHI-BOU 4/ENHANCER OF PINOID encodes a NPH3-like protein and reveals similarities between organogenesis and phototropism at the molecular level. Development **134,** 3849-3859.

Furutani, M., Sakamoto, N., Yoshida, S., Kajiwara, T., Robert, H.S., Friml, J., and Tasaka, M. (2011). Polar-localized NPH3-like proteins regulate polarity and endocytosis of PIN-FORMED auxin efflux carriers. Development **138,** 2069-2078.

Galvan-Ampudia, C.S., and Offringa, R. (2007). Plant evolution: AGC kinases tell the auxin tale. Trends Plant Sci **12,** 541-547.

Galweiler, L., Guan, C., Muller, A., Wisman, E., Mendgen, K., Yephremov, A., and Palme, K. (1998). Regulation of polar auxin transport by AtPIN1 in *Arabidopsis* vascular tissue. Science **282,** 2226-2230.

Gao, H.B., Chu, Y.J., and Xue, H.W. (2013). Phosphatidic acid (PA) binds PP2AA1 to regulate PP2A activity and PIN1 polar localization. Mol Plant **6,** 1692-1702.

Geisler, M., and Murphy, A.S. (2006). The ABC of auxin transport: the role of p-glycoproteins in plant development. FEBS Lett **580,** 1094-1102.

Geisler, M., Blakeslee, J.J., Bouchard, R., Lee, O.R., Vincenzetti, V., Bandyopadhyay, A., Titapiwatanakun, B., Peer, W.A., Bailly, A., Richards, E.L., Ejendal, K.F., Smith, A.P., Baroux, C., Grossniklaus, U., Muller, A., Hrycyna, C.A., Dudler, R., Murphy, A.S., and Martinoia, E. (2005). Cellular efflux of auxin catalyzed by the *Arabidopsis* MDR/PGP transporter AtPGP1. Plant J **44,** 179-194.

Geldner, N. (2009). Cell polarity in plants: a PARspective on PINs. Curr Opin Plant Biol **12,** 42-48.

Geldner, N., Friml, J., Stierhof, Y.D., Jurgens, G., and Palme, K. (2001). Auxin transport inhibitors block PIN1 cycling and vesicle trafficking. Nature **413,** 425-428.

Geldner, N., Richter, S., Vieten, A., Marquardt, S., Torres-Ruiz, R.A., Mayer, U., and Jurgens, G. (2004). Partial loss-of-function alleles reveal a role for GNOM in auxin transport-related, post-embryonic development of *Arabidopsis*. Development **131,** 389-400.

Geldner, N., Anders, N., Wolters, H., Keicher, J., Kornberger, W., Muller, P., Delbarre, A., Ueda, T., Nakano, A., and Jurgens, G. (2003). The *Arabidopsis* GNOM ARF-GEF mediates endosomal recycling, auxin transport, and auxin-dependent plant growth. Cell **112,** 219-230.

Grossmann, K. (2010). Auxin herbicides: current status of mechanism and mode of action. Pest Manag Sci **66,** 113-120.

Habets, M.E., and Offringa, R. (2014). PIN-driven polar auxin transport in plant developmental plasticity: a key target for environmental and endogenous signals. New Phytol **203,** 362-377.

Haga, K., Hayashi, K., and Sakai, T. (2014). PINOID AGC kinases are necessary for phytochrome-mediated enhancement of hypocotyl phototropism in *Arabidopsis*. Plant Physiol **166,** 1535-1545.

Hager, A., Debus, G., Edel, H.G., Stransky, H., and Serrano, R. (1991). Auxin induces exocytosis and the rapid synthesis of a high-turnover pool of plasma-membrane H+-ATPase. Planta **185,** 527-537.

Heisler, M.G., Ohno, C., Das, P., Sieber, P., Reddy, G.V., Long, J.A., and Meyerowitz, E.M. (2005). Patterns of auxin transport and gene expression during primordium development revealed by live imaging of the *Arabidopsis* inflorescence meristem. Curr Biol **15,** 1899-1911.

Heisler, M.G., Hamant, O., Krupinski, P., Uyttewaal, M., Ohno, C., Jonsson, H., Traas, J., and Meyerowitz, E.M. (2010). Alignment between PIN1 polarity and microtubule orientation in the shoot apical meristem reveals a tight coupling between morphogenesis and auxin transport. PLoS Biol **8,** e1000516.

Huang, F., Zago, M.K., Abas, L., van Marion, A., Galvan-Ampudia, C.S., and Offringa, R. (2010). Phosphorylation of conserved PIN motifs directs *Arabidopsis* PIN1 polarity and auxin transport. Plant Cell **22,** 1129-1142.

Isono, E., Katsiarimpa, A., Muller, I.K., Anzenberger, F., Stierhof, Y.D., Geldner, N., Chory, J., and Schwechheimer, C. (2010). The deubiquitinating enzyme AMSH3 is required for intracellular trafficking and vacuole biogenesis in *Arabidopsis* thaliana. Plant Cell **22,** 1826-1837.

Ito, J., Sono, T., Tasaka, M., and Furutani, M. (2011). MACCHI-BOU 2 is required for early embryo patterning and cotyledon organogenesis in *Arabidopsis*. Plant Cell Physiol **52,** 539-552.

Jia, W., Li, B., Li, S., Liang, Y., Wu, X., Ma, M., Wang, J., Gao, J., Cai, Y., Zhang, Y., Wang, Y., Li, J., and Wang, Y. (2016). Mitogen-Activated Protein Kinase Cascade MKK7-MPK6 Plays Important Roles in Plant Development and Regulates Shoot Branching by Phosphorylating PIN1 in *Arabidopsis*. PLoS Biol **14,** e1002550.

Kamimoto, Y., Terasaka, K., Hamamoto, M., Takanashi, K., Fukuda, S., Shitan, N., Sugiyama, A., Suzuki, H., Shibata, D., Wang, B., Pollmann, S., Geisler, M., and Yazaki, K. (2012). *Arabidopsis* ABCB21 is a facultative auxin importer/exporter regulated by cytoplasmic auxin concentration. Plant Cell Physiol **53,** 2090-2100.

Kitakura, S., Vanneste, S., Robert, S., Lofke, C., Teichmann, T., Tanaka, H., and Friml, J. (2011). Clathrin mediates endocytosis and polar distribution of PIN auxin transporters in *Arabidopsis*. Plant Cell **23,** 1920-1931.

Kleine-Vehn, J., Langowski, L., Wisniewska, J., Dhonukshe, P., Brewer, P.B., and Friml, J. (2008a). Cellular and molecular requirements for polar PIN targeting and transcytosis in plants. Mol Plant **1,** 1056-1066.

Kleine-Vehn, J., Ding, Z., Jones, A.R., Tasaka, M., Morita, M.T., and Friml, J. (2010). Gravity-induced PIN transcytosis for polarization of auxin fluxes in gravity-sensing root cells. Proc Natl Acad Sci U S A **107,** 22344-22349.

Kleine-Vehn, J., Leitner, J., Zwiewka, M., Sauer, M., Abas, L., Luschnig, C., and Friml, J. (2008b). Differential degradation of PIN2 auxin efflux carrier by retromer-dependent vacuolar targeting. Proc Natl Acad Sci U S A **105,** 17812-17817.

Kleine-Vehn, J., Huang, F., Naramoto, S., Zhang, J., Michniewicz, M., Offringa, R., and Friml, J. (2009). PIN auxin efflux carrier polarity is regulated by PINOID kinase-mediated recruitment

into GNOM-independent trafficking in *Arabidopsis*. Plant Cell **21,** 3839-3849.

Kleine-Vehn, J., Dhonukshe, P., Sauer, M., Brewer, P.B., Wisniewska, J., Paciorek, T., Benkova, E., and Friml, J. (2008c). ARF GEF-dependent transcytosis and polar delivery of PIN auxin carriers in *Arabidopsis*. Curr Biol **18,** 526-531.

Krecek, P., Skupa, P., Libus, J., Naramoto, S., Tejos, R., Friml, J., and Zazimalova, E. (2009). The PIN-FORMED (PIN) protein family of auxin transporters. Genome Biol **10,** 249.1-249.11.

Laxmi, A., Pan, J., Morsy, M., and Chen, R. (2008). Light plays an essential role in intracellular distribution of auxin efflux carrier PIN2 in *Arabidopsis* thaliana. PLoS One **3,** e1510.

Lee, S.H., and Cho, H.T. (2006). PINOID positively regulates auxin efflux in Arabidopsis root hair cells and tobacco cells. Plant Cell **18,** 1604-1616.

Liscum, E., and Briggs, W.R. (1995). Mutations in the NPH1 locus of *Arabidopsis* disrupt the perception of phototropic stimuli. Plant Cell **7,** 473-485.

Liscum, E., Askinosie, S.K., Leuchtman, D.L., Morrow, J., Willenburg, K.T., and Coats, D.R. (2014). Phototropism: growing towards an understanding of plant movement. Plant Cell **26,** 38-55.

Ljung, K., Bhalerao, R.P., and Sandberg, G. (2001). Sites and homeostatic control of auxin biosynthesis in *Arabidopsis* during vegetative growth. Plant J **28,** 465-474.

Ljung, K., Hull, A.K., Celenza, J., Yamada, M., Estelle, M., Normanly, J., and Sandberg, G. (2005). Sites and Regulation of Auxin Biosynthesis in *Arabidopsis* Roots. Plant Cell **17,** 1090-1104.

Luschnig, C., Gaxiola, R.A., Grisafi, P., and Fink, G.R. (1998). EIR1, a root-specific protein involved in auxin transport, is required for gravitropism in *Arabidopsis* thaliana. Genes Dev **12,** 2175-2187.

Marchant, A., Kargul, J., May, S.T., Muller, P., Delbarre, A., Perrot-Rechenmann, C., and Bennett, M.J. (1999). AUX1 regulates root gravitropism in *Arabidopsis* by facilitating auxin uptake within root apical tissues. EMBO J **18,** 2066-2073.

Marhavy, P., Duclercq, J., Weller, B., Feraru, E., Bielach, A., Offringa, R., Friml, J., Schwechheimer, C., Murphy, A., and Benkova, E. (2014). Cytokinin controls polarity of PIN1-dependent auxin transport during lateral root organogenesis. Curr Biol **24,** 1031-1037.

Marten, I., Lohse, G., and Hedrich, R. (1991). Plant growth hormones control voltage-dependent activity of anion channels in plasma membrane of guard cells. Nature **353,** 758-762.

McCaffrey, L.M., and Macara, I.G. (2009). Widely Conserved Signaling Pathways in the Establishment of Cell Polarity. Cold Spring Harb Perspect Biol **1,** a001370

Mellman, I., and Nelson, W.J. (2008). Coordinated protein sorting, targeting and distribution in polarized cells. Nat Rev Mol Cell Biol **9,** 833-845.

Mettbach, U., Strnad, M., Mancuso, S., and Baluska, F. (2017). Immunogold-EM analysis reveal brefeldin a-sensitive clusters of auxin in *Arabidopsis* root apex cells. Commun Integr Biol **10,** e1327105.

Michniewicz, M., Brewer, P.B., and Friml, J.I. (2007a). Polar auxin transport and asymmetric auxin distribution. *Arabidopsis* Book **5,** e0108.

Michniewicz, M., Zago, M.K., Abas, L., Weijers, D., Schweighofer, A., Meskiene, I., Heisler, M.G., Ohno, C., Zhang, J., Huang, F., Schwab, R., Weigel, D., Meyerowitz, E.M., Luschnig, C., Offringa, R., and Friml, J. (2007b). Antagonistic regulation of PIN phosphorylation by PP2A and PINOID directs auxin flux. Cell **130,** 1044-1056.

Muller, A., Guan, C., Galweiler, L., Tanzler, P., Huijser, P., Marchant, A., Parry, G., Bennett, M.,

Wisman, E., and Palme, K. (1998). AtPIN2 defines a locus of *Arabidopsis* for root gravitropism control. EMBO J **17,** 6903-6911.

Mullins, R.D. (2010). Cytoskeletal Mechanisms for Breaking Cellular Symmetry. Cold Spring Harb Perspect Biol **2,** a003392

Munro, E., and Bowerman, B. (2009). Cellular Symmetry Breaking during Caenorhabditis elegans Development. Cold Spring Harb Perspect Biol **1,** a003400

Nagawa, S., Xu, T., Lin, D., Dhonukshe, P., Zhang, X., Friml, J., Scheres, B., Fu, Y., and Yang, Z. (2012). ROP GTPase-dependent actin microfilaments promote PIN1 polarization by localized inhibition of clathrin-dependent endocytosis. PLoS Biol **10,** e1001299.

Normanly, J. (2010). Approaching cellular and molecular resolution of auxin biosynthesis and metabolism. Cold Spring Harb Perspect Biol **2,** a001594.

Okada, K., Ueda, J., Komaki, M.K., Bell, C.J., and Shimura, Y. (1991). Requirement of the Auxin Polar Transport System in Early Stages of *Arabidopsis* Floral Bud Formation. Plant Cell **3,** 677-684.

Orlando, K., and Guo, W. (2009). Membrane Organization and Dynamics in Cell Polarity. Cold Spring Harb Perspect Biol **1,** a001321

Ottenschlager, I., Wolff, P., Wolverton, C., Bhalerao, R.P., Sandberg, G., Ishikawa, H., Evans, M., and Palme, K. (2003). Gravity-regulated differential auxin transport from columella to lateral root cap cells. Proc Natl Acad Sci U S A **100,** 2987-2991.

Paciorek, T., Zazimalova, E., Ruthardt, N., Petrasek, J., Stierhof, Y.D., Kleine-Vehn, J., Morris, D.A., Emans, N., Jurgens, G., Geldner, N., and Friml, J. (2005). Auxin inhibits endocytosis and promotes its own efflux from cells. Nature **435,** 1251-1256.

Paponov, I.A., Paponov, M., Teale, W., Menges, M., Chakrabortee, S., Murray, J.A., and Palme, K. (2008). Comprehensive transcriptome analysis of auxin responses in *Arabidopsis*. Mol Plant **1,** 321-337.

Petersson, S.V., Johansson, A.I., Kowalczyk, M., Makoveychuk, A., Wang, J.Y., Moritz, T., Grebe, M., Benfey, P.N., Sandberg, G., and Ljung, K. (2009). An auxin gradient and maximum in the *Arabidopsis* root apex shown by high-resolution cell-specific analysis of IAA distribution and synthesis. Plant Cell **21,** 1659-1668.

Petrasek, J., and Friml, J. (2009). Auxin transport routes in plant development. Development **136,** 2675-2688.

Petrasek, J., Mravec, J., Bouchard, R., Blakeslee, J.J., Abas, M., Seifertova, D., Wisniewska, J., Tadele, Z., Kubes, M., Covanova, M., Dhonukshe, P., Skupa, P., Benkova, E., Perry, L., Krecek, P., Lee, O.R., Fink, G.R., Geisler, M., Murphy, A.S., Luschnig, C., Zazimalova, E., and Friml, J. (2006). PIN proteins perform a rate-limiting function in cellular auxin efflux. Science **312,** 914-918.

Petricka, J.J., Van Norman, J.M., and Benfey, P.N. (2009). Symmetry Breaking in Plants: Molecular Mechanisms Regulating Asymmetric Cell Divisions in *Arabidopsis*. Cold Spring Harb Perspect Biol **1,** a000497.

Peyroche, A., Antonny, B., Robineau, S., Acker, J., Cherfils, J., and Jackson, C.L. (1999). Brefeldin A acts to stabilize an abortive ARF-GDP-Sec7 domain protein complex: involvement of specific residues of the Sec7 domain. Mol Cell **3,** 275-285.

Rademacher, E.H., and Offringa, R. (2012). Evolutionary Adaptations of Plant AGC Kinases: From Light Signaling to Cell Polarity Regulation. Front Plant Sci **3,** 250.

Rahman, A., Takahashi, M., Shibasaki, K., Wu, S., Inaba, T., Tsurumi, S., and Baskin, T.I. (2010). Gravitropism of *Arabidopsis* thaliana roots requires the polarization of PIN2 toward the root tip in meristematic cortical cells. Plant Cell **22,** 1762-1776.

Rakusova, H., Gallego-Bartolome, J., Vanstraelen, M., Robert, H.S., Alabadi, D., Blazquez, M.A., Benkova, E., and Friml, J. (2011). Polarization of PIN3-dependent auxin transport for hypocotyl gravitropic response in *Arabidopsis* thaliana. Plant J **67,** 817-826.

Ramakrishna, A., Giridhar, P., and Ravishankar, G.A. (2011). Phytoserotonin: a review. Plant Signal Behav **6,** 800-809.

Rashotte, A.M., DeLong, A., and Muday, G.K. (2001). Genetic and chemical reductions in protein phosphatase activity alter auxin transport, gravity response, and lateral root growth. Plant Cell **13,** 1683-1697.

Rayle, D.L., and Cleland, R.E. (1992). The Acid Growth Theory of auxin-induced cell elongation is alive and well. Plant Physiol **99,** 1271-1274.

Reinhardt, D., Pesce, E.R., Stieger, P., Mandel, T., Baltensperger, K., Bennett, M., Traas, J., Friml, J., and Kuhlemeier, C. (2003). Regulation of phyllotaxis by polar auxin transport. Nature **426,** 255-260.

Richter, S., Geldner, N., Schrader, J., Wolters, H., Stierhof, Y.-D., Rios, G., Koncz, C., Robinson, D.G., and Jurgens, G. (2007). Functional diversification of closely related ARF-GEFs in protein secretion and recycling. Nature **448,** 488-492.

Richter, S., Muller, L.M., Stierhof, Y.D., Mayer, U., Takada, N., Kost, B., Vieten, A., Geldner, N., Koncz, C., and Jurgens, G. (2012). Polarized cell growth in *Arabidopsis* requires endosomal recycling mediated by GBF1-related ARF exchange factors. Nat Cell Biol **14,** 80-86.

Roberts, D., Pedmale, U.V., Morrow, J., Sachdev, S., Lechner, E., Tang, X., Zheng, N., Hannink, M., Genschik, P., and Liscum, E. (2011). Modulation of phototropic responsiveness in *Arabidopsis* through ubiquitination of phototropin 1 by the CUL3-Ring E3 ubiquitin ligase CRL3(NPH3). Plant Cell **23,** 3627-3640.

Rubery, P.H., and Sheldrake, A.R. (1973). Effect of pH and surface charge on cell uptake of auxin. Nat New Biol **244,** 285-288.

Rubery, P.H., and Sheldrake, A.R. (1974). Carrier-mediated auxin transport. Planta **118,** 101-121.

Sabatini, S., Beis, D., Wolkenfelt, H., Murfett, J., Guilfoyle, T., Malamy, J., Benfey, P., Leyser, O., Bechtold, N., Weisbeek, P., and Scheres, B. (1999). An auxin-dependent distal organizer of pattern and polarity in the *Arabidopsis* root. Cell **99,** 463-472.

Sano, H., Kane, S., Sano, E., Miinea, C.P., Asara, J.M., Lane, W.S., Garner, C.W., and Lienhard, G.E. (2003). Insulin-stimulated phosphorylation of a Rab GTPase-activating protein regulates GLUT4 translocation. J Biol Chem **278,** 14599-14602.

Sauer, M., and Friml, J. (2010). Immunolocalization of proteins in plants. Methods Mol Biol **655,** 253-263.

Sauer, M., Balla, J., Luschnig, C., Wisniewska, J., Reinohl, V., Friml, J., and Benkova, E. (2006). Canalization of auxin flow by Aux/IAA-ARF-dependent feedback regulation of PIN polarity. Genes Dev **20,** 2902-2911.

Scarpella, E., Marcos, D., Friml, J., and Berleth, T. (2006). Control of leaf vascular patterning by polar auxin transport. Genes Dev **20,** 1015-1027.

Schlicht, M., Strnad, M., Scanlon, M.J., Mancuso, S., Hochholdinger, F., Palme, K., Volkmann, D., Menzel, D., and Baluska, F. (2006). Auxin immunolocalization implicates vesicular neu-

rotransmitter-like mode of polar auxin transport in root apices. Plant Signal Behav **1,** 122-133.

Senn, A.P., and Goldsmith, M.H. (1988). Regulation of electrogenic proton pumping by auxin and fusicoccin as related to the growth of Avena coleoptiles. Plant Physiol **88,** 131-138.

Shao, W., and Dong, J. (2016). Polarity in plant asymmetric cell division: Division orientation and cell fate differentiation. Dev Biol **419,** 121-131.

Shin, H., Shin, H.S., Guo, Z., Blancaflor, E.B., Masson, P.H., and Chen, R. (2005). Complex regulation of *Arabidopsis* AGR1/PIN2-mediated root gravitropic response and basipetal auxin transport by cantharidin-sensitive protein phosphatases. Plant J **42,** 188-200.

Simon, M.L.A., Platre, M.P., Marquès-Bueno, M.M., Armengot, L., Stanislas, T., Bayle, V., Caillaud, M.-C., and Jaillais, Y. (2016). A PtdIns(4)P-driven electrostatic field controls cell membrane identity and signalling in plants **2,** 16089.

Slaughter, B.D., Smith, S.E., and Li, R. (2009). Symmetry Breaking in the Life Cycle of the Budding Yeast. Cold Spring Harb Perspect Biol **1,** a003384

Sorefan, K., Girin, T., Liljegren, S.J., Ljung, K., Robles, P., Galvan-Ampudia, C.S., Offringa, R., Friml, J., Yanofsky, M.F., and Ostergaard, L. (2009). A regulated auxin minimum is required for seed dispersal in *Arabidopsis*. Nature **459,** 583-586.

Steinmann, T., Geldner, N., Grebe, M., Mangold, S., Jackson, C.L., Paris, S., Galweiler, L., Palme, K., and Jurgens, G. (1999). Coordinated polar localization of auxin efflux carrier PIN1 by GNOM ARF GEF. Science **286,** 316-318.

Su, T., Bryant, D.M., Luton, F., Vergés, M., Ulrich, S.M., Hansen, K.C., Datta, A., Eastburn, D.J., Burlingame, A.L., Shokat, K.M., and Mostov, K.E. (2010). A kinase cascade leading to Rab11-FIP5 controls transcytosis of the polymeric immunoglobulin receptor. Nat Cell Biol **12,** 1143-1153.

Sukumar, P., Edwards, K.S., Rahman, A., Delong, A., and Muday, G.K. (2009). PINOID kinase regulates root gravitropism through modulation of PIN2-dependent basipetal auxin transport in *Arabidopsis*. Plant Physiol **150,** 722-735.

Swarup, K., Benkova, E., Swarup, R., Casimiro, I., Peret, B., Yang, Y., Parry, G., Nielsen, E., De Smet, I., Vanneste, S., Levesque, M.P., Carrier, D., James, N., Calvo, V., Ljung, K., Kramer, E., Roberts, R., Graham, N., Marillonnet, S., Patel, K., Jones, J.D., Taylor, C.G., Schachtman, D.P., May, S., Sandberg, G., Benfey, P., Friml, J., Kerr, I., Beeckman, T., Laplaze, L., and Bennett, M.J. (2008). The auxin influx carrier LAX3 promotes lateral root emergence. Nat Cell Biol **10,** 946-954.

Takahashi, K., Hayashi, K., and Kinoshita, T. (2012). Auxin activates the plasma membrane H+-ATPase by phosphorylation during hypocotyl elongation in *Arabidopsis*. Plant Physiol **159,** 632-641.

Tanaka, H., Dhonukshe, P., Brewer, P.B., and Friml, J. (2006). Spatiotemporal asymmetric auxin distribution: a means to coordinate plant development. Cell Mol Life Sci **63,** 2738-2754.

Tanaka, H., Kitakura, S., Rakusova, H., Uemura, T., Feraru, M.I., De Rycke, R., Robert, S., Kakimoto, T., and Friml, J. (2013). Cell polarity and patterning by PIN trafficking through early endosomal compartments in *Arabidopsis* thaliana. PLoS Genet **9,** e1003540.

Tanaka, H., Nodzylski, T., Kitakura, S., Feraru, M.I., Sasabe, M., Ishikawa, T., Kleine-Vehn, J., Kakimoto, T., and Friml, J. (2014). BEX1/ARF1A1C is required for BFA-sensitive recycling of PIN auxin transporters and auxin-mediated development in *Arabidopsis*. Plant Cell Physiol **55,** 737-749.

Teale, W.D., Paponov, I.A., and Palme, K. (2006). Auxin in action: signalling, transport and the control of plant growth and development. Nat Rev Mol Cell Biol **7,** 847-859.

Teh, O.K., and Moore, I. (2007). An ARF-GEF acting at the Golgi and in selective endocytosis in polarized plant cells. Nature **448,** 493-496.

Terasaka, K., Blakeslee, J.J., Titapiwatanakun, B., Peer, W.A., Bandyopadhyay, A., Makam, S.N., Lee, O.R., Richards, E.L., Murphy, A.S., Sato, F., and Yazaki, K. (2005). PGP4, an ATP binding cassette P-glycoprotein, catalyzes auxin transport in *Arabidopsis* thaliana roots. Plant Cell **17,** 2922-2939.

Treml, B.S., Winderl, S., Radykewicz, R., Herz, M., Schweizer, G., Hutzler, P., Glawischnig, E., and Ruiz, R.A. (2005). The gene ENHANCER OF PINOID controls cotyledon development in the *Arabidopsis* embryo. Development **132,** 4063-4074.

Tuma, P.L., and Hubbard, A.L. (2003). Transcytosis: Crossing Cellular Barriers. Physiol Rev **83,** 871-932.

Ulmasov, T., Hagen, G., and Guilfoyle, T.J. (1997a). ARF1, a transcription factor that binds to auxin response elements. Science **276,** 1865-1868.

Ulmasov, T., Liu, Z.B., Hagen, G., and Guilfoyle, T.J. (1995). Composite Structure of Auxin Response Elements. Plant Cell **7,** 1611-1623.

Ulmasov, T., Murfett, J., Hagen, G., and Guilfoyle, T.J. (1997b). Aux/IAA Proteins Repress Expression of Reporter Genes Containing Natural and Highly Active Synthetic Auxin Response Elements. Plant Cell **9,** 1963-1971.

Utsuno, K., Shikanai, T., Yamada, Y., and Hashimoto, T. (1998). Agr, an Agravitropic locus of *Arabidopsis* thaliana, encodes a novel membrane-protein family member. Plant Cell Physiol **39,** 1111-1118.

Vernoux, T., Besnard, F., and Traas, J. (2010). Auxin at the Shoot Apical Meristem. Cold Spring Harb Perspect Biol **2,** a001487.

Vernoux, T., Brunoud, G., Farcot, E., Morin, V., Van den Daele, H., Legrand, J., Oliva, M., Das, P., Larrieu, A., Wells, D., Guedon, Y., Armitage, L., Picard, F., Guyomarc'h, S., Cellier, C., Parry, G., Koumproglou, R., Doonan, J.H., Estelle, M., Godin, C., Kepinski, S., Bennett, M., De Veylder, L., and Traas, J. (2011). The auxin signalling network translates dynamic input into robust patterning at the shoot apex. Mol Syst Biol **7,** 508.

Viaene, T., Delwiche, C.F., Rensing, S.A., and Friml, J. (2013). Origin and evolution of PIN auxin transporters in the green lineage. Trends Plant Sci **18,** 5-10.

Vida, T.A., and Emr, S.D. (1995). A new vital stain for visualizing vacuolar membrane dynamics and endocytosis in yeast. J Cell Biol **128,** 779-792.

Vieten, A., Vanneste, S., Wisniewska, J., Benkova, E., Benjamins, R., Beeckman, T., Luschnig, C., and Friml, J. (2005). Functional redundancy of PIN proteins is accompanied by auxin-dependent cross-regulation of PIN expression. Development **132,** 4521-4531.

Went, F.W. (1926). On growth-accelerating substances in the coleoptile of Avena sativa. Proc. Kon. Ned. Akad. Wet., 10-19.

Wildman, S.G. (1997). The auxin-A,B enigma: scientific fraud or scientific ineptitude? Plant Growth Regul **1,** 37-68

Willige, B.C., Ahlers, S., Zourelidou, M., Barbosa, I.C., Demarsy, E., Trevisan, M., Davis, P.A., Roelfsema, M.R., Hangarter, R., Fankhauser, C., and Schwechheimer, C. (2013). D6PK AGCVIII kinases are required for auxin transport and phototropic hypocotyl bending in *Ara-*

bidopsis. Plant Cell **25,** 1674-1688.

Wiśniewska, J., Xu, J., Seifertová, D., Brewer, P.B., Růžička, K., Blilou, I., Rouquié, D., Benková, E., Scheres, B., and Friml, J. (2006). Polar PIN Localization Directs Auxin Flow in Plants. Science **312,** 883.

Wolters, H., Anders, N., Geldner, N., Gavidia, R., and Jurgens, G. (2011). Coordination of apical and basal embryo development revealed by tissue-specific GNOM functions. Development **138,** 117-126.

Yang, H., and Murphy, A.S. (2009). Functional expression and characterization of *Arabidopsis* ABCB, AUX 1 and PIN auxin transporters in Schizosaccharomyces pombe. Plant J **59,** 179-191.

Yang, Y., Hammes, U.Z., Taylor, C.G., Schachtman, D.P., and Nielsen, E. (2006). High-affinity auxin transport by the AUX1 influx carrier protein. Curr Biol **16,** 1123-1127.

Zadnikova, P., Petrasek, J., Marhavy, P., Raz, V., Vandenbussche, F., Ding, Z., Schwarzerova, K., Morita, M.T., Tasaka, M., Hejatko, J., Van Der Straeten, D., Friml, J., and Benkova, E. (2010). Role of PIN-mediated auxin efflux in apical hook development of *Arabidopsis* thaliana. Development **137,** 607-617.

Zeigerer, A., McBrayer, M.K., and McGraw, T.E. (2004). Insulin stimulation of GLUT4 exocytosis, but not its inhibition of endocytosis, is dependent on RabGAP AS160. Mol Biol Cell **15,** 4406-4415.

Zhang, J., Nodzynski, T., Pencik, A., Rolcik, J., and Friml, J. (2010). PIN phosphorylation is sufficient to mediate PIN polarity and direct auxin transport. Proc Natl Acad Sci U S A **107,** 918-922.

Zourelidou, M., Muller, I., Willige, B.C., Nill, C., Jikumaru, Y., Li, H., and Schwechheimer, C. (2009). The polarly localized D6 PROTEIN KINASE is required for efficient auxin transport in *Arabidopsis* thaliana. Development **136,** 627-636.

Zourelidou, M., Absmanner, B., Weller, B., Barbosa, I.C., Willige, B.C., Fastner, A., Streit, V., Port, S.A., Colcombet, J., de la Fuente van Bentem, S., Hirt, H., Kuster, B., Schulze, W.X., Hammes, U.Z., and Schwechheimer, C. (2014). Auxin efflux by PIN-FORMED proteins is activated by two different protein kinases, D6 PROTEIN KINASE and PINOID. Elife **3,** e02860.

Acknowledgements

Zuerst bedanke ich mich bei Prof. Dr. Claus Schwechheimer für die engagierte Betreuung meiner Arbeit, die spannenden Forschungsprojekte und das kreieren eines inspirierenden Wissenschaftsumfelds.

Bedanken möchte ich mich auch bei Prof. Dr. Schneitz für die Übernahme des Vorsitzenden der Prüfungskommission.

Bei PD Dr. Hammes bedanke ich mich vor allem dafür, dass er sich bereit erklärt hat dieses Werk als einer der wenigen wirklich zu lesen. Seine Insider-Infos zur bayrischen Pflanzenforschungswelt und seiner Rocker-Vergangenheit an heißen Tagen im hot-Lab seien allerdings natürlich auch erwähnt.

Ganz speziell möchte ich auch Dr. Inês Barbosa danken, ihr Name taucht nicht ohne Grund überall in dieser Arbeit auf.

Mein Dank geht auch an Mr. Western-Blot, Dr. Björn C. Willige, die alles-Könner Dr. Hiromasa Shitaka und Dr. Melina Zourelidou und natürlich an Jutta Elgner.

Ansonsten bin ich vor allem dankbar dafür, beim Rest der Truppe Freunde für's Leben gewonnen zu haben.

Appendix

PNAS PLUS

Dynamic PIN-FORMED auxin efflux carrier phosphorylation at the plasma membrane controls auxin efflux-dependent growth

Benjamin Weller[a], Melina Zourelidou[a], Lena Frank[a,1], Inês C. R. Barbosa[a], Astrid Fastner[b], Sandra Richter[c], Gerd Jürgens[c], Ulrich Z. Hammes[b], and Claus Schwechheimer[a,2]

[a]Plant Systems Biology, Technical University of Munich, 85354 Freising, Germany; [b]Department of Cell Biology and Biochemistry, Regensburg University, 93053 Regensburg, Germany; and [c]Developmental Genetics, Center for Plant Molecular Biology, 72076 Tübingen, Germany

Edited by Mark Estelle, University of California, San Diego, La Jolla, CA, and approved December 27, 2016 (received for review August 29, 2016)

The directional distribution of the phytohormone auxin is essential for plant development. Directional auxin transport is mediated by the polarly distributed PIN-FORMED (PIN) auxin efflux carriers. We have previously shown that efficient PIN1-mediated auxin efflux requires activation through phosphorylation at the four serines S1–S4 in *Arabidopsis thaliana*. The Brefeldin A (BFA)-sensitive D6 PROTEIN KINASE (D6PK) and the BFA-insensitive PINOID (PID) phosphorylate and activate PIN1 through phosphorylation at all four phosphosites. PID, but not D6PK, can also induce PIN1 polarity shifts, seemingly through phosphorylation at S1–S3. The differential effects of D6PK and PID on PIN1 polarity had so far been attributed to their differential phosphosite preference for the four PIN1 phosphosites. We have mapped PIN1 phosphorylation at S1–S4 in situ using phosphosite-specific antibodies. We detected phosphorylation at PIN1 phosphosites at the basal (rootward) as well as the apical (shootward) plasma membrane in different root cell types, in embryos, and shoot apical meristems. Thereby, PIN1 phosphorylation at all phosphosites generally followed the predominant PIN1 distribution but was not restricted to specific polar sides of the cells. PIN1 phosphorylation at the basal and apical plasma membrane was differentially sensitive to BFA treatments, suggesting the involvement of different protein kinases or trafficking mechanisms in PIN1 phosphorylation control. We conclude that phosphosite preferences are not sufficient to explain the differential effects of D6PK and PID on PIN1 polarity, and suggest that a more complex model is needed to explain the effects of PID.

auxin transport | protein kinase | *Arabidopsis* | PIN1 | polarity

The phytohormone auxin is a central regulator of plant development and tropic growth (1, 2). Proper plant development strictly requires the directed cell-to-cell transport of auxin, which is achieved by a system of auxin influx and efflux transporters (1). AUXIN RESISTANT1 (AUX1)/LIKE-AUX1 (LAX) proteins are auxin influx transporters and PIN-FORMED (PIN) proteins are auxin efflux transporters that may act together with ABC transporters (3–8). Auxin transport gains its directionality through the often polar distribution of the plasma membrane-resident PIN auxin efflux carriers, PIN1–PIN4 and PIN7 in *Arabidopsis thaliana* (1, 9). Directional auxin transport results in the formation of cellular auxin maxima and minima that provide essential cues for plant growth and differentiation at the level of individual cells and tissues (1, 2). PIN1 localizes to the basal (rootward) plasma membrane in root stele cells and directs auxin transport toward the root tip (3). PIN2 localizes differentially to the basal (rootward) and apical (shootward) plasma membrane in cortex and epidermis cells, respectively, and the opposing auxin transport streams in cortex and epidermis are important for gravitropic root growth (10, 11).

Efficient PIN1-mediated auxin efflux requires activation by phosphorylation (12, 13). In the case of PIN1, the AGCVIII protein kinases D6 PROTEIN KINASE (D6PK) and PINOID (PID) activate auxin efflux through phosphorylation at the PIN1 serines S1 (S231), S2 (S252), S4 (S271), and S3 (S290), respectively (Fig. 1 *A* and *B*) (12). In in vitro kinase assays, PID preferentially phosphorylates PIN1 at S1–S3 (12, 14, 15). S1–S3 are embedded in motifs that share striking sequence similarity to each other and that are highly conserved between PIN1–PIN4 and PIN7 (Fig. 1 *A* and *B*). D6PK preferentially phosphorylates PIN1 at S4 but it also phosphorylates S1–S3, albeit less efficiently than PID (12). Functional analyses of protein kinase-dependent PIN1-mediated auxin efflux support the relevance of the respective phosphosite preferences detected in vitro for kinase-activated auxin transport (12). There, PIN1 S1–S3 mutations affect PIN1 activation by PID more strongly than PIN1 S4 mutations and, conversely, PIN1 S4 mutations affect PIN1 activation by D6PK more strongly than PIN1 S1–S3 mutations. However, mutations of all four phosphosites are required to fully impair PID- and D6PK-dependent PIN1 activation, indicating that both kinases are able to target all four PIN1 phosphosites (2, 12). S5, an additional phosphosite in PIN3, related to S4 and preferentially targeted by D6PK, is not conserved in PIN1 and will therefore not be discussed further (Fig. 1 *A* and *B*) (12, 13).

In vivo, inactivation of D6PK and the functionally related D6PKL1–3 (D6PK-LIKE1–3), achieved either by chemical inhibitor-mediated removal of D6PK and D6PKLs from the plasma membrane or by the gradual mutational inactivation of the *D6PK* genes, correlates strongly with decreases in PIN1 phosphorylation as well

Significance

The distribution of the hormone auxin controls most processes in plant development. Auxin distribution within the plant requires PIN transporters and efficient PIN-mediated transport requires PIN phosphorylation. Phosphorylation seemingly also controls auxin transport by targeting PINs to specific sides of the cell. Understanding how auxin is directed and activated through phosphorylation is essential to understand plant growth. Two different protein kinases targeting the same phosphosites in PIN1 can activate auxin efflux. Surprisingly, however, only one affects PIN1 polar distribution. Here, we show that the differential effects of the two kinases on PIN1 cannot be explained by phosphorylation at the established phosphosites, and suggest that a more complex model is needed to explain the effects of the kinase on PIN1 polarity.

Author contributions: B.W., G.J., U.Z.H., and C.S. designed research; B.W., M.Z., L.F., I.C.R.B., A.F., and S.R. performed research; M.Z., L.F., and I.C.R.B. contributed new reagents/analytic tools; B.W., A.F., S.R., G.J., U.Z.H., and C.S. analyzed data; and B.W. and C.S. wrote the paper.

The authors declare no conflict of interest.

This article is a PNAS Direct Submission.

[1]Present address: Research Unit Environmental Simulation, Helmholtz Zentrum München, 85764 Neuherberg, Germany.

[2]To whom correspondence should be addressed. Email: claus.schwechheimer@wzw.tum.de.

This article contains supporting information online at www.pnas.org/lookup/suppl/doi:10.1073/pnas.1614380114/-/DCSupplemental.

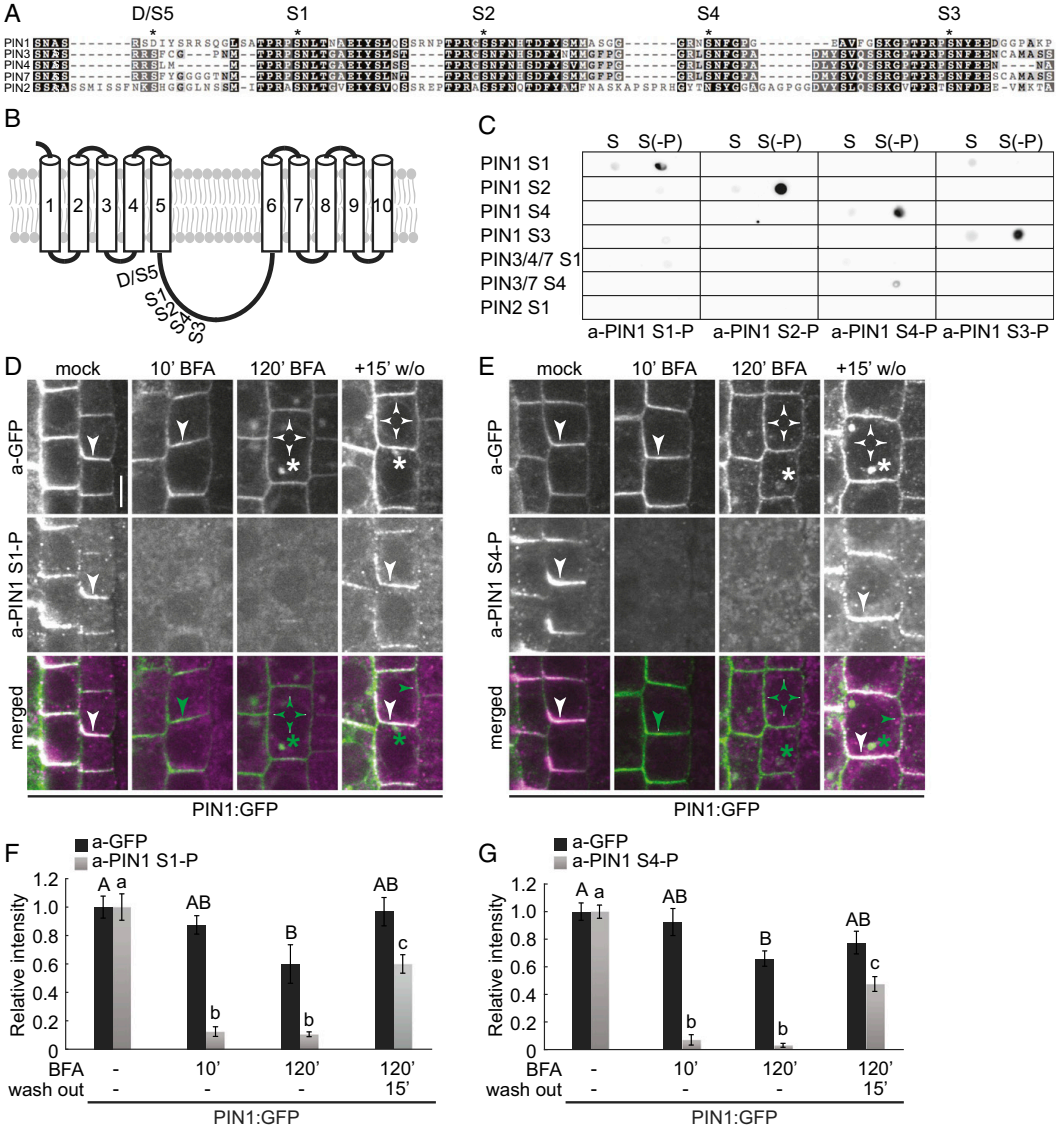

Fig. 1. Phosphosite-specific PIN1 antibodies detect PIN1 phosphorylation in a BFA-sensitive manner. (*A*) Pretty box protein sequence alignment of a region of the intracellular hydrophilic loop of *A. thaliana* PIN1–PIN4 and PIN7. The S1–S5 phosphosites described for PINs are marked with asterisks. S5 is not conserved in PIN1, where it aligns with a D (aspartic acid; S5/D), and examining S5 phosphorylation was therefore not relevant for this study. (*B*) Predicted topology of PIN1 with 10 transmembrane domains and the intracellular hydrophilic loop with the relative positions of the phosphosites marked. (*C*) Dot blot immunoblot against unphosphorylated (S) and phosphorylated peptides S(-P) probed with anti-PIN1 S1-P through S4-P antibodies. (*D* and *E*) Representative confocal images of primary root stele cells after immunostaining of 4-d-old PIN1:GFP *Arabidopsis* seedlings with anti-GFP (a-GFP; PIN1:GFP) (green), a-PIN1 S1-P (*D*) (magenta) and a-PIN1 S4-P (*E*) (magenta) antibodies. Seedlings were mock-treated or BFA-treated (50 μM) for 10 and 120 min, respectively. A 15-min washout (w/o) followed the 120-min BFA treatment. Arrowheads mark strong and weak plasma membrane staining, asterisks mark intracellular BFA compartments. Overlap of green and magenta signals is indicated by white arrowheads in the merged images. Green arrowheads and asterisks indicate the absence of a corresponding magenta signal from a-PIN1 S1-P or a-PIN1 S4-P immunostaining. The corresponding experiments with a-PIN1 S2-P and a-PIN1 S3-P are shown in Fig. S1 *A* and *B*; images of entire roots immunostained with a-PIN1 S1-P through S4-P are shown in Fig. S4, supporting the representative nature of the images shown here. (Scale bar, 5 μm.) (*F* and *G*) Quantification of fluorescence intensity at the basal plasma membrane after immunostaining as shown in *D* and *E*. Data represent the average from two independent experiments ($n = 50$ cells). Student's *t* test datasets with no statistical difference fall in one group and were labeled accordingly. Upper and lowercase letters serve to distinguish the results obtained with a-GFP and a-PIN1 S1-P or a-PIN1 S4-P, respectively.

as with decreases in directional auxin transport in stems and hypocotyls (13, 16, 17). Thus, PIN1 phosphorylation is essential for auxin transport *in planta* and may allow predicting PIN1 activity in situ.

Although D6PK and PID activate PIN1 through phosphorylation of the same phosphosites in vitro, the two kinases have differential effects on PIN1 in vivo. Overexpression of *PID* but not of *D6PK* promotes the retargeting of PIN1 from the basal (rootward) to the apical (shootward) plasma membrane in root cells (14, 15). PID-dependent PIN1 phosphorylation has been proposed to mediate this effect because PIN1 becomes insensitive to *PID* overexpression in transgenic lines where PIN1 S1–S3 are replaced by the nonphosphorylatable A (alanine) (14, 15). Furthermore, PIN1 is targeted to the apical plasma membrane in a PID-independent manner when S1–S3 are replaced by the supposedly phosphorylation-mimicking E (glutamic acid) (14, 15). These observations suggested that PID-dependent PIN1 S1–S3 phosphorylation serves as a sorting signal for differential PIN1 intracellular transport and targeting. As yet, the differential effects of PID and D6PK on PINs could only be explained by the differential phosphosite preferences of the two kinases (2, 12). Here, we show that this distinction cannot be the main feature underlying their differential cell biological effects.

Besides their differential phosphosite preference, D6PK and PID also differ from each other in regard to a number of cell biological criteria. Whereas PID is localized to the plasma membrane in a nonpolar manner, D6PK localizes to the basal plasma membrane of most cells (13, 18). D6PK, as well as PIN1, are constitutively recycling to and from the plasma membrane and both proteins are internalized after treatment with Brefeldin A (BFA), a fungal inhibitor that blocks the GN (GNOM) ARF-GEF–dependent recycling of endosomal cargo from the *trans*-Golgi network to the plasma membrane (13, 19). However, whereas D6PK is rapidly and completely internalized within minutes after BFA treatment, PIN1 has a comparatively slow response and remains detectable at the plasma membrane, even after prolonged BFA treatments (13). In contrast, the plasma membrane targeting of PID cannot be efficiently blocked by BFA inhibitor treatments (18). Thus, D6PK, PID, and PINs differ from each other in regard to their cell biological behavior and their BFA sensitivity.

Here, we monitor PIN1 phosphorylation as a proxy for the spatial and temporal dynamics of PIN1 activation and localization at the subcellular level. To this end, we have generated PIN1 S1–S4 phosphosite-specific antibodies and examine PIN1 phosphorylation patterns in situ. We detected PIN1 phosphorylation at the basal (rootward) as well as the apical (shootward) plasma membranes in different root cell types and in embryos, as well as in shoot meristems. PIN1 phosphorylation generally followed the predominant PIN1 distribution but was not restricted to specific plasma membrane domains. PIN1 phosphorylation at the basal and apical plasma membrane was differentially sensitive to BFA treatments, suggesting the involvement of different protein kinases or trafficking mechanisms in PIN1 phosphorylation control. We concluded that phosphosite preferences are not sufficient to explain the differential effects of D6PK and PID on PIN1 polarity, and suggest that a more complex model is needed to explain PID-dependent PIN1 polarity control.

Results

Phosphosite-Specific Antibodies Detect PIN1 Phosphorylation in Situ. PIN1 S1–S4 are phosphorylation targets for PID and D6PK (12, 14, 15). To monitor PIN1 phosphorylation at these specific sites individually in situ, we generated peptide antibodies directed against phosphorylated PIN1 S1–S4, designated a-PIN1 S1-P to a-PIN1 S4-P (Fig. 1 *A* and *B*). Dot blot immunoblotting showed that the antibodies are specific for the respective PIN1 phosphopeptides, with little or no cross-reactivity toward the respective other PIN1 phospho-peptides or sequence-related phosphopeptides from other PINs (Fig. 1*C*).

We tested the *in planta* specificity of these antibodies using transgenic lines expressing wild-type PIN1:GFP or PIN1:YFP and their variants carrying A (alanine) mutations at one of the four phosphosite serines (S1A, S2A, S3A, and S4A) in a *pin1* loss-of-function mutant background (12). We detected PIN1:GFP or PIN1:YFP with all four phosphorylation-specific antibodies as well as with an a-GFP antibody at the basal (rootward) plasma membrane of root stele cells in the entire root (Fig. 1 *D–G* and Fig. S1). In turn, the a-PIN1 S1-P, a-PIN1 S2-P, and a-PIN1 S4-P antibodies did not recognize PIN1:GFP or PIN1:YFP with alanine substitutions at the respective S1, S2, or S4 phosphosites (Fig. S2 *A–C*). Only a-PIN1 S3-P still detected basally localized PIN1:YFP in PIN1:YFP S3A lines (Fig. S2*D*). We concluded that three phosphosite antibodies are highly specific to phosphorylated PIN1 serine residues and could thus be used to monitor PIN1 phosphorylation in situ.

PIN1 S1–S4 Phosphorylation at the Basal Plasma Membrane Is BFA-Sensitive. Short-term BFA treatments (10 min) result in the complete internalization of D6PK. In turn, D6PK rapidly relocalizes to the basal plasma membrane following short (15 min) washout treatments (Fig. S3) (13). Over the duration of a 10-min BFA treatment, PIN1 or PID abundance at the plasma membrane are not detectably affected. After a 120-min BFA treatment, however, PIN1 reportedly becomes apolarly distributed and internalized (Fig. 1 *D–G* and Figs. S1 and S3*A*) (13, 18). We exploited this differential BFA sensitivity of D6PK and PIN1 to examine PIN1 phosphorylation after the depletion of BFA-sensitive kinases from the plasma membrane. Interestingly, phosphorylation at all four PIN1 phosphosites was strongly reduced, if not lost, after a 10-min BFA treatment, when D6PK was completely internalized but PIN1 protein was still clearly detectable at the basal plasma membrane (Fig. 1 *D–G* and Figs. S1 and S3*A*). After a 120-min BFA treatment, PIN1 was apolarly distributed at the plasma membrane and also detected in intracellular BFA compartments (Fig. 1 *D–G* and Fig. S1). However, PIN1 phosphorylation at any of the four sites could not be detected, either at the plasma membrane or in the intracellular compartments (Fig. 1 *D–G* and Fig. S1). Although the phosphosite-specific antibodies recognized intracellular structures, these signals did not consistently overlap with a-GFP (PIN1) signals and also occurred outside of the *PIN1* expression domain, indicating that they are unspecific background signals. When the 120-min BFA treatment was followed by a 15-min washout, resulting in the polar retargeting of D6PK to the basal plasma membrane, PIN1 phosphorylation was again detected preferentially at the basal plasma membrane at all four phosphosites (Fig. 1 *D–G* and Fig. S1) (12, 13). These phosphorylation patterns were observed throughout the entire root meristem (Fig. S4). The phosphosite-specific antibodies thereby mirrored the apparent phosphorylation pattern detected for PIN1 with an anti-GFP antibody in immunoblots of total root cell extracts exposed to the same BFA treatments (Fig. S5) (12, 13). This finding suggested that BFA-sensitive protein kinases may be required to maintain PIN1 phosphorylation at all four PIN1 phosphosites and that dephosphorylation by protein phosphatases rapidly antagonizes PIN1 phosphorylation. Even though we had observed a residual signal with the a-PIN1 S3-P antibody in PIN1:YFP S3A *pin1* lines, a-PIN1 S3-P showed the same behavior as the other phosphosite-specific antibodies with regard to BFA sensitivity (Figs. S2*D*, S4, and S5). We therefore judged that a-PIN1 S3-P may interact with one of the highly related PIN phosphosites in one of the other functionally redundant PINs (Fig. 1*A*). Because all antibodies showed comparable behaviors in the experimental conditions tested to this point, PIN1 S1-P

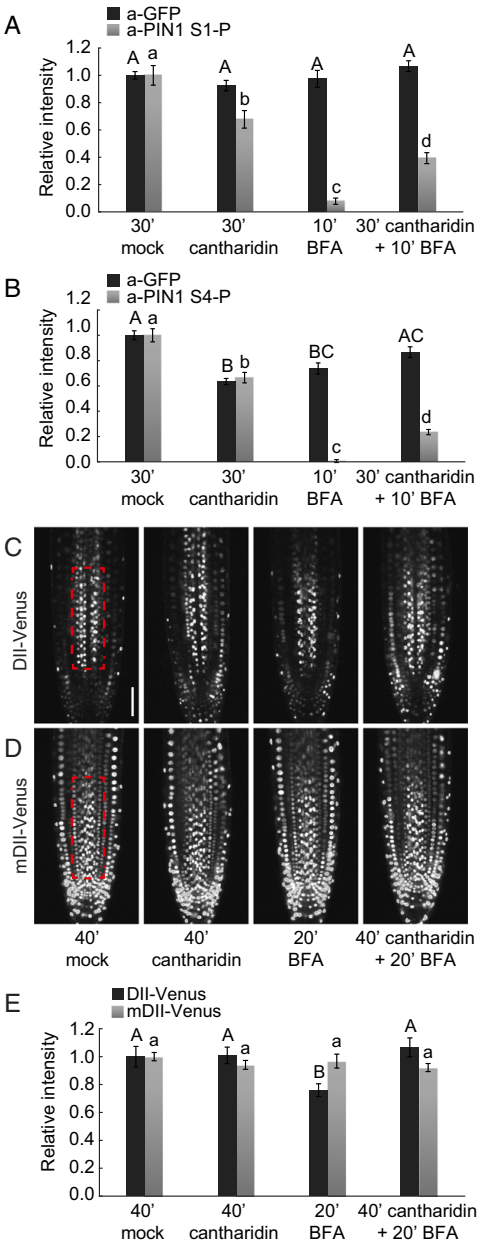

Fig. 2. Cantharidin inhibits PIN1 dephosphorylation and alters auxin distribution patterns. (*A* and *B*) Quantification of fluorescence intensity in the root stele after immunostaining following BFA (50 μM, 10 min) and cantharidin or mock (30 min) treatments. The average from three independent experiments is shown (total $n \geq 44$). Representative images of entire roots immunostained with a-PIN1 S1-P and a-PIN1 S4-P as used for quantifications are shown in Fig. S7. (*C* and *D*) Representative live fluorescence microscopy images of root tips of 4-d-old *Arabidopsis* seedlings expressing the auxin-sensitive DII-VENUS (*C*) or the auxin-insensitive mDII-VENUS markers (*D*) subjected to BFA (50 μM, 20 min) and cantharidin or mock (40 min) treatments. (Scale bar, 50 μm.) (*E*) Quantification of fluorescence intensities in the framed areas of the root stele after live imaging as shown in *C* and *D*. The average from three independent experiments ($n \geq 21$) is shown. The slightly longer treatments in *C*–*E* were chosen because the downstream responses of the primary effects shown in *A* and *B* were being examined. In *A*, *B*, and *E*, Student's *t* test datasets with no statistical difference fall in one group and were labeled accordingly. Upper and lowercase letters serve to distinguish the results obtained with the different series.

and PIN1 S4-P were chosen as representative phosphosites for further investigations.

PIN1 Phosphorylation Is GNOM-Dependent. The ARF-GEF GNOM is inhibited by BFA and functional GN is required for PIN1 and D6PK trafficking (13, 19). To test the GN-dependency of the observed BFA effects on PIN1 phosphorylation, we used transgenic lines expressing BFA-sensitive wild-type GN^{wt} or the BFA-insensitive but functional GN^{M696L} variant (19). Indeed, after 30-min BFA treatments, PIN1 S1 and S4 phosphorylation at the plasma membrane was maintained in GN^{M696L} but impaired in GN^{wt}. We concluded that PIN1 phosphorylation at the basal plasma membrane is mediated by BFA-sensitive GN trafficking-dependent kinases (Fig. S6).

The Phosphatase Inhibitor Cantharidin Delays PIN1 Dephosphorylation. The rapid decrease in PIN1 phosphorylation following BFA treatment can be explained by the activity of phosphatases. We tested whether PIN1 phosphorylation was affected by cantharidin, a phosphatase inhibitor previously used to manipulate PIN-dependent auxin transport (20–22). Indeed, cantharidin pretreatments delayed PIN1 dephosphorylation following BFA treatments significantly, albeit not completely (Fig. 2 *A* and *B* and Fig. S7).

The effects of cantharidin on PIN1 phosphorylation should affect PIN1 auxin efflux activity and consequently auxin distribution patterns in the root. We monitored auxin distribution with the auxin-labile DII-VENUS reporter (23). Because, following the interference with auxin transport, changes in auxin responses are expected to occur with a delay, we conducted these experiments using slightly longer BFA (20 min vs. 10 min) and cantharidin (40 min vs. 30 min) treatments, respectively. As expected from an increase in cellular auxin levels as a consequence of reduced auxin efflux, DII-VENUS fluorescence intensities decreased rapidly following BFA treatments (Fig. 2 *C*–*E*). This decrease was attenuated when BFA was applied together with cantharidin, indicative for a comparatively more active auxin efflux (Fig. 2 *C*–*E*). At the same time, mDII-VENUS, the stabilized auxin-insensitive control variant of DII-VENUS, did not respond to any of the treatments (Fig. 2 *C*–*E*). Thus, the inhibition of PIN1 dephosphorylation may have direct effects on auxin efflux and result, as suggested by the changes in DII-VENUS abundance, in differential cellular accumulations of auxin.

PIN1 Phosphorylation Can Be Detected at Apical and Lateral Plasma Membranes. Ectopic *PID* expression causes PIN1 polarity shifts, which had been proposed to be promoted by PIN1 S1–S3 phosphorylation (14, 15, 24). We used *PID* overexpressing seedlings (35S:PID) to examine the consequences of altered PIN1 plasma membrane distribution on PIN1 phosphorylation. In 2-d-old *PID* overexpressing seedlings, PIN1 became detectable at the lateral and apical plasma membranes of many root cells. Interestingly, PIN1 S1 and S4 phosphorylation, after *PID* overexpression, was not found exclusively at either the apical or basal end of the cell, as had been hypothesized (18, 25), but followed the general distribution pattern of PIN1 (Fig. 3*A*). Similarly, PIN1 phosphorylation patterns followed the distribution of PIN1 in lines expressing *PID* under control of an estradiol-inducible system (*XVE>>PID:GFP*)

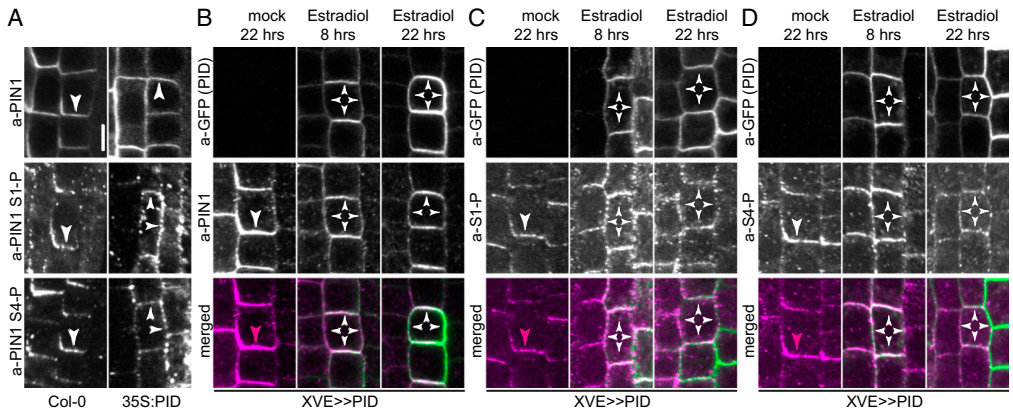

Fig. 3. PIN1 phosphorylation follows PIN1 polarity changes after *PID* overexpression. (*A*) Representative confocal images of primary root stele cells after immunostaining of 4-d-old Col-0 wild-type and 35S:PID seedlings with anti-PIN1 (a-PIN1), a-PIN1 S1-P, and a-PIN1 S4-P antibodies. (*B–D*) Representative confocal images of primary root stele cells after immunostaining of 4-d-old estradiol-inducible XVE>>PID seedlings with anti-GFP (PID) (green) and (*B*) anti-PIN1 (a-PIN1; magenta), (*C*) a-PIN1 S1-P (a-S1-P; magenta), and (*D*) a-PIN1 S4-P (a-S4-P; magenta). Seedlings were mock- or estradiol-treated for 8 and 22 h, respectively. Arrowheads mark strong and weak plasma membrane staining. Overlap of green and magenta signals is indicated by white arrowheads in merged images. Magenta arrowheads indicate the absence of a corresponding green signal from a-GFP (PID) immunostaining. (Scale bar, 5 μm.)

(15). Whereas PIN1 often lost its initial basal polarity and became apolar after 8 h of *PID* induction, PIN1 became detectable at the apical plasma membrane only after prolonged inductions (22 h). The distribution of phosphorylated PIN1, as detected with a-PIN1 S1-P or a-PIN1 S4-P, followed again the distribution of PIN1 but was not associated with specific plasma membrane subdomains (Fig. 3 *B–D*). Thus, PIN1 polar distribution is not associated with specific PIN1 phosphorylation patterns.

PIN1 Phosphorylation in Cortex and Epidermal Cells Is Independent of PIN1 Polar Localization. Root epidermis and cortex cells differentially localize PIN2 at the apical and basal plasma membranes, respectively (10). The same differential polar distribution in cortex and epidermis cells is obtained when PIN1, harboring a GFP-tag in the cytoplasmic loop, is expressed from the *PIN2* promoter fragment in a *pin2* mutant background (PIN2p::PIN1:GFP3) (26). Differential positioning of the GFP-tag in PIN2p::PIN1:GFP2, however, results in the divergent polar targeting, where PIN1:GFP2 is preferentially localized at the basal plasma membrane in both cortex and epidermis cells (26). We examined PIN1:GFP2 and PIN1:GFP3 phosphorylation and detected, with both types of transgenic lines, PIN1:GFP at the respective apical or basal domains with phosphorylations at S1 and S4 (Fig. 4). Thus, PIN1 phosphorylation followed PIN1 distribution, but did not correlate with the presence of PIN1 at either the apical or basal end of the cell, as could be hypothesized (18, 25).

Whereas PID is apolarly distributed at the plasma membranes of root epidermis and cortex cells, D6PK localizes to the basal plasma membrane in all cell types of the root meristem (Fig. S3) (13, 18). We reasoned that the differential BFA sensitivity of the PIN1 regulatory kinases should have differential effects on PIN1 phosphorylation after BFA treatment. Indeed, PIN1 phosphorylation of the basally localized PIN1:GFP2 in cortex and epidermis cells, as well as PIN1 phosphorylation of basally localized PIN1:GFP3 in the cortex, were strongly BFA-sensitive. Importantly, however, phosphorylation of apical PIN1:GFP3 in the epidermis was strongly insensitive to BFA, suggesting that a BFA-insensitive protein kinase or a BFA-insensitive trafficking machinery promotes PIN1 phosphorylation at the apical side of the cell (Fig. 4 *C* and *D*). With regard to the strong BFA sensitivity of PIN1 phosphorylation at the basal plasma membrane, these results correlate well with the known behavior and basal distribution of D6PK. With regard to the BFA-insensitive PIN1 phosphorylation at the apical plasma membrane, PIN1 phosphorylation may be maintained by the BFA-insensitive PID. This would, however, also lead to the question why the apolarly distributed BFA-insensitive PID, after BFA treatment, cannot maintain PIN1 phosphorylation at the basal plasma membrane and may invite the hypothesis that additional BFA-sensitive cofactors function together with PID at this side of the cell.

Differential Effects of BFA on Root Gravitropism Correlate with PIN1 Phosphorylation Patterns and Hypothetical Auxin Transport in the *PIN2* Expression Domain. PIN1:GFP3 displays the same plasma membrane distribution as PIN2 in root cortex and epidermis cells and PIN1:GFP3 can suppress the *pin2* gravitropism defect in PIN2p::PIN1:GFP3 (26). PIN1:GFP3 can thus functionally replace PIN2 in these contexts. Because the root gravitropism response is dependent on shoot-directed auxin transport in the root epidermis (10, 11, 27), the rescue of *pin2* by PIN1:GFP3 should only occur when the apically localized epidermal PIN1:GFP3 carried auxin transport-activating phosphorylation. Because PIN1:GFP3 phosphorylation at the epidermal apical plasma membrane was not impaired after BFA treatment, we hypothesized that the rescue of the *pin2* gravitropism defect by PIN1:GFP3 should be maintained following BFA treatments. We could indeed confirm this hypothesis and show that root gravitropism was maintained in PIN1:GFP3 when seedlings were grown on BFA-containing medium (Fig. 5 *A* and *B*).

In *pin2* PIN2p::PIN1:GFP2, BFA treatments lead to a dephosphorylation of basally localized PIN1:GFP2 in epidermis and cortex cells. BFA treatments should thus impair root-directed PIN1:GFP2-dependent auxin transport in this line. We reasoned that the inability of PIN1:GFP2 to rescue the gravitropism defect of *pin2* should, at least in part, be suppressed by BFA treatments in *pin2* PIN2p::PIN1:GFP2. Interestingly, we detected, specifically after BFA treatment, a surprisingly strong rescue of the gravitropism defect in BFA-treated *pin2* PIN2p::PIN1:GFP2 seedlings

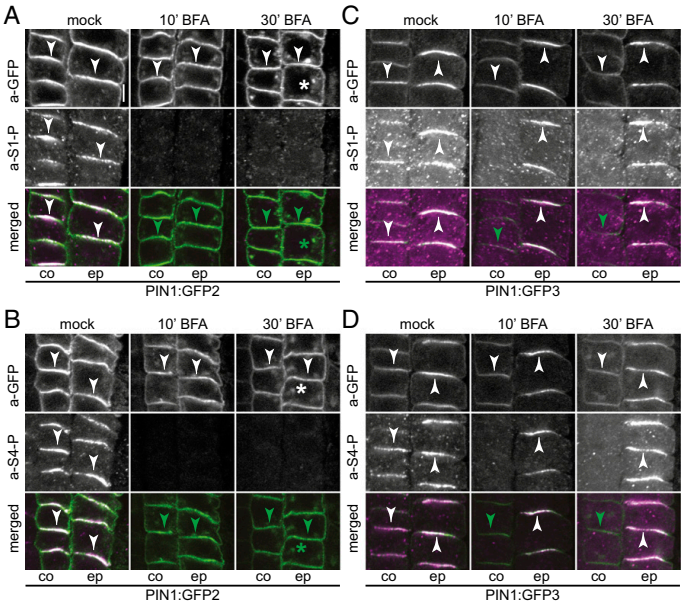

Fig. 4. PIN1 phosphorylation at the basal and apical plasma membranes is differentially BFA-sensitive. Representative confocal images of root cortex (c) and epidermal (e) cells after immunostaining of 4-d-old PIN1:GFP2 and PIN1:GFP3 seedlings following mock or BFA treatments (50 μM; 10 and 30 min) with anti-GFP (PIN1:GFP2 or PIN1:GFP3; green) and (*A* and *B*) a-PIN1 S1-P (a-S1-P; magenta) or (*C* and *D*) a-PIN1 S4-P (a-S4-P; magenta). Arrowheads mark plasma membrane staining, asterisks mark intracellular compartments. Overlap of green and magenta signals is indicated by white arrowheads in merged images. Green arrowheads and asterisks indicate the absence of a corresponding magenta signal from a-PIN1 S1-P or a-PIN1 S4-P immunostaining. (Scale bar, 5 μm.)

(Fig. 5 *A* and *B*). To understand the molecular mechanism underlying this rescue, we analyzed the localization and phosphorylation of PIN1:GFP2 by immunostaining in seedlings grown on BFA-containing medium or a corresponding control medium. We found that this resulted in a depolarization and sometimes apicalization of PIN1:GFP2 from the basal plasma membrane and, in all cells with an immunostaining signal (n = 92, a-PIN1 S1-P; n = 81; a-PIN1 S4-P) also to PIN1:GFP2 phosphorylation at the apical membrane (Fig. 5 *C* and *D*). This finding suggested that the BFA-induced rescue of *pin2* by PIN1:GFP2 may, at least in part, be because of a reversal of PIN1:GFP2-mediated and BFA-sensitive root-directed auxin transport to BFA-insensitive shoot-directed auxin transport in the epidermis.

PIN1 Is Not Activated by Phosphomimicking Mutations of PIN1 S1–S4. Phosphorylation events at phosphosites may be mimicked by replacing the phosphorylated residues by negatively charged D (aspartic acid) or E (glutamic acid). Phosphorylation-mimicking mutations of PIN1 S1–S3 (PIN1 S123E) were reported to result in PIN1 targeting to the apical plasma membrane (14, 15). Because PIN1 phosphorylation is also required for PIN1 auxin efflux activation, we examined the activity of PIN1 S123E in *Xenopus laevis* oocyte-based auxin transport assays. Neither PIN1 S123E nor the additionally generated PIN1 S4E and PIN1 S1234E variants showed any kinase-independent auxin efflux activity in this assay (Fig. S8). What is more, the PIN1 S123E and PIN1 S1234E could not be efficiently activated by D6PK or PID, and therefore behaved like loss-of-function rather than gain-of-function variants with regard to auxin transport activity (Fig. S8). Thus, phosphorylation-mimicking mutations that were reported to be sufficient for PIN1 polarity changes *in planta* are not sufficient for the activation of PIN1-mediated auxin efflux in a heterologous auxin transport assay (14).

PIN1 Phosphorylation Can Be Detected at the Basal Domains in *Arabidopsis* Embryos and in Shoot Meristems. Differential auxin transport and differential PIN polarity are crucial during early plant development (28). Cotyledon-directed PIN1 in the epidermis directs auxin transport toward incipient cotyledon initiation sites, whereas root-directed PIN1 in the inner cells helps to establish a critical auxin maximum that forms above the hypophysis (29). Because the *Arabidopsis* embryo is amenable to immunostaining and differential PIN1 polarities can be examined in the embryo in a wild-type context, we examined PIN1 phosphorylation in different embryo developmental stages. There, we observed PIN1 S1 and S4 phosphorylation at the basal as well as apical plasma membranes in PIN1:GFP embryos (Fig. 6 *A* and *B*). Similar to our observations made in stele cells of the primary root, PIN1 was phosphorylated at S1 and S4 at the basal membrane of embryonic inner cells (Fig. 6 *A* and *B*). In each case, PIN1 phosphorylation correlated with PIN1 distribution but not with specific PIN1 localization at the basal or apical plasma membrane. Furthermore, we examined PIN1 phosphorylation in the undifferentiated shoot apical meristems of *pid* mutants and showed that S1- and S4-phosphorylated PIN1, contrary to the expectation based on published literature (24, 25), accumulated at the basal membrane of epidermal cells (Fig. 6 *C* and *D*).

Unknown Kinases Act Redundantly with D6PK and PID in Phosphorylating PIN1 in the Root. D6PK and PID belong to the family of AGCVIII protein kinases, which is comprised of 23 sequence-related kinases in *Arabidopsis* (30). *D6PK* and *PID* supposedly act redundantly with their closest homologs, *D6PK-LIKE1* through *D6PK-LIKE3,* and *PID2*, *WAG1*, and *WAG2*, respectively (15, 31). When we examined PIN1 phosphorylation in loss-of-function mutants of *d6pk d6pkl1 d6pkl2* (*d6pk012*) and *pid pid2 wag1 wag2* (*pid/wag*), we found that

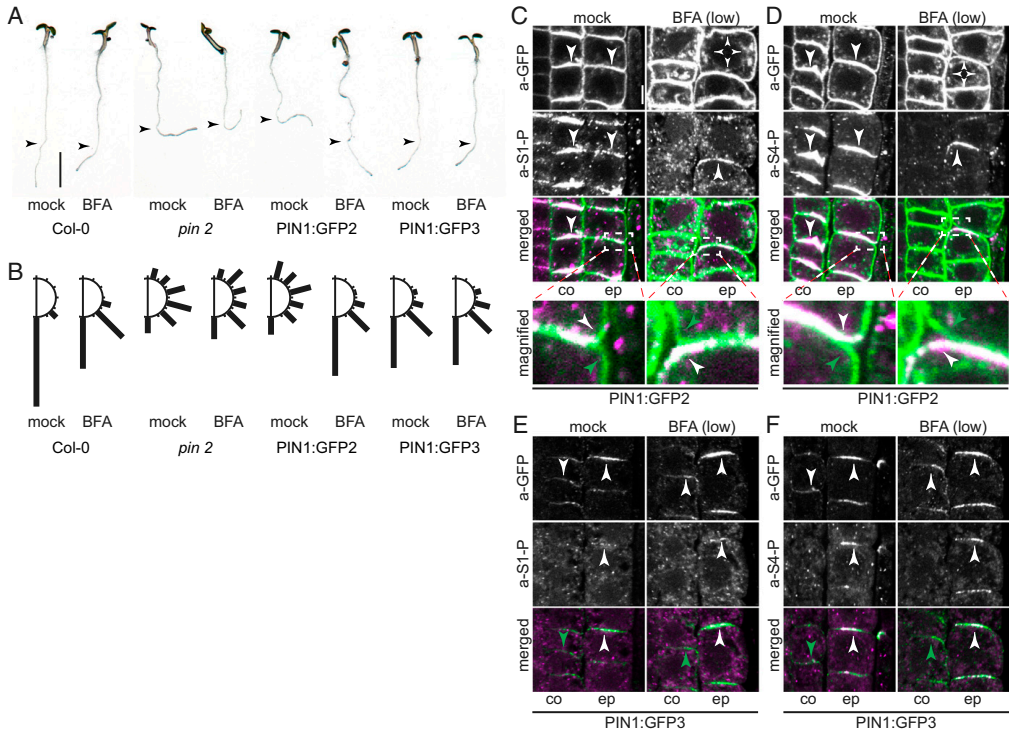

Fig. 5. Differential BFA sensitivity of apical and basal PIN1 phosphorylation correlate with BFA-sensitive rescue of the gravitropism defect in *pin2* seedlings. (*A*) Representative photographs of 5-d-old light-grown *Arabidopsis* seedlings transferred for 18 h to medium with or without BFA (10 μM). The arrowheads point to the position of the root tip at the point of transfer. (Scale bar, 4 mm.) (*B*) Quantification of root gravitropism in 30° windows from seedlings as shown in *A*. The sum of seedlings with root angles corresponding to 30° windows left and right from the vertical axis were combined. Cumulative data from three independent experiments are shown ($n \geq 128$ seedlings). (*C*–*F*) Representative confocal images of root cortex (co) and epidermis (ep) cells after immunostaining of 5-d-old PIN1:GFP2 (*C* and *D*) and PIN1:GFP3 (*E* and *F*) seedlings following the same treatment as in *A* with anti-GFP (a-GFP; PIN1:GFP; green), a-PIN1 S1-P (magenta), and a-PIN1 S4-P (magenta). Arrowheads mark strong and weak plasma membrane staining. Overlap of green and magenta signals is indicated by white arrowheads in merged images. Green arrowheads indicate the absence of a corresponding magenta signal from a-PIN1 S1-P or a-PIN1 S4-P immunostaining. In *C*, immunostained epidermal cells (51 of 79) showed a basal plasma membrane signal following the mock treatment and an apical signal after BFA treatment (92 of 240). In *D*, immunostained cells showed a basal plasma membrane signal (128 of 140) following the mock treatment and an apical signal after BFA treatment (81 of 177). In all cases, the remaining cells showed either no signal for a-PIN1 S1-P or a-PIN1 S4-P, or the polarity of that signal could not be unequivocally determined, based on the criteria as shown in the magnifications. (Scale bar, 5 μm.)

PIN1 phosphorylation at S1 and S4 was maintained, suggesting that other kinases may act redundantly with D6PKs and PID/WAGs in PIN1 phosphorylation, at least in the root stele cells examined here (Fig. S9*A*). Because many other kinases of the AGCVIII family had not been tested with regard to their phosphorylation activity toward PIN proteins, we performed phosphorylation experiments with previously uncharacterized family members, namely D6PKL3 (AT3G27580) but also AGC1–5 (AT3G12690) and KIPK (AT3G52890), using the PIN1 cytoplasmic loop as a substrate. Each of these protein kinases phosphorylated the PIN1 substrate and therefore qualifies as additional kinase that can phosphorylate PIN1 in the *d6pk012* or *pid/wag* mutants (Fig. S9*B*).

Discussion

PIN1 phosphorylation was previously linked to the control of PIN1 activity and polarity (2, 12, 13, 24, 25, 32, 33). In the present study, we established phosphosite-specific antibodies against PIN1 S1–S4. At least three of these antibodies, directed against PIN1 S1, S2, and S4, enabled us to examine specific PIN1 phosphorylation events in situ in the context of PIN1 activity and polarity control.

PIN1 phosphorylation at PIN1 S1–S3 by the BFA-insensitive PID kinase has been proposed to control PIN1 polarity (15, 33). Because phosphorylated PIN1 should be targeted to the apical plasma membrane in root cells, it would be expected that PIN1 S1–S3 phosphorylation is detected at the apical but not at the basal plasma membrane. In contrast, we detected PIN1 phosphorylation at S1–S3 at the basal and, after *PID* overexpression, also at the apical plasma membrane of root stele cells. Thereby, PIN1 phosphorylation followed the general distribution pattern of PIN1 and was not associated with the plasma membrane at a specific side of the cell. This finding was also true in lines expressing differentially GFP-tagged PIN1 in the *PIN2* expression domain, where PIN1 phosphorylation could be detected at the basal and the apical plasma membrane in root epidermis or cortex cells (26). In addition, in the complex tissue

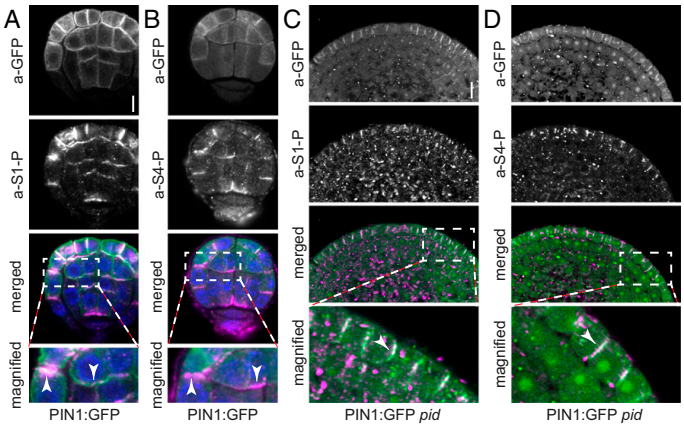

Fig. 6. PIN1 phosphorylation follows PIN1 distribution in *Arabidopsis* embryos and *pid* shoot apical meristems. (*A* and *B*) Representative confocal images of *Arabidopsis* PIN1:GFP embryos stained with a-GFP (PIN1; green) and a-PIN1 S1-P (*A*; magenta) or a-PIN1 S4-P antibodies (*B*; magenta). Arrowheads mark the immunostaining at the plasma membrane. Merged images also include DAPI staining of nuclei (blue). (Scale bar, 5 μm.) (*C and D*) Representative confocal images of nondifferentiated *pid* PIN1:GFP mutant shoot apical meristems stained with a-GFP (PIN1; green) and a-PIN1 S1-P (*C*; magenta) or a-PIN1 S4-P antibodies (*D*; magenta). White arrowheads mark the immunostaining at the plasma membrane in the merged images. (Scale bar, 10 μm.)

of a differentiating *Arabidopsis* embryo, we observed PIN1 phosphorylation at the apical and basal plasma membrane of embryonic cells and no correlation between PIN1 phosphorylation and specific sides of the cell. In epidermal cells of *pid* mutant shoot apical meristems where, according to previous models (24, 25), PIN1 phosphorylation should lead to PIN1 apicalization, we detected PIN1 phosphorylation also at the basal plasma membrane. In addition, we also obtained no evidence that PIN1 might be phosphorylated during intracellular transport, for example when it accumulated in BFA compartments after BFA treatment. There is thus no obvious correlation between PIN1 polar distribution and PIN1 phosphorylation at the phosphosites examined.

Previous studies had supported the model explaining PIN1 polarity changes by PIN1 S1–S3 phosphorylation by examining PIN1 variants, in which S1–S3 phosphorylation was prevented through mutations to alanines (S123A) or mimicked through mutations to glutamic acid (S123E). There, PIN1 S123A and PIN1 S123E were detected at the basal and apical plasma membranes of root cells, respectively (33). In line with the expectation that dynamic PIN1 trafficking to different polar sides of the cell, and consequently differential and dynamic auxin distribution, was required for the implementation of complex developmental processes, neither of these mutant variants could rescue *pin1* mutant phenotypes (14). We had previously shown that PIN1 S123A variants were, as expected, impaired in kinase-dependent PIN1 activation and auxin efflux when tested in *Xenopus* oocytes (12). Interestingly, we now found that PIN1 S123E variants were functionally impaired in their ability to promote auxin export from oocytes when coexpressed with D6PK or PID. In contrast to the expectation that the glutamic acid replacement mutations would mimic PIN1 phosphorylation and—as we would assume—activation, neither PIN1 S123E nor the more complex PIN1 S1234E variant exported auxin from oocytes in a protein kinase-independent manner. Thus, at least with regard to auxin transport activation and the responsiveness to protein kinases, the phosphomimicking variants behaved like variants with reduced PIN1 function. Of course, this observation cannot be easily related to the mechanisms controlling PIN1 polarity because it cannot be excluded that the PIN1 trafficking machinery may recognize the phosphomimicking variants as a result of distinct affinity requirements for phosphorylated PIN1.

We had previously argued that the phosphosite preferences of the two kinases may be the relevant distinguishing feature that could explain the differential effects of PID and D6PK on PIN1 polarity control (2, 12, 13, 15). Previous work had established that PID and D6PK phosphorylate PIN1 S1–S4 but that PID preferentially phosphorylated S1–S3, whereas D6PK preferentially phosphorylated S4 (2, 12, 13, 15). However, we obtained no evidence for a differential phosphorylation at the PIN1 phosphosites in any experimental setting. Rather, all four PIN1 phosphorylations, or at least PIN1 S1 and S4 phosphorylation, coincided in all cases tested. Taken together, these findings suggested that the phosphorylation of all four serines may be mediated by the same protein kinases. We thus propose that the differential phosphorylation at these sites, as detected in vitro, may not be biologically relevant in vivo. Hence, differential phosphosite preference may not be suitable to explain the differences between D6PK and PID in PIN1 polarity control. The fact that differential antibody affinities preclude stringent quantitative comparisons of phosphorylation levels between the PIN1 phosphosites in immunostaining experiments is a limiting technical factor in this analysis.

Our observations thus show that the prevalent model explaining PIN1 polarity by PID-dependent phosphorylation can no longer hold true. As previously reported, and confirmed here with transgenic lines generated independently for our study, PIN1 polarity is clearly altered after *PID* overexpression. However, phosphorylation of the preferential PID phosphorylation site PIN1 S1 was not specifically associated with the respective polarity change. Therefore, as yet unknown factors must control PIN1 polarity together with PID. These could be PID-specific protein interactors that may not be able to bind or act in concert with D6PK. Although PID and D6PK belong to the same class of AGCVIII protein kinases, D6PK and PID have substantial differences that would allow for such regulatory protein interactions to take place (e.g., in their N and C termini, as well as in an insertion domain that resides within the kinase domains of both proteins) (30). PID has already been reported to engage in interactions with proteins other than PINs and these may play an additional role in controlling PID activity (34). Based on our experiments with an inducible *PID* expression line, we also argue that the respective mechanism does not have the fast dynamics that could be expected for a phosphorylation-controlled PIN1

repolarization process. Instead, and in line with previous reports, we detected in our experiments a clear change in PIN1 polarity only after an extended induction period of 22 h (24).

PIN1 phosphorylation controls PIN1 auxin efflux activity (12). Here, we report on several settings where predictions on auxin transport activity and consequently auxin distribution could be made based on PIN1 phosphorylation. We observed in root stele cells that the interference with PIN1 phosphorylation resulted in the apparent accumulation of auxin within cells, as judged with the auxin-sensitive DII-VENUS marker. We could further explain the suppression of the gravitropism defect of a *pin2* mutant expressing PIN1:GFP2 after BFA treatment, not only by the effects of BFA on BFA-sensitive kinases at the basal plasma membrane, but also by the effects of activated phosphorylated PIN1 at the apical plasma membrane, where PIN1 phosphorylation is maintained after BFA treatment by apparently BFA-insensitive protein kinases or trafficking machineries. Therefore, the availability of phosphosite-specific PIN1 antibodies will, in the future, allow understanding PIN1-mediated auxin efflux in a given cell or tissue context based on PIN1 phosphorylation rather than based solely on PIN1 abundance.

Genetic studies indicate that *D6PK* acts in a functionally redundant manner with at least three other sequence-related *D6PK-LIKE* genes (12, 16, 17). Based on genetic and cell biological studies, functional redundancy was also proposed between *PID*, *WAG1*, and *WAG2*, and possibly with *PID2*, which are all members of a distinct subclade within the *Arabidopsis* AGCVIII protein kinase family (30, 31). We found that PIN1 phosphorylation was not detectably impaired in complex mutants of the *D6PK* and *PID*-related kinases, suggesting that other protein kinases (e.g., other protein kinases of the AGCVIII family) also regulate PIN phosphorylation in addition to D6PKs and PID/WAGs. This hypothesis finds indirect support in the observation that root growth and gravitropism are not as severely impaired in the complex *d6pk* or *pid/wag* mutants as may be expected from mutants with severely impaired PIN and auxin transport function (10, 17, 20, 31, 35). Several of the phosphorylation events observed in our experiments support the notion that these, as yet, unknown PIN1-regulatory protein kinases are related—in their cell biological behavior—to D6PK and PID. D6PK is a strongly BFA-sensitive protein kinase and PIN1 phosphorylation at the basal plasma membrane of root cells was very sensitive to BFA treatments. In contrast, PID is a BFA-insensitive kinase and may maintain PIN1 phosphorylation at the apical plasma membrane where PIN1 phosphorylation was not responsive to BFA treatments. Solely based on structural and sequence criteria, several hitherto uncharacterized members of the AGCVIII protein kinase family could qualify as candidate PIN regulators (30). We showed that uncharacterized AGCVIII kinases can phosphorylate PIN1 in vitro and these may control PINs by phosphorylation in vivo (e.g., in the *d6pk012* or *pid/wag* backgrounds examined here). In other recently published work, we provide evidence that these kinases also localize to the plasma membrane (36), providing further support for the hypothesis that also these kinases may regulate activities at the plasma membrane. We also noted with interest that the BFA-insensitive PID was seemingly not sufficient to maintain PIN1 phosphorylation at the basal plasma membrane after BFA treatment, even though it is apolarly distributed in these cells and expected to function at the basal plasma domain. Thus, phosphorylation control of PIN1 activity and polarity by PID must be more complex than previously anticipated. Understanding the transcriptional and posttranslational mechanisms controlling the expression and abundance of the different functionally related protein kinases will therefore be an important topic for future research aiming at mapping the complexities of PIN regulation. Phosphosite-sepcific antibodies, as established here for PIN1, will then be an important tool to monitor the activity and effects of these phosphorylation events.

Materials and Methods

Biological Material. All *A. thaliana* lines used in this study are in the Columbia ecotype. The following lines have been described previously: *pin1* (SALK_047613) PIN1p::PIN1:GFP (PIN1:GFP) and *pin1* (SALK_047613) PIN1p::PIN1:YFP (PIN1:YFP) (37); *pin2* PIN2p::PIN1:GFP2 and *pin2* PIN2p::PIN1:GFP3 (26); *pin1* PIN1p::PIN1:GFP S1A (14); estradiol-inducible G10-90::XVE>>PID (15); BFA-sensitive GNOM^{wt} and BFA-insensitive GNOM^{M696L} (19); DII-VENUS and mDII-VENUS (38); *d6pk d6pkl1 d6pkl2* (*d6pk012*) and 35S::YFP:D6PK (17); and *pid/PID pid2 wag1 wag2* (31). *pid pid2 wag1 wag2* quadruple mutants were isolated from the progeny of *pid/PID pid2 wag1 wag2* based on the cotyledon formation-deficient phenotype specific for the quadruple mutant (31). The *pin1* (SALK_047613) mutant backgrounds were genotyped for homozygosity using primers as listed in Table S1.

Molecular Cloning. PIN1p::PIN1:YFP (PIN1:YFP) is a previously described plant transformation construct for the expression of a functional YFP-tagged PIN1 under control of the *PIN1* promoter fragment (12). Mutagenesis of the PIN1 S2 and S3 phosphosites to alanine yielded PIN1:YFP S2A and S3A, which were introduced in PIN1:YFP as previously described for PIN1:YFP S4A (12). The constructs were transformed into heterozygous *PIN1/pin1* (SALK_047613) plants by *Agrobacterium*-mediated transformation and *pin1* homozygous lines carrying the PIN1:YFP transgenes were isolated from the progeny and used for immunostaining (39). PIN1:GFP S1A was previously described (33).

For auxin transport assays in *X. laevis* oocytes, PIN1 S (serine) phosphosites were mutagenized in p002:PIN1 to potentially phosphorylation-mimicking E (glutamic acid) through several rounds of PCR mutagenesis with primers PIN1 S1E, PIN1 S2E, PIN1 S3E, and PIN1 S4E (12).

The *PID* overexpression construct 35S:PID was obtained by PCR amplification of the *PID* coding sequence with primers PID-GW-FW and PID-GW-RV. The resulting fragment was inserted into pDONR201 (LifeTechnologies) and from there into pGW-35S-MYC (a gift from Jane Parker, Max Planck Institute for Plant Breeding Research, Cologne, Germany). A stop codon in PID-GW-RV prevents the in-frame fusion with the C-terminal MYC-tag of this vector. 35S:PID was introduced in the Col-0 wild-type background using the floral dip method (39).

A construct for the expression of YFP-tagged PID (YFP:PID) in *Arabidopsis* was obtained by PCR amplification of the *PID* coding sequence, insertion of the PCR fragment into pDONR201 followed by the transfer into pExtag-YFP-GW (a gift from Jane Parker, Max Planck Institute for Plant Breeding Research, Cologne, Germany). The transgenic construct was introduced into the Col-0 wild-type using the floral-dip method (39).

cDNAs of protein kinases were amplified using forward and reverse primers for the respective gene and amplification products were transferred, via pDONR201, into pDEST15 using the Gateway cloning system (Invitrogen). Expression constructs for D6PK and PID were previously described (12).

All primer sequences are listed in Table S1.

Phosphosite-Specific Antibodies. Phosphosite-specific antibodies were generated by Eurogentec using the following peptides for immunization and affinity purification of rabbit sera: PIN1 S1 N′-LSATPRP-S(P)-NLTNA-C′, PIN1 S2 N′-RNPTPRG-S(P)-SFNHT-C′, PIN1 S3 N′-GPTPRP-S(P)-NYEEDG-C′, and PIN1 S4 N′-SGGGRN-S(P)-NFGPGE-C′.

ACKNOWLEDGMENTS. The authors thank Jutta Elgner for excellent technical assistance; Jiri Friml (Institute of Science and Technology Austria, Klosterneuburg, Austria), Remko Offringa (University of Leiden, Leiden, The Netherlands), Teva Vernoux (Ecole normale supérieur de Lyon, Lyon, France), and Tatsuya Sakai (Niigata University, Niigata, Japan) for mutant or transgenic seed lines and constructs; and Hannelore Daniel (Technical University of Munich, Freising, Germany) for the generous and uncomplicated supply of *Xenopus* oocytes. Financial support for this work came from Deutsche Forschungsgemeinschaft Grants SCHW751/12-1 (to C.S.), SFB1101 (to G.J.), and SFB924 and HA3468/6-1 (to U. Z.H.); as well as a Fundação para a Ciência e a Tecnologia Fellowship SFRH/BD/73187/2010 (to I.C.R.B.).

1. Teale WD, Paponov IA, Palme K (2006) Auxin in action: Signalling, transport and the control of plant growth and development. *Nat Rev Mol Cell Biol* 7(11):847–859.
2. Barbosa IC, Schwechheimer C (2014) Dynamic control of auxin transport-dependent growth by AGCVIII protein kinases. *Curr Opin Plant Biol* 22:108–115.
3. Gälweiler L, et al. (1998) Regulation of polar auxin transport by AtPIN1 in *Arabidopsis* vascular tissue. *Science* 282(5397):2226–2230.
4. Friml J, et al. (2002) AtPIN4 mediates sink-driven auxin gradients and root patterning in *Arabidopsis*. *Cell* 108(5):661–673.

5. Noh B, Bandyopadhyay A, Peer WA, Spalding EP, Murphy AS (2003) Enhanced gravi- and phototropism in plant mdr mutants mislocalizing the auxin efflux protein PIN1. *Nature* 423(6943):999–1002.
6. Geisler M, et al. (2005) Cellular efflux of auxin catalyzed by the *Arabidopsis* MDR/PGP transporter AtPGP1. *Plant J* 44(2):179–194.
7. Bainbridge K, et al. (2008) Auxin influx carriers stabilize phyllotactic patterning. *Genes Dev* 22(6):810–823.
8. Péret B, et al. (2012) AUX/LAX genes encode a family of auxin influx transporters that perform distinct functions during *Arabidopsis* development. *Plant Cell* 24(7):2874–2885.
9. Krecek P, et al. (2009) The PIN-FORMED (PIN) protein family of auxin transporters. *Genome Biol* 10(12):249.
10. Müller A, et al. (1998) AtPIN2 defines a locus of *Arabidopsis* for root gravitropism control. *EMBO J* 17(23):6903–6911.
11. Rahman A, et al. (2010) Gravitropism of *Arabidopsis thaliana* roots requires the polarization of PIN2 toward the root tip in meristematic cortical cells. *Plant Cell* 22(6): 1762–1776.
12. Zourelidou M, et al. (2014) Auxin efflux by PIN-FORMED proteins is activated by two different protein kinases, D6 PROTEIN KINASE and PINOID. *eLife*, 10.7554/eLife.02860.
13. Barbosa IC, Zourelidou M, Willige BC, Weller B, Schwechheimer C (2014) D6 PROTEIN KINASE activates auxin transport-dependent growth and PIN-FORMED phosphorylation at the plasma membrane. *Dev Cell* 29(6):674–685.
14. Huang F, et al. (2010) Phosphorylation of conserved PIN motifs directs *Arabidopsis* PIN1 polarity and auxin transport. *Plant Cell* 22(4):1129–1142.
15. Dhonukshe P, et al. (2010) Plasma membrane-bound AGC3 kinases phosphorylate PIN auxin carriers at TPRXS(N/S) motifs to direct apical PIN recycling. *Development* 137(19):3245–3255.
16. Willige BC, et al. (2013) D6PK AGCVIII kinases are required for auxin transport and phototropic hypocotyl bending in *Arabidopsis*. *Plant Cell* 25(5):1674–1688.
17. Zourelidou M, et al. (2009) The polarly localized D6 PROTEIN KINASE is required for efficient auxin transport in *Arabidopsis thaliana*. *Development* 136(4):627–636.
18. Kleine-Vehn J, et al. (2009) PIN auxin efflux carrier polarity is regulated by PINOID kinase-mediated recruitment into GNOM-independent trafficking in *Arabidopsis*. *Plant Cell* 21(12):3839–3849.
19. Geldner N, et al. (2003) The *Arabidopsis* GNOM ARF-GEF mediates endosomal recycling, auxin transport, and auxin-dependent plant growth. *Cell* 112(2):219–230.
20. Sukumar P, Edwards KS, Rahman A, Delong A, Muday GK (2009) PINOID kinase regulates root gravitropism through modulation of PIN2-dependent basipetal auxin transport in *Arabidopsis*. *Plant Physiol* 150(2):722–735.
21. Shin H, et al. (2005) Complex regulation of *Arabidopsis* AGR1/PIN2-mediated root gravitropic response and basipetal auxin transport by cantharidin-sensitive protein phosphatases. *Plant J* 42(2):188–200.
22. Rashotte AM, DeLong A, Muday GK (2001) Genetic and chemical reductions in protein phosphatase activity alter auxin transport, gravity response, and lateral root growth. *Plant Cell* 13(7):1683–1697.
23. Vernoux T, et al. (2011) The auxin signalling network translates dynamic input into robust patterning at the shoot apex. *Mol Syst Biol* 7:508.
24. Friml J, et al. (2004) A PINOID-dependent binary switch in apical-basal PIN polar targeting directs auxin efflux. *Science* 306(5697):862–865.
25. Michniewicz M, et al. (2007) Antagonistic regulation of PIN phosphorylation by PP2A and PINOID directs auxin flux. *Cell* 130(6):1044–1056.
26. Wisniewska J, et al. (2006) Polar PIN localization directs auxin flow in plants. *Science* 312(5775):883.
27. Abas L, et al. (2006) Intracellular trafficking and proteolysis of the *Arabidopsis* auxin-efflux facilitator PIN2 are involved in root gravitropism. *Nat Cell Biol* 8(3):249–256.
28. Lau S, Slane D, Herud O, Kong J, Jürgens G (2012) Early embryogenesis in flowering plants: Setting up the basic body pattern. *Annu Rev Plant Biol* 63:483–506.
29. Steinmann T, et al. (1999) Coordinated polar localization of auxin efflux carrier PIN1 by GNOM ARF GEF. *Science* 286(5438):316–318.
30. Galván-Ampudia CS, Offringa R (2007) Plant evolution: AGC kinases tell the auxin tale. *Trends Plant Sci* 12(12):541–547.
31. Haga K, Hayashi K, Sakai T (2014) PINOID AGC kinases are necessary for phytochrome-mediated enhancement of hypocotyl phototropism in *Arabidopsis*. *Plant Physiol* 166(3):1535–1545.
32. Zhang J, Nodzynski T, Pencík A, Rolcík J, Friml J (2010) PIN phosphorylation is sufficient to mediate PIN polarity and direct auxin transport. *Proc Natl Acad Sci USA* 107(2):918–922.
33. Offringa R, Huang F (2013) Phosphorylation-dependent trafficking of plasma membrane proteins in animal and plant cells. *J Integr Plant Biol* 55(9):789–808.
34. Benjamins R, Ampudia CS, Hooykaas PJ, Offringa R (2003) PINOID-mediated signaling involves calcium-binding proteins. *Plant Physiol* 132(3):1623–1630.
35. Blilou I, et al. (2005) The PIN auxin efflux facilitator network controls growth and patterning in *Arabidopsis* roots. *Nature* 433(7021):39–44.
36. Barbosa IC, et al. (2016) Phospholipid composition and a polybasic motif determine D6 PROTEIN KINASE polar association with the plasma membrane and tropic responses. *Development* 143(24):4687–4700.
37. Benková E, et al. (2003) Local, efflux-dependent auxin gradients as a common module for plant organ formation. *Cell* 115(5):591–602.
38. Brunoud G, et al. (2012) A novel sensor to map auxin response and distribution at high spatio-temporal resolution. *Nature* 482(7383):103–106.
39. Clough SJ, Bent AF (1998) Floral dip: A simplified method for Agrobacterium-mediated transformation of *Arabidopsis thaliana*. *Plant J* 16(6):735–743.
40. Sauer M, Friml J (2010) Immunolocalization of proteins in plants. *Methods Mol Biol* 655:253–263.
41. Geldner N, Friml J, Stierhof YD, Jürgens G, Palme K (2001) Auxin transport inhibitors block PIN1 cycling and vesicle trafficking. *Nature* 413(6854):425–428.
42. Bröer S (2010) *Xenopus laevis* oocytes. *Methods Mol Biol* 637:295–310.